Prepared for:

RIKZ

Furthur development and first application of a mud transport model for the Scheldt estuary

In the framework of LTV

Report

December 2007

Prepared for:

RIKZ

Further development and first application of a mud transport model for the Scheldt estuary

In the framework of LTV

Phase 2

Thijs van Kessel, Joris Vanlede, Kees Kuijper, Johan de Kok

Report

November 2007

WL | delft hydraulics

Client:	RIKZ / WD
Title:	Further development and first application of a mud transport model for the Scheldt estuary

Abstract:

In 2006, a work plan was conceived for the development of a mud transport model for the Scheldt estuary in the framework of LTV (Long Term Vision) (Winterwerp and De Kok, 2006). The purpose of this model is to support managers of the Scheldt estuary with the solution of a number of managerial issues. Also in 2006, the first two phases were initiated. The present report discusses the activities that have been carried out during 2007, *i.e.* further improvement of the hydrodynamic and mud transport model and first application of the mud model to the release of fine sediment dredged from Sloe harbour, Vlissingen.

At a technical level, all model improvements scheduled for 2007 have been implemented. The most important developments are: longer hydrodynamic simulation period (3 month), more accurate concentration boundary conditions, variable wave effects and biological effects.

The hydrodynamic simulation demonstrates realistic values for water levels, salinities and residual currents. Upstream of Antwerpen, the propagation of the tidal wave is modelled less accurately.

Regarding the mud transport simulations, the following is concluded:

1. A minor shift of two dumping locations near Antwerp much improves the proper modelling of the ETM.
2. New concentration BC at sea result in more realistic SPM concentrations and longshore SPM fluxes at sea.
3. The difference between simulations with 5 and 10 horizontal layers is only minor.
4. Variable waves temporarily enhance the concentration in the western part of the Western Scheldt during storms.
5. The biological impact on large-scale SPM concentrations in the Scheldt estuary appears to be minor.
6. The SPM levels appear to be rather sensitive to the volume of harbour siltation and dumping.
7. The model computes an unrealistically high residual sediment flux towards the North Sea (about 2 MT/y).

If sediment dumping is in equilibrium with harbour siltation, this net export results in too low equilibrium SPM levels. Application of the model to the dumping of sediment dredged from Sloe harbour shows that a shift of the release location in western direction may be favourable because of a small reduction in local SPM levels and siltation rates.

References:	contract RKZ – 1872

Ver	Author		Date	Remarks	Review		Approved by	
1.1	Thijs van Kessel	TvK	30/11/2007		Winterwerp	ww	Schilperoort	

Project number:	Z4375
Keywords:	mud transport, three-dimensional models, estuary models, Scheldt
Number of pages:	139
Classification:	None
Status:	Final

Contents

1 Introduction

In 2006, a work plan was conceived for the development of a mud transport model for the Scheldt estuary in the framework of LTV (Long Term Vision) (Winterwerp and De Kok, 2006). The purpose of this model is to support managers of the Scheldt estuary with the tools to evaluate a number of managerial issues.

In the work plan five phases have been defined:
1. set-up of mud model
2. elaboration of managerial questions
3. year simulations
4. detail studies
5. sediment mixtures.

In 2006, the first two phases were initiated. The set-up of the hydrodynamic and mud transport model was reported in Van Kessel *et al.* (2006), whereas the managerial issues were elaborated in Bruens *et al.* (2006). The present report discusses the activities that have been carried out during 2007. These activities are based on the original work plan (items 1 through 3), but take also into account the findings from the set-up of the mud model and the discussions with Scheldt estuary managers during 2006.

In short, most activities for 2007 fall into the following two categories:
1. further improvement of the mud transport model
2. providing support for a few managerial issues

This report deals with both activities. In chapters 2–4 , the work on the model improvements is further elaborated. In chapter 5, the model is applied to support the management of the Scheldt estuary. Conclusions are drawn and recommendations are made in chapter 6. This year's application deals with optimisation of dredging and dumping strategies for harbour maintenance.

Because of the decision to continue work on model improvement during the second phase of the 2007 project on LTV-mud, the first part of this report (chapters 2–4) is an extension and revision of the final report of the first phase as described in Van Kessel *et al.* (2007). As such, this report can be read independently from the Phase 1 report from August 2007.

2 Data analysis

In Van Kessel *et al.* (2006) a data analysis is made regarding the suspended particulate matter (SPM) levels and sedimentation in the Scheldt estuary. Here only two aspects are elaborated:

1. selection of simulation year
2. SPM boundary concentrations

2.1 Year selection

The selection of a representative year is constrained by the following limitations:

- Boundary conditions for water level and salinity from the ZUNO model are readily available for the period 1996 – 2003;
- Validation data at DOW jetty (Terneuzen) with a high temporal resolution are available for the period 12/1998 – 2/2002.

These constraints limit the selection of years 1999 – 2001. Of these years, the year 2000 appears to be most typical regarding average wind speed, number of storms and river discharge (191 m^3/s at Schaar van Ouden Doel). The average wind speed at HIRLAM grid point (86, 34) (at the North Sea approximately halfway between IJmuiden and Lowestoft) is 7.5 m/s with a direction of 263.4 deg. The number of storms is 11. For the year 2000 the western component of the wind is quite strong, resulting in an above-average residual current through Dover Strait (128,000 m^3/s or 0.128 Sv). The wind climate for the year 2000 is shown in Fig. 2.1.

Because of limitations on disk storage and simulation time, it was decided not to use a complete year initially, but the 3-month period January 2000 – March 2000. At a later stage, the whole year will be simulated. Compared with the 14-day hydrodynamic simulation used in the 2006 project, a three month period already means a major extension.

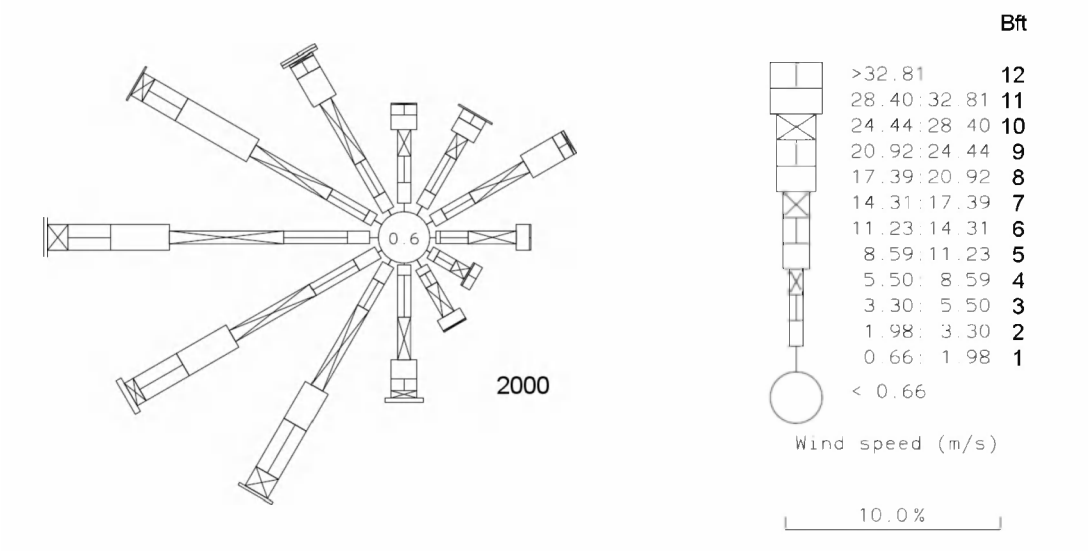

Fig. 2.1: Wind climate at HIRLAM gridpoint (86, 34) for the year 2000. Left: wind rose. Right: wind classes.

2.2 SPM boundary conditions

In the 2006 study, the southern boundary conditions were derived from the Appelzak transect, which is the southernmost transect from the silt atlas (Suijlen and Duin, 2001) based on the MWTL monitoring stations. However, the Appelzak transect is located quite far from the southern model boundary near the border between France and Belgium. Also, the Appelzak transect runs through the turbidity maximum north of Zeebrugge. As a result, the SPM levels applied at the southern boundary are probably too high. Therefore remote sensing images on the SPM levels near the Belgian-French border have been utilised in the present phase of the study, as recommended in the 2006 study.

Recently, Fettweis *et al.* (2007) analysed SeaWiFs images with regard to SPM levels in the Belgian part of the southern North Sea. Supported by a numerical model, they produced maps of the seasonal SPM surface and depth-averaged concentrations (see Fig. 2.2). The depth-averaged SPM boundary conditions applied in the present study were based on these SeaWiFs data. The approximate locations of the model boundaries are delineated in the upper left panel of Fig. 2.2. Figure 2.3 shows the applied cross-shore SPM concentration gradients, both at the southern and the northern model boundary.

Although the applied SPM boundary concentrations are best on the best information available, they may be biased towards lower concentration levels, as satellite images are impaired by cloud cover. Also, the derivation of depth-average concentrations and fluxes from surface observation includes some uncertainty.

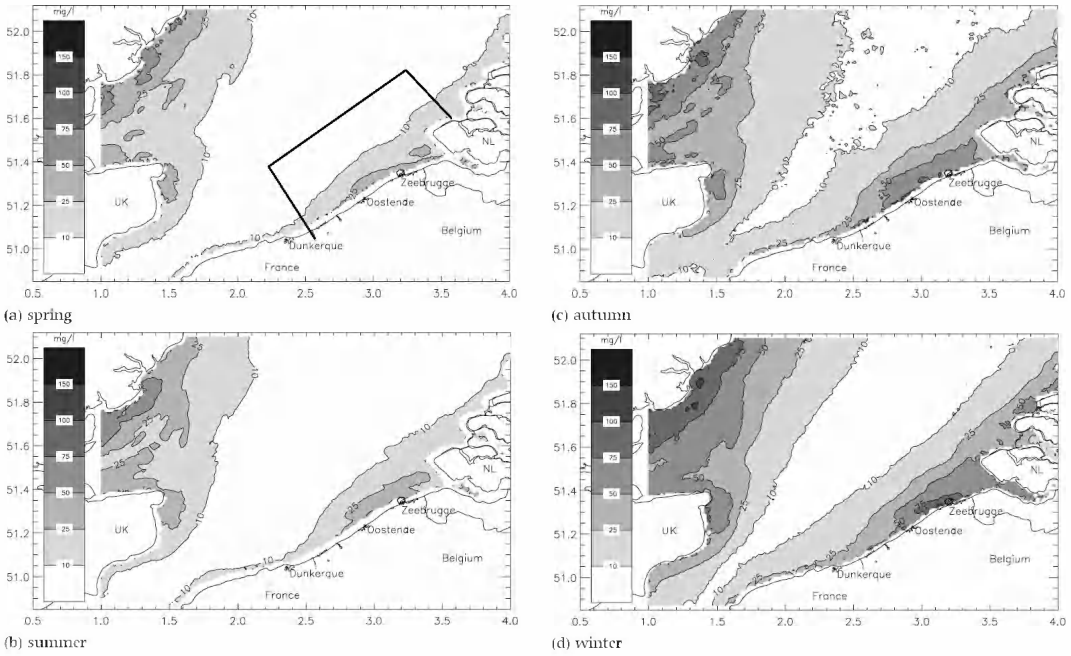

Fig. 2.2: Seasonal averages of SPM surface concentration in the southern North Sea derived from 362 SeaWiFs images (1997 – 2004). From Fettweis *et al.* (2007). The model boundaries are delineated in the upper left panel.

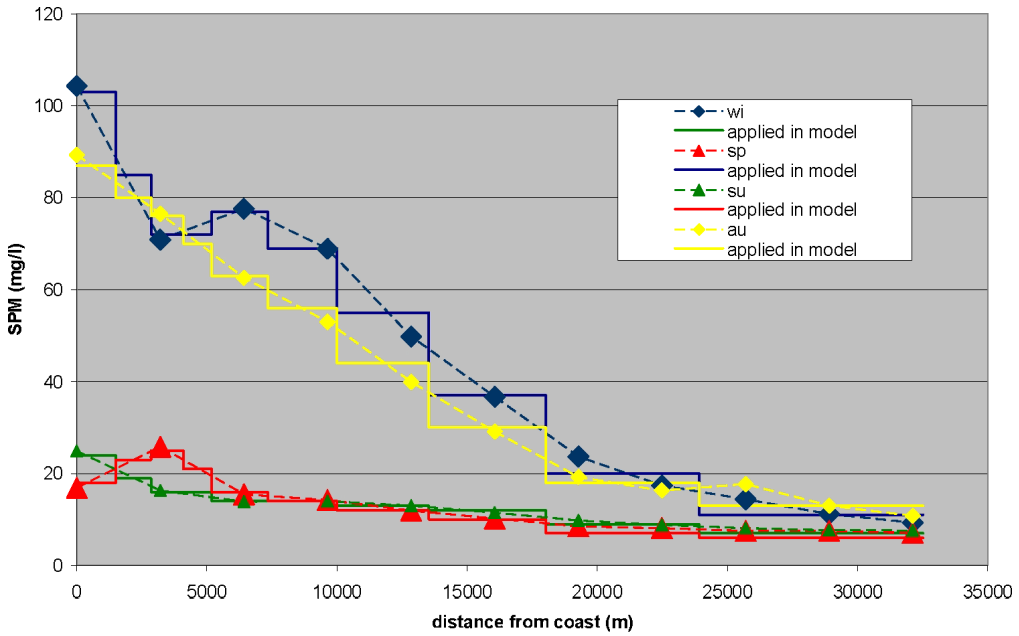

Fig. 2.3a: Applied concentration at northern boundary based on SeaWiFs images (wi = winter, sp = spring, su = summer and au = autumn observations converted to depth-averaged values).

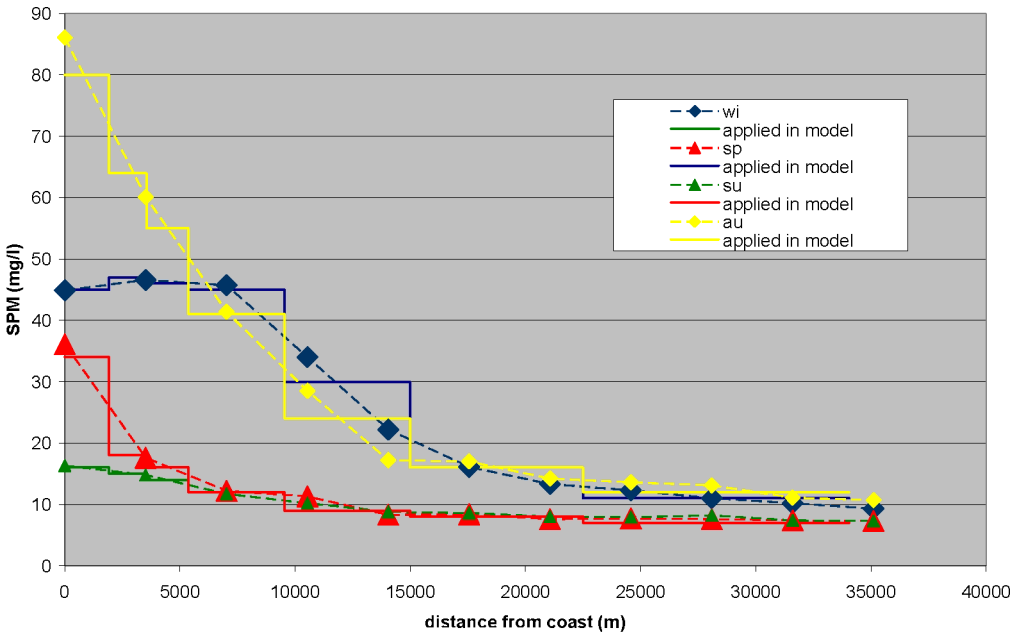

Fig. 2.3b: Applied concentration at southern boundary based on SeaWiFs images (wi = winter, sp = spring, su = summer and au = autumn observations converted to depth-averaged values).

3 Hydrodynamic model

3.1 Introduction

This chapter describes the hydrodynamic model that is used in the LTV-mud project. The description of boundary conditions, hard- and software is followed by a discussion of the results (water levels and salinities). Special attention is paid to the differences with the hydrodynamic results that were obtained in the previous phase of the project, as described in Van Kessel *et al.* (2006) (14-day hydrodynamics) and Van Kessel *et al.* (2007) (3-month hydrodynamics `runllf`, requiring further improvements). The figures that complement the description of the hydrodynamic model can be found in Appendix A.

3.2 Selection of simulation period

One of the targeted improvements for the LTV-mud project in 2007 was to move from a 14 day hydrodynamic simulation to a longer period (possibly one year). Another suggestion was to increase the vertical resolution of the hydrodynamic model from 5 layers to 10 layers. The main challenge would be to provide for enough storage capacity to store the model output, besides the computational time (wall clock time, not merely CPU time) needed to simulate longer time periods. Table 3.1 gives an overview of estimates for both storage capacity and computational time needed for different model set-ups.

	Simulation period	
Computational time [days] **(storage capacity [GB])**	3 months	1 year
5 layer model	7 d. **(315 GB)**	28 d. **(1.260 GB)**
10 layer model	14 d. **(630 GB)**	56 d. **(2.520 GB)**

Table 3.1: Estimates of storage capacity and computational time for different model set-ups.

In order to avoid excessive storage needs and due to the limited time available to calculate the hydrodynamics, it was decided to select a 3 month simulation period. In the feasibility phase of the project, model results were compared for a 5- and a 10-layer model. The vertical parabolic profile of diffusivity proved to be comparable in both cases, as indicated in Figure A-3 for locations "Antwerpen loodsgebouw" and "Vlakte van de Raan". Increasing the vertical resolution of the model from 5 to 10 vertical layers will therefore only have a small effect on the calculated suspended sediment transports, which was confirmed in a test calculation of mud transport with both vertical resolutions (see Chapter 4.3).

The months January to March 2000 were selected for the 3-month simulation. Both the monthly averaged values for wind speed and fresh water inflow are far from the extremes of the period 1995 – 2005 (Figures A-1 and A-2, respectively). In contrast, the months May,

June, July and October 2000 show very high values for fresh water inflow while strong winds occurred in November 2000.

3.3 Hydrodynamic model

The set-up of the model (grid, bathymetry, etc) is covered extensively in Van Kessel *et al.* (2006) and will not be repeated in this report. The hydrodynamic model simulation runs from 1/1/2000 22h30 (HW) until 3/4/2000 22h30. A hydrodynamics simulation of 93 days is carried out. For the 3 month period, a combination of water level and velocity boundary conditions was applied at the sea boundaries, where for previous simulations covering a 14-day period only water levels were applied. This change was made to improve the modelling of the residual longshore current, which was too strong for the previous 14-day simulations.

3.3.1 Initial values

Initial values of water levels and velocities are read-in from a 4 day run of hydrodynamics. This avoids the wiggles in the first time-steps, which were observed in the 2006 version of the hydrodynamic model. The initial values of salinity are based on the available measurements (represented in Figure A-7). The following values are implemented:

Location	Salinity [ppt]
Sea	32.5
Vlakte van de Raan	32.5
Hoofdplaat	25
Overloop van Hansweert	17.5
Baalhoek	7.5
Oosterweel	0.4
Gent	0.3

Table 3.2: Initial salinity values.

In between these locations, salinity is linearly interpolated between the (m, n) points of the computational grid. Time series of salinity of Vlakte van de Raan, Hoofdplaat, Overloop Hansweert and Baalhoek were retrieved from HMCZ (www.hmcz.nl) on 25/07/2007. The time series of salinity at Oosterweel were provided by Flanders Hydraulics Research.

3.3.2 Seaward boundary condition

The downstream boundary of the LTV model is located at sea (Figure A-4). In the 2006 version of the LTV model, 96 harmonic constituents of water level were prescribed at different points along the boundary. In the 2007 version of the model, the downstream boundary conditions for water level and velocity are read-in from a run of the ZUNO model. In order to have an optimal fit of the LTV model to the ZUNO model, a different (somewhat smaller) enclosure was chosen than the 2006 HD model, as is illustrated in Figure A-4. The downstream boundary condition is defined as a set of time-series with a 30 minute interval. Velocities and salinities are prescribed uniformly over the depth.

Along both the north side and sea (i.e. west) side of the downstream model boundary (different parts of the downstream boundary of the model are defined on Figure A-4), water levels are prescribed obtained from the ZUNO model. At the south downstream boundary, the along-shore component of velocity is prescribed. At every point of the sea boundary a time series of salinity is prescribed obtained from the ZUNO model. Typical salinity values for the northward, seaward and southward boundary are depicted in Figures A-5 and A-6. The salinity values at the northward boundary are significantly lower than the salinity values at the seaward and southward boundary. A possible explanation for this is the influence of the diffusive and advective mixing of the fresh water discharge of the river Rhine, which is modelled in ZUNO.

3.3.3 Fresh water inflow

At the upstream boundary of the tidal region, daily values of freshwater inflow are prescribed. The values were provided by Flanders Hydraulics Research. There is inflow in the model from the tributaries Kleine Nete, Grote Nete, Zenne, Dijle and Bovenschelde. The fresh water inflow from the "Bathse Spuikanaal" were provided by Leen Dekker on 06/09/2007. The daily values are presented in Figure A-8.

The monthly average fresh water inflow is higher in February (230 m^3/s) than in January and March (170 m^3/s). On a monthly timescale, one can indeed observe an increasing trend in the salinity in January and March and a slight decreasing trend in February (Figures A-9 through A-11). This effect is particularly visible in stations Baalhoek and Overloop van Hansweert. The daily salinity values reflect a peak discharge event of 550 m^3/s on 04/03/2000 (Figure A-8). This peak discharge has a clear effect on the observations of salinity. A drop in the observed salinities is noticeable in stations Baalhoek and Overloop van Hansweert in the beginning of March (Figure A-11).

3.3.4 Wind forcing

Wind measurements of Vlissingen were retrieved from the website of KNMI (www.knmi.nl) on 23/07/2007. Hourly values of wind speed at 10 m height, together with the wind direction are applied uniformly over the computational grid. The wind drag coefficient is set to 0.0026 (default). The Smith and Banke (1975) formulations are used to relate wind velocity to interfacial shear stress. The hourly values of wind speed and direction are represented in Figures A-12 to A-14.

The monthly mean wind speed varies between 6 and 7 m/s (Figure A-1). Noticeable peaks in wind speed (10 minute mean > 17 m/s) occur at the end of January, and in the beginning of March, together with the peak of fresh water inflow. The main wind direction varies between NW and SW direction (225 to 315 ° from North).

3.3.5 Hardware

The hydrodynamic model was run on the Linux cluster of Flanders Hydraulics Research. The run is performed on 10 dual core nodes, thus using 20 processors. Each node is a HP proliant G3 node with a 2.33 GHz dual core Xeon 5140 processor and 2GB RAM. In this set-up, hydrodynamics are calculated 13.5 times faster than reality (i.e. a one-year

simulation takes 27 days). However, if the heavy model output of 1 map of hydrodynamics every 30 minutes is switched off, the hydrodynamics are calculated 28.8 times faster than reality. A part of this difference can be explained by the extra communication needed to write the results to SDS-file.

3.3.6 Software

The model is run in the SIMONA software suite of Rijkswaterstaat, release 0612. The WAQPRE module is used for pre-processing, and WAQPRO for processing. Postprocessing is done using the getdata routine to generate netCDF files of different variables (time series and spatial distributions). These files are then read-in and further processed in Matlab. netCDF is an open source standard of a binary data container for scientific datasets. netCDF-files are read in in Matlab using the mexcdf software package (freeware, retrieved from http://mexcdf.sourceforge.net/ on 25/04/2007).

3.4 Validation of results

3.4.1 Hydrodynamics

Simulated water levels are compared to measurements at the locations Vlakte van de Raan, Vlissingen, Overloop Hansweert, Bath, Liefkenshoek and Antwerpen. Measurements of water level were retrieved from HMCZ (www.hmcz.nl) on 23/07/2007. Both measurements and simulations are represented in two-week graphs for the period 26/02/2000 to 09/03/2000 (Figure A-16 to A-18) and for 25/03/2000 to 06/04/2000 (Figure A-19 to A-21).

A harmonic analysis on M2 and M4 components of the water level of the complete three-month period (both for measurements and for model results) is shown from Figure A-22 to Figure A-24. Figure A-22 shows M2 amplitude of model results and measurements. Run11 in this figure refers to the hydrodynamic model as it was presented at the end of phase 1 of the project (van Kessel et al, 2007). Run13 represents the current version of the hydrodynamic model. A new set of boundary conditions successfully lowered the M2 amplitude at the downstream boundary from 1.75 m to 1.55 m at Vlakte van de Raan, bringing it closer to the measured amplitude of 1.5 m. Lowering the M2 component of the boundary condition with 20 cm (from run 11 to run 13) had a similar effect throughout the entire modelling domain.

The computed M2 phase lags 5° behind the measured phase, which corresponds to a 10 minute phase lag. The phase lag between run 13 and the measurements remains more or less constant throughout the modelling domain, which indicates that the tidal wave propagates at a correct speed.

Figure A-22 also shows that once further upstream than Liefkenshoek, the amplitude of M2 starts to decrease, a trend which is not observed in the measurements. The harmonic analysis was not performed in the zone upstream of Antwerpen, so at present it is not known how the difference in M2 amplitude between predictions and observations evolves further down the estuary.

Figures A-23 and A-24 learn that the model underestimates the amplitude ratio of M4 to M2 by 1 or 2 % (depending on the location; upstream of Antwerpen the difference increases). The amplitude ratio M4/M2 is an indication of the non-linear response to tidal forcing (Aubrey and Speer, 1985). A part of M4 amplitude in the estuary is indeed generated by M2 through non-linear response to M2 tidal forcing (e.g. by friction or by geometry effects) but another part of M4 amplitude is already present in the boundary condition, as can be seen from Figure A-23. The curve of M4 amplitude shows a decreasing trend downstream beyond Overloop Hansweert which is not observed in the measurements. The computed phase of M4 shows a trend upstream from Baalhoek that is not observed in the measurements. Speer and Aubrey (1985) state that harmonic growth and particularly relative phase of M4 depend on the size of tidal flats, time variability of channel geometry and the level of friction.

The general underestimation of M4 phase upstream of Baalhoek also has an important effect on the M2–2M4 phase difference graph, which is an indication of tidal asymmetry. A relative phase between 0° and 180° indicates that the duration of water level fall exceeds water level rise, i.e. the tide is flood-dominant, and otherwise if it is ebb-dominant (Wang *et al.*, 2002). Figure A-24 indicates that the simulated hydrodynamics is more ebb-dominant than according to the measurements in between the seaward boundary and Liefkenshoek, and that it becomes more flood dominant than according to the measurements further upstream. This indicates that tidal asymmetry (flood and ebb dominance) is predicted correctly in a qualitative sense, but that the magnitude of tidal asymmetry is overpredicted. It is remarked that this analysis based on the M2–2M4 phase difference is most relevant for transport-limited conditions (such as for sand). For supply-limited conditions (such as is often the case for mud transport), the relative duration of the high water and low water slack may be more relevant.

Figures A-25 through A-27 give an image of Eulerian residual velocity fields of the horizontal velocity components, calculated over 1 tidal cycle as follows:

$$\frac{\int_{T_0}^{T_0+\Delta T} \vec{u}_{bottom}\,dt}{\Delta T}$$

The presented results are valid for the bottom boundary layer, which has a fixed depth of 1m. The results show residual velocity fields with maximum values of up to 10 cm/s. At the mouth of the estuary (Figure A-25) there is a certain amount of convergence of residual velocities in the bottom layer of the model, influencing estuarine circulation. More analysis on different tidal cycles and on a longer timescale is still required.

In between Deurganckdok and Kallo sluice, a similar convergence is observed in Figure A-27. Between Deurganckdok and the Boudewijn – van Cauwelaert sluice complex, the net residual bottom velocity is upstream. Further upstream, between Boudewijn – Van Cauwelaert and Kallo sluice, the net residual bottom velocity points downstream. In both cases, the dominating residual velocity vectors are situated on the right bank side. It is believed that this pattern induces a second turbidity maximum between Deurganckdok and Kallo sluice.

3.4.2 Salinity

Model results of salinity are compared to continuous observations at fixed locations in Figures A-28 to A-35. Salinity measurements are available at stations Vlakte van de Raan, Hoofdplaat, Overloop van Hansweert, Baalhoek and Oosterweel. The measurements of all the stations are summarised in Figures A-9 to A-11. The measurements show that the amplitude of salinity variations reach a maximum in stations Overloop Hansweert and Baalhoek (Figure A-9 to A-11). Typical amplitudes of salinity variation during one tidal cycle are 3 ppt at Vlakte van de Raan, 5 ppt at Hoofdplaat, 6 to 8 ppt at Overloop Hansweert and Baalhoek, and 2 to 3 ppt at Oosterweel.

In general the modelled salinities are in good agreement with the observations. Both the amplitude of salinity variations, and the tidally averaged value are within a 2 ppt margin of error. The most important difference between model results and observations is found at Hoofdplaat and to a lesser extent at Overloop Hansweert in March. The observed salinity at these stations is lower in March then the predicted values. Considering measurements and predictions of salinity in all stations during January and February, it is believed that the model is capable of predicting salinity values within a reasonable margin of error. This would suggest that the difference between measured and predicted salinity in March at stations Hoofdplaat and Overloop Hansweert might be explained by a peak discharge through the channel of Gent-Terneuzen in the beginning of March. At present, this hypothesis is not backed by measurements however.

3.5 Conclusions

The simulation of hydrodynamics has resulted in an SDS file containing every 30 min. water levels, velocities, and vertical mixing coefficients (among other parameters). The simulated period extends from 01/01/2000 22u30 to 03/04/2000 22u30, which spans a period of 93 days.

1. Tidal analysis of modelled and predicted water levels shows that the amplitude of the tidal signal is predicted well throughout the modelling domain. There is a 5° phase lag of M2 and a 10° phase lag of M4 in the boundary condition. In the current modelling set-up, the boundaries are read-in as time series out of a larger model (ZUNO) which makes phase corrections of separate harmonic components a tedious task.
2. Upstream Antwerp the model predicts a drop in M2 amplitude that is not represented in the measurements. This difference is considered important for possible future applications of the model in the region upstream of Antwerp, and is under current investigation at WLBorgerhout.
3. Plots of the horizontal components of the residual velocity vectors in the lowest layer show a convergent pattern close to the mouth of the estuary, and between Deurganckdok and Kallo sluice. At these locations the measurements show enhanced SPM concentrations.

4 Mud transport model

In this chapter, a number of improvements to the mud transport model are discussed, following the recommendations from the previous phase of the LTV project. A major limitation of the 2006 model was the unsatisfactory reproduction of the turbidity maximum near Antwerp. The following simulations are discussed:

1. a minor shift of the dumping locations of dredged material near Antwerp;
2. new concentration boundary conditions based on SeaWiFs images;
3. comparison between simulations with 5 and 10 horizontal layers (regarding both hydrodynamics and mud transport);
4. incorporation of variable wave forcing;
5. effect of stabilizing and destabilizing effects of biological activity;
6. matching of sediment dumping and siltation fluxes, including the development of a dredging and dumping module in Delwaq;
7. potential effect of shipping traffic;
8. validation on 3-month hydrodynamics;

For points 4, 6 and 8 use is made of the improved hydrodynamics as described in chapter 3 of this report. For the sensitivity simulations 1, 2, 3, 5 and 7 that were made earlier, the 14-day hydrodynamics from 2006 has been used, as the 3-month hydrodynamics was not yet available at the time these simulations were made. However, the developments investigated herein have also been implemented in the simulations based on the 3-month hydrodynamics when deemed necessary: shift in dumping locations (point 1) and new concentration BC (point 2). Note that the 14-day hydrodynamics is not perfect cyclical (many tidal components were applied at the sea boundary), therefore closure errors may accumulate after many repeated periods.

The final parameter settings used for validation run `q10` are shown in Table 4.1. For a description of the model formulations reference is made to Van Kessel *et al.* (2006). Here only the meaning of the parameters is explained:

w_s = settling velocity;
α = fraction of the flux settling towards the second bed layer
τ_{crit1} = critical shear stress for erosion for the first bed layer
M_1 = resuspension parameter for the first bed layer
τ_{crit2} = critical shear stress for erosion for the second bed layer
M_2 = resuspension parameter for the second bed layer
d = thickness of second bed layer

The only parameter differing from the 2006 settings is τ_{crit1}, which was reduced from 0.2 to 0.1 Pa following the inclusion of variable wave forcing and the application of different hydrodynamic boundary conditions (see chapter 3). All mud transport simulations are performed for a period of one year. As the period for which hydrodynamic results are available is much shorter (either 2 weeks or 3 months), this shorter period is applied repeatedly to fill up a complete year. Depending on the spin-up time for the mud transport

model, it may be required to simulate a second year to reach a dynamic steady-state condition. As the applied boundary conditions and wave-induced bed shear stress exhibit seasonal dynamics, also the mud model may show seasonal behaviour.

parameter	value	units	value	units
	fraction 1: marine		*fraction 2: fluvial*	
w_s	1.0	mm/s	1.0	mm/s
α	0.1	–	0.05	–
τ_{crit1}	0.1	Pa	0.1	Pa
M_1	2.3×10^{-5}	s^{-1}	2.3×10^{-5}	s^{-1}
d	0.05	m	0.05	m
τ_{crit2}	0.5	Pa	0.5	Pa
M_2	$3.5\ 10^{-7}$	$kg/m^2/s$	$3.5\ 10^{-7}$	$kg/m^2/s$

Table 4.1: Final parameter settings used in 3D model (q10). Note that the settings for the marine and fluvial fraction are equal apart from α.

4.1 Shift of dumping locations

First the effect of a shift of the dumping locations Punt van Merelse and Plaat van Boomke by a few 100 m towards the navigation channel (see Fig. 4.1) was studied, as it appeared that the grid cells at the original locations remained inactive during the 14-day hydrodynamic simulation. As a result, all sediment dumped accumulated permanently in these cells and did not become available for transport. Accretion in the access channels and harbours was therefore not compensated by dumping, causing sediment depletion and low SPM levels near Antwerp. At the new locations, however, sediment can be resuspended and further dispersed. This results in higher SPM concentrations near Antwerp that are in better agreement with observations. This is illustrated in Fig. 4.2, showing the computed concentration levels near Doel and Zuidergat for the original and new dumping locations. The observed 10 and 90 percentile, summer and winter mean SPM concentrations are indicated herein with coloured horizontal lines. The horizontal and vertical SPM concentration distributions are shown in Appendix B.1.

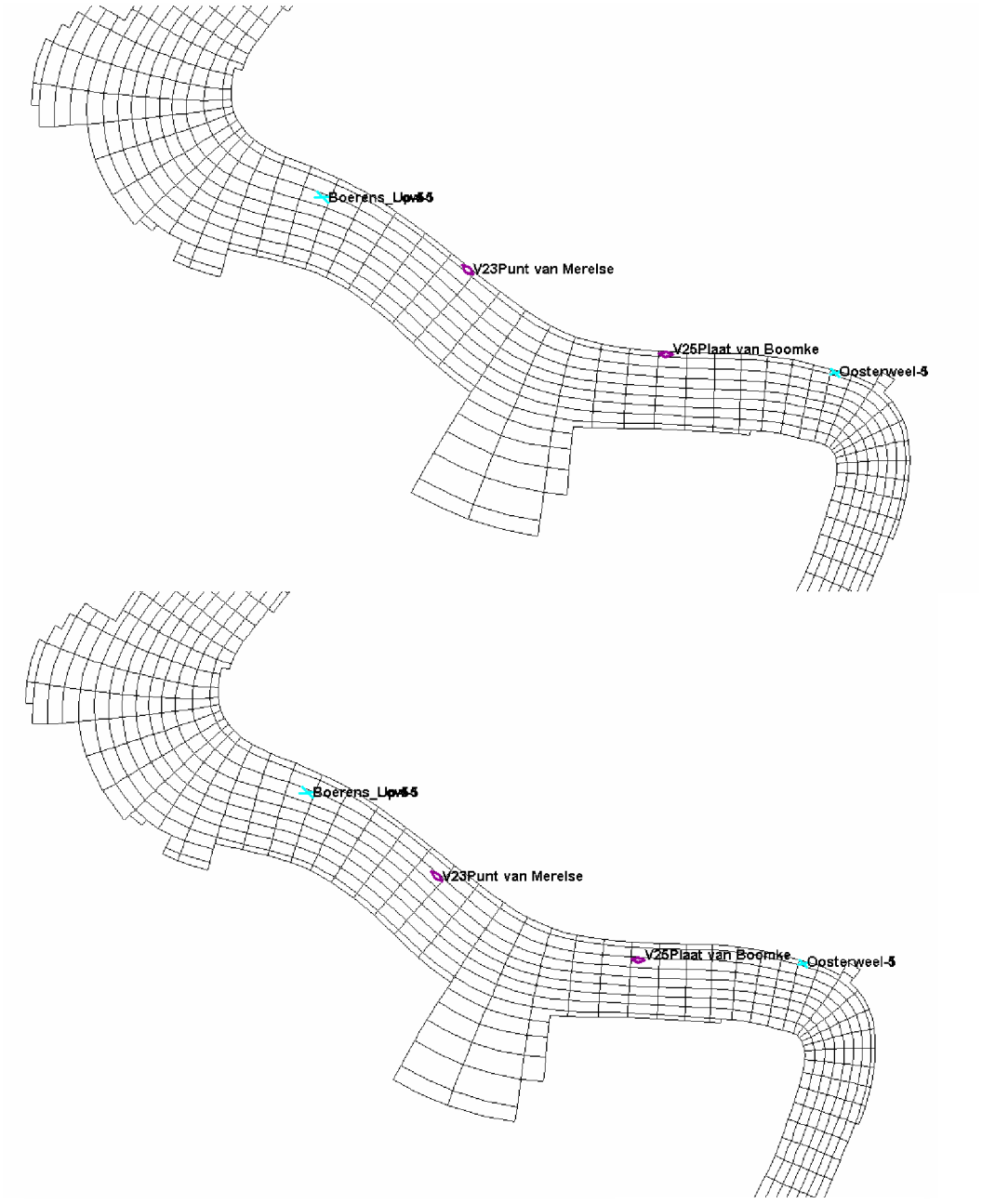

Fig. 4.1: Shift of dumping locations. Top: original locations Punt van Merelse and Plaat van Boomke; Down: new locations. (N.B. light-blue markers such as Boerenschans and Oosterweel designate observation points).

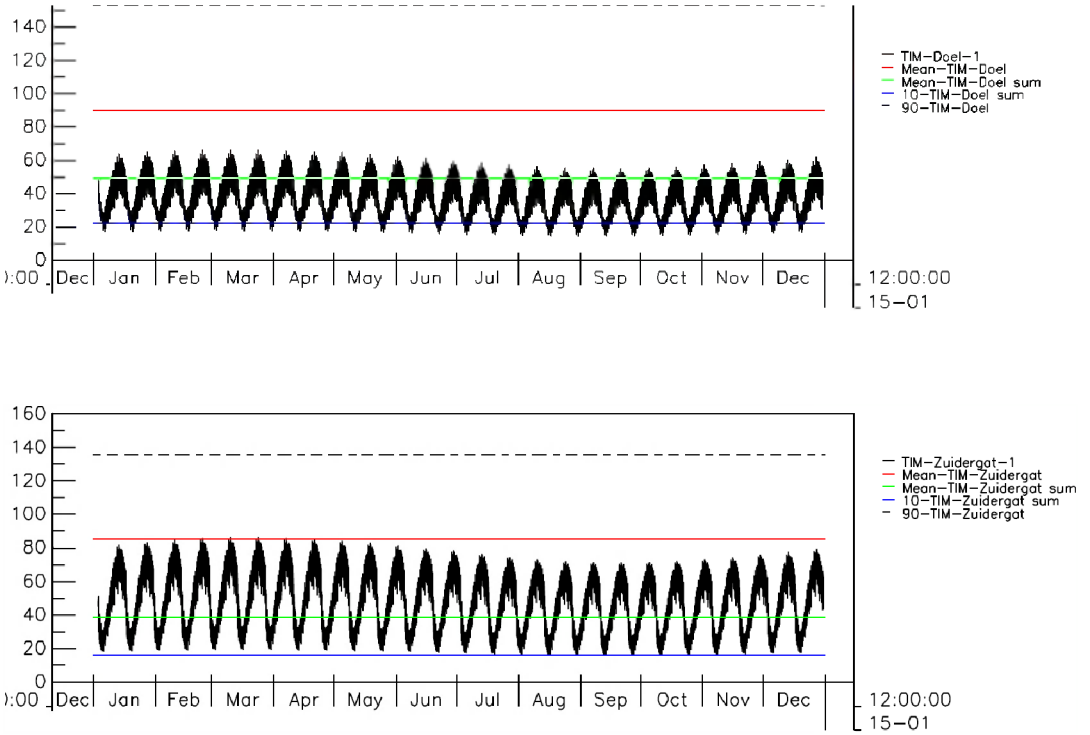

a)

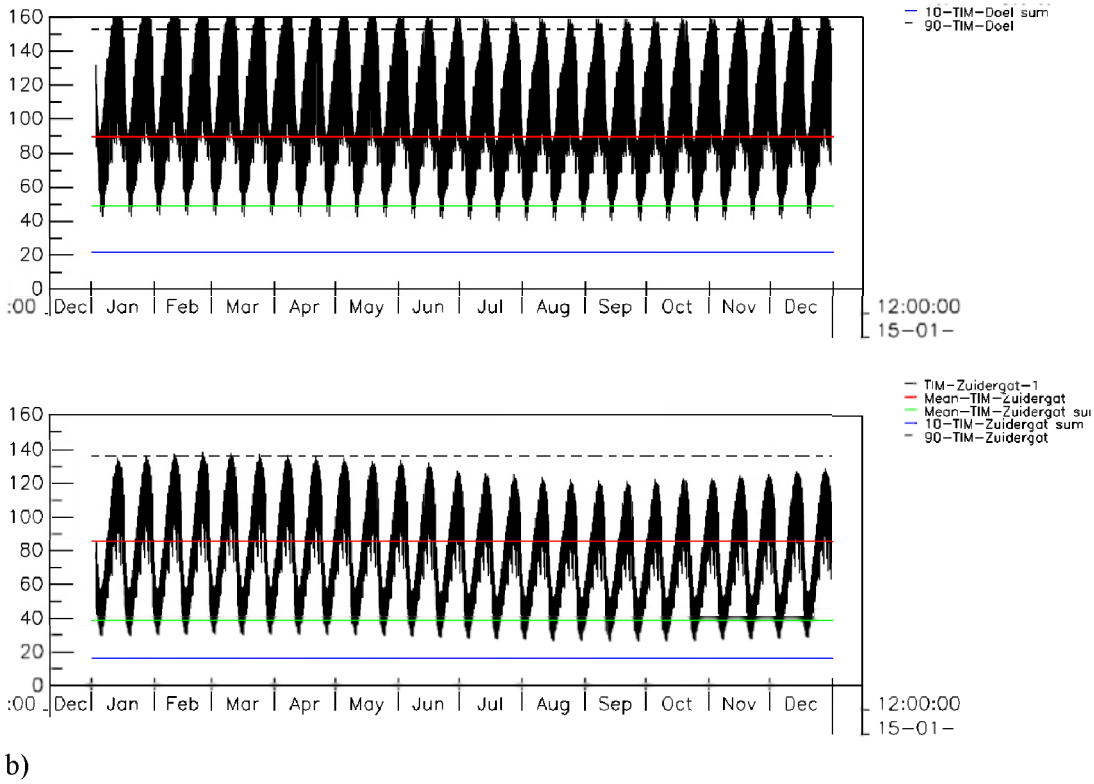

b)

Figure 4.2: Computed SPM surface concentration near Doel and Zuidergat. a) original dumping locations; b) new dumping locations. Observed mean levels are indicated with horizontal lines. In blue: 10-percentile level; in green: mean summer level; in red: mean winter level; dashed black: 90-percentile level.

4.2 New concentration boundary conditions

Figure 4.4 shows the horizontal distribution of the 14-day average SPM surface concentration for the original and new concentration boundary conditions (see Chapter 2.2). The new boundary conditions result in a significant decrease of the SPM levels at the North Sea, which are in a better agreement with observations. This is illustrated in Appendix B-2, in which the modelled and observed SPM concentrations at Wielingen are shown. The concentration maximum near the port of Zeebrugge is maintained with the new boundary condition, which agrees with the SeaWiFs observations (Fig. 2.1).

With the new boundary condition, the alongshore residual sediment flux ranges between 32 MT/y and 66 MT/y for summer and winter condition, respectively (see Fig. B.6c). Although this flux is substantially less than that for the original BC (up to 174 MT/y), it is still fairly high compared with estimates of the residual SPM flux through Dover Strait (between 22 in June and 58 MT/y in January according to McManus and Prandle, 1997) and along the Belgian coast (approximately 25 g/ms according to Fettweis *et al.*, 2007, which is equivalent with 28 MT/y for a 35 km long transect normal to the coastline, see Fig. 2.2). It is remarked that the analysis by McManus and Prandle (1997) was based on 15 monthly survey cruises between August 1988 and October 1989.

As a 14-day hydrodynamic period is too short to draw well-founded conclusions on residual fluxes in view of the large variability of the residual currents, also a 3-month simulation has been analysed (q10). The flux through the southern model boundary is about 22 MT/y, which is in good agreement with the estimate by Fettweis *et al.* (2007) of 28 MT/y. It is therefore concluded that the model performance of the 3-month simulation is satisfactory with regard to the residual longshore SPM flux. The mixed application of water levels and velocities at the sea boundaries for the 3-month simulation has probably contributed to this improvement compared to the 14-day simulation.

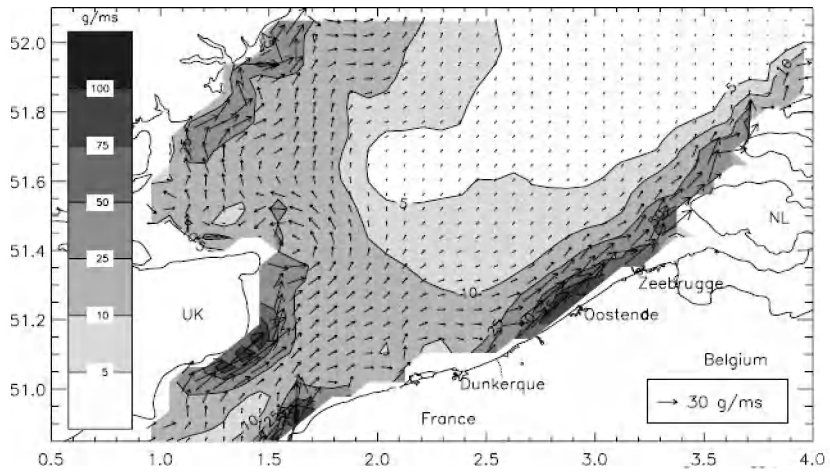

Figure 4.3: Yearly averaged SPM transport per unit width (g/ms) in the southern North Sea. The SPM concentration from the satellite images has been corrected vertically to obtain depth-averaged values (after Fettweis *et al.*, 2007).

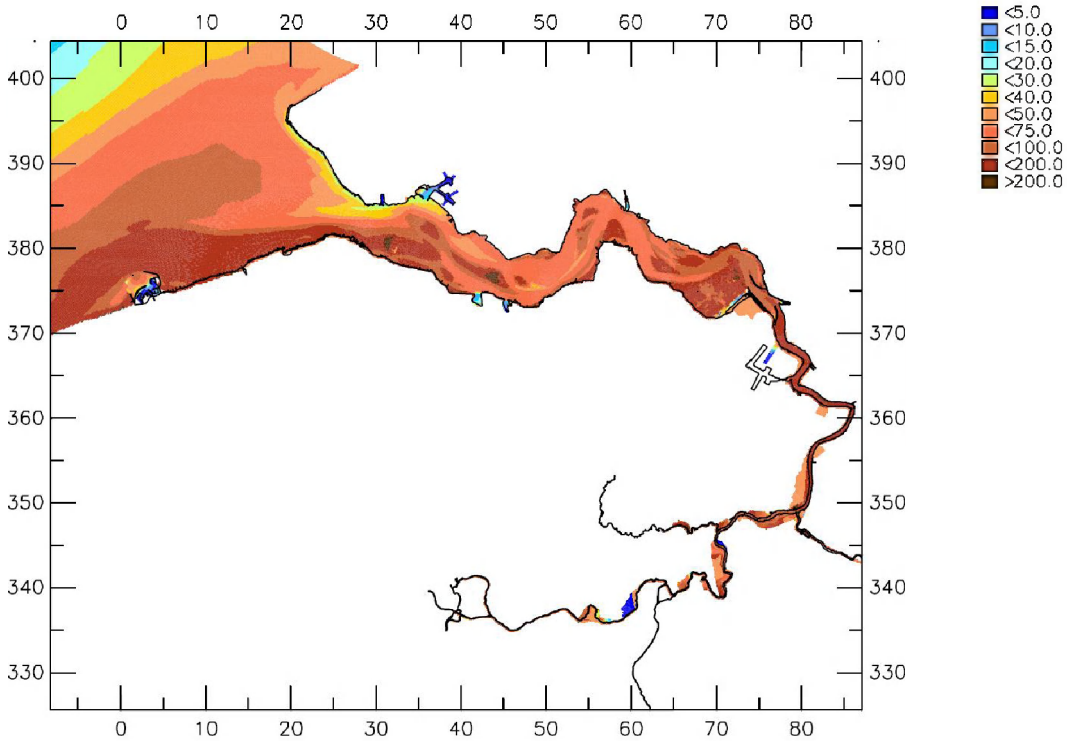

Fig. 4.4a: 14-day winter averaged SPM surface concentration (mg/l), original BC (ws19).

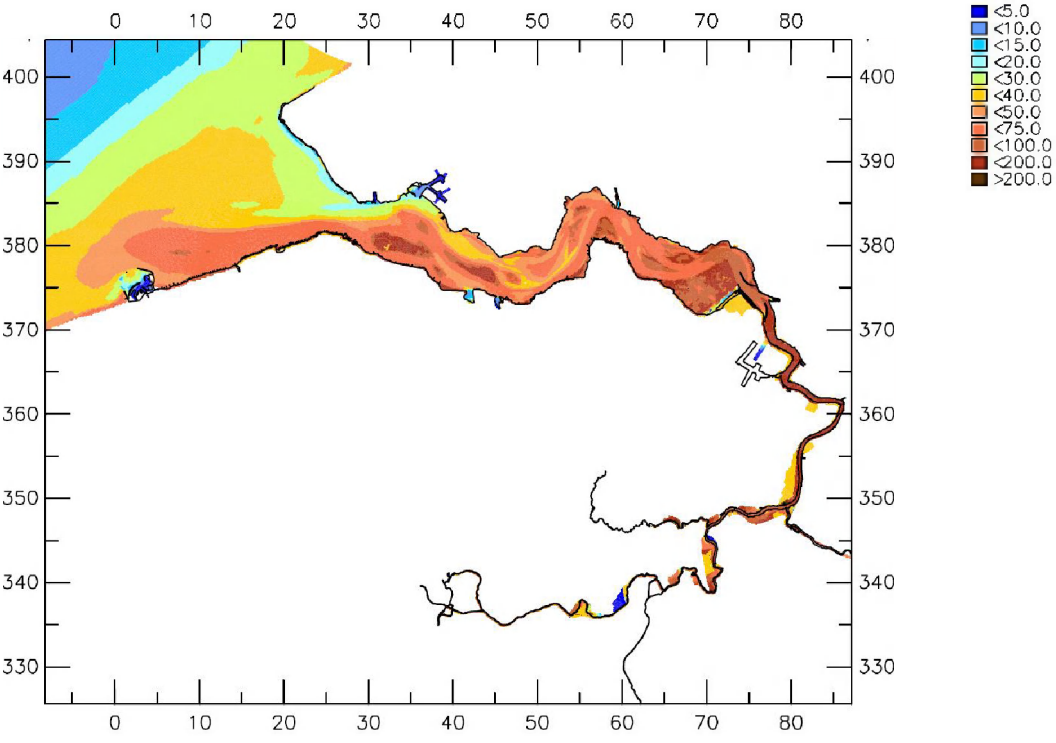

Fig. 4.4b: 14-day winter averaged SPM surface concentration (mg/l), new SeaWiFs BC (ws20)

4.3 Comparison between 5 and 10 layers

A proper simulation of the estuarine circulation requires sufficient vertical detail. The number of 5 layers used in the base simulation is considered to be a bare minimum. To investigate the sensitivity of the simulation results on the vertical resolution, also a 14-day hydrodynamic period was also computed with 10 horizontal layers. Results on the vertical current and eddy viscosity profiles for 5 and 10 layers were already discussed in Chapter 3.2 (see also Fig. A-3). It was concluded that the 5-layer profiles did not deviate significantly from the 10-layer profiles.

The same conclusion is drawn from the mud transport simulations. Figure 4.5 shows the 14-day winter averaged vertical SPM concentration transects along a gridline in the Scheldt estuary in case of 5 and 10 horizontal layers. Although the near-bed concentrations do increase moderately, concentration levels in the remainder of the water column are similar. Also the spatial distribution of SPM remains largely unaffected (see Figs. B.3). It is therefore concluded that at this phase of the project, the limited benefit of 5 additional layers does not justify the required twofold increase in CPU time and disk storage capacity.

4.4 Wave effects

In 2006, wave effects were included by applying a constant, year-averaged wind speed of 7 m/s and assuming a constant fetch length of 25 km. Subsequently, the wave-induced bed shear stress was computed from the equilibrium wave height as a function of the local water depth throughout the model domain.

In this phase of the project, wave effects are included based on a SWAN wave model of the Scheldt estuary forced by observed wave conditions at the North Sea boundary (observations from location Scheur West, see Fig. 4.6) and observed wind speed and direction measured at Vlissingen. The wave fields are computed at a two-hourly interval for the year 2000, resulting in approximately 4400 wave fields. The computations were made with a variable water depth supplied by the hydrodynamic model, which is especially important for the shallow areas. With a Matlab-script, the wave fields computed by SWAN are converted into map fields for the wave-induced bed shear stress that are imported into the DELWAQ mud transport model.

The results presented in this report do not yet cover the complete year 2000, but only the first three months of this year. However, this is sufficient to evaluate the method.

The results of the simulation with variable wave forcing are shown in Appendix B-4. For comparison, also the results of the simulation with constant wave forcing are shown herein. The most pronounced changes do occur at the North Sea and in the western part of the Western Scheldt, where the typical wave energy is significant compared to the tidal energy. Towards Antwerp, the tidal energy is by far dominant. Nevertheless, high-concentration peaks generated by wave-induced resuspension in the western part of the estuary may be advected up-estuary by tidal pumping and result in temporarily higher SPM concentrations.

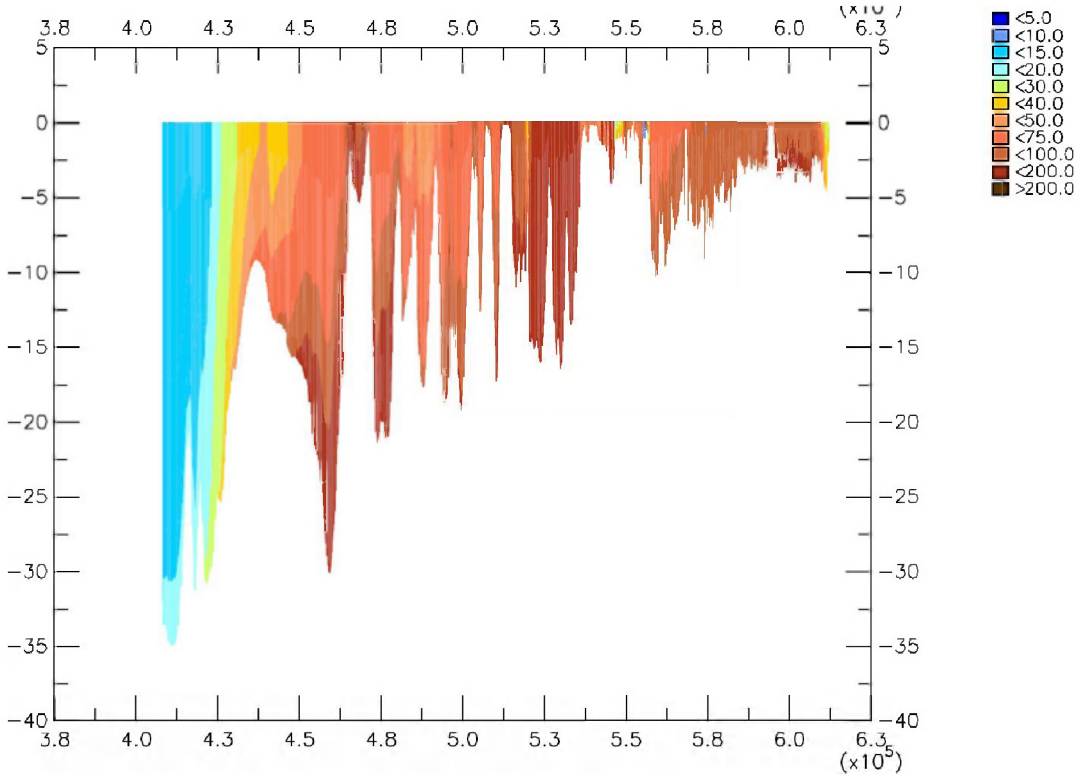

Fig. 4.5a: 14-day winter averaged vertical SPM concentration transect (mg/l) along the estuary (left = sea) , 5 horizontal layers (05L01).

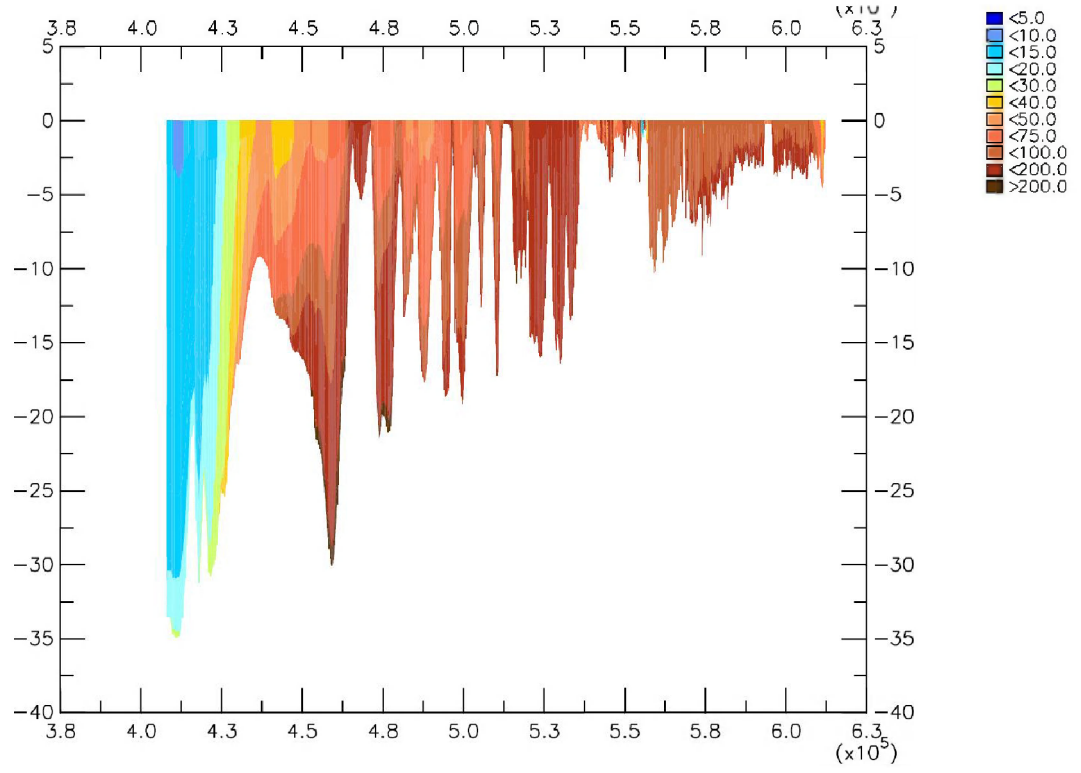

Fig. 4.5b: 14-day winter averaged vertical SPM concentration transect (mg/l) along the estuary (left = sea), 10 horizontal layers (10L01).

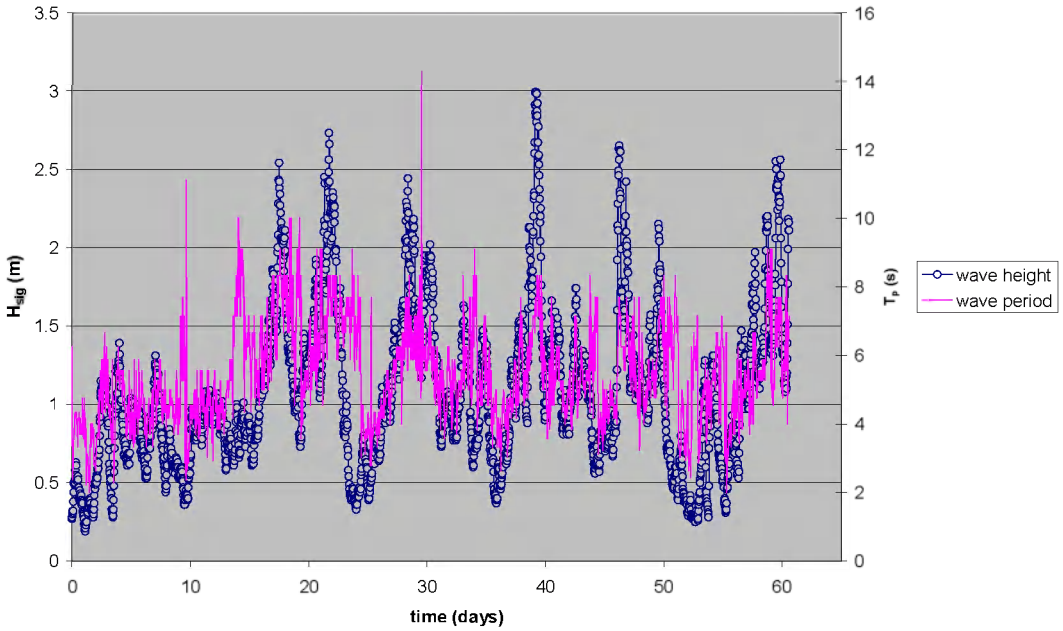

Fig. 4.6: Wave boundary conditions at North Sea (location Scheur Wes, depth 15 m offshore Zeebrugge). Start date 01/01/2000.

Because of the variable waves, the average SPM concentration tend to increase in the western part of the model domain. This can be explained by the peaks in bed shear stress during storm, which do not occur for the simulation with a constant wave-induced bed shear stress.

It is concluded that the technique for applying variable wave forcing is available and gives sensible results. Note that the simulations presented in this concept report are still based on a hydrodynamic simulation period of 14 days. In the final report they will be replaced by simulations based on 3-month hydrodynamics.

4.5 Influence of biology

Stabilisation and destabilisation of the seabed by biological activity may have an impact on the SPM levels in the Scheldt. Biological activity plays a role notably in the shallow parts of the estuary. In the deeper parts (below NAP –3 m), physical effects are dominant (Borsje *et al.*, 2007).

Diatoms have a stabilising influence on the sediment surface, whereas the clam *Macoma bathica* and the mud snail *Hydrobia ulvae* have a destabilising influence. The biomass of these organisms shows a seasonal variation, with low values in winter and high values in summer. In summer, the biological impact is therefore expected to be more pronounced than in winter.

As an initial step, the variation of the biomass of diatoms, *Macoma* and *Hydrobia* as a function of depth and season is assumed to be equal to the variation in the Wadden Sea

reported by Borsje *et al*. (2007). At a later stage, values more representative for the Scheldt estuary may be applied. Also other stabilising or destabilising species may be considered. A first comparison with data from De Jong and De Jonge (1995) on the chlorophyll-*a* distribution in the Western Scheldt does not reveal large discrepancies.

The relative effect of biology on the critical shear stress for erosion τ_c and the resuspension parameter *M* during summer (acting equally on bed layers one and two) is shown in Fig. 4.7. At a level above 0 m NAP, the stabilising effect of diatoms dominates, resulting in an increase in τ_c and a decrease in *M*. At levels between −3 and 0 m NAP the destabilising effect of *Macoma* and *Hydrobia* dominates, resulting in a decrease in τ_c and an increase in *M*. At levels below −3 m NAP, the biomass is set at zero and therefore no effect of biology is found.

Fig. 4.8 shows the 14-day average surface SPM concentration at Terneuzen with and without biology. The biological impact results in a concentration decrease in summer and a concentration increase in winter. Also, the concentration minimum occurs approximately one month earlier in the year, which is in better agreement with observations (*e.g.* see Fig. 3.10 in the previous report by Van Kessel *et al*., 2006). However, for the settings presently applied the overall effect of biology on the SPM concentration is quite small: the increase and decrease is in the order of 1 mg/l only.

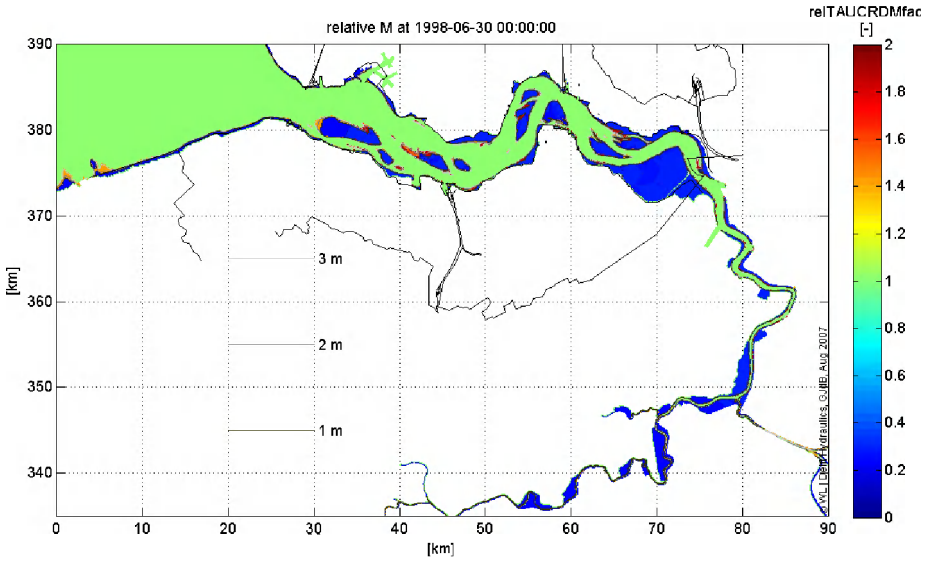

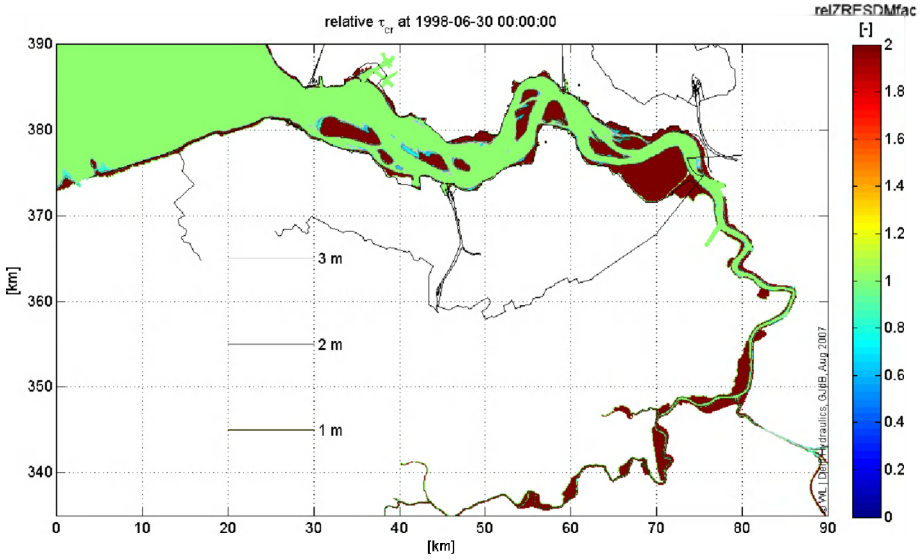

Fig. 4.7: Relative influence of biology on resuspension parameter M (upper panel) and critical shear stress for erosion τ_c (lower panel) on June 30. 1 = no biological effect.

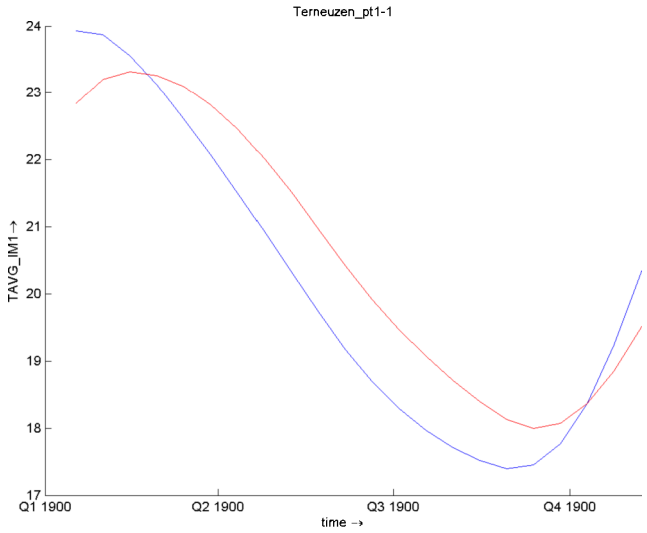

Fig. 4.8: Year variation of the 14-day averaged SPM surface concentration (mg/l) at Terneuzen; red line: without biology; blue line: with biology.

It should be realised that the surface area above −3 m NAP in the Scheldt area is relatively much smaller than in the Wadden Sea, thus reducing the potential impact of biological effects.

Appendix B-5 shows both the 14-day average SPM surface concentration and the mud content in the bed in summer. It is clear that although the computed overall effects of biology in the estuary are minor, the biological effects are significant on the intertidal flats: because of stabilisations, the mud content is locally increased in summer, whereas the SPM concentration is decreased.

It is concluded that:

1. The technical (software) infrastructure required to include biological effects is available.
2. Assuming that the settings in the Wadden Sea are representative for the Scheldt estuary, the biological impact on the overall SPM levels appears to be minor. SPM levels appear to be much more influenced by physical processes such as waves.
3. However, local effects on bed composition and SPM levels appear to be significant.
4. The biological settings should be more tailored for the conditions in the Scheldt, *e.g.* by optimising biomass availability, considering other species and taking into account the effect of salinity gradients on the distribution of species.

4.6 Matching of siltation and dumping flux

The 2006 mud transport simulations were not yet balanced regarding the rate of harbour siltation and dumping of dredged material from harbours. Table 4.1 shows the rate of siltation and dumping for a simulation with 2006 settings, apart from the new SeaWiFs concentration BC (ws20) (see §4.2). The simulations are based on a hydrodynamic period of 14 days. Harbour siltation amounted to 3 MT/y, whereas sediment dumping amounted to 7.7 MT/y.

Location	siltation (kT/y)		dumping (kT/y)	
	ws20	**ws24**	**ws20**	**ws24**
Zeebrugge + Western Scheldt	1714	1915	5436	2718
Sea Scheldt	1286	1316	2075	2075
TOTAL	3000	3131	7511	4793

Table 4.1 Siltation and dumping rates for original settings (ws20) and new settings (ws24).

To improve the balance between siltation and dumping, two actions have been taken:

1. Enhance sedimentation by increasing τ_c in the harbour basins.
2. Reduce the rate of dumping.

The first action has most effect at Zeebrugge, where in reality waves do not propagate into the harbour basins. However, the jetties have not yet been included in the wave model. Therefore too little siltation is computed at Zeebrugge. A local increase in τ_c will compensate for this unrealistic behaviour. The second action is justified in view of the uncertain (and highly variable) data on sediment dumping, including the mud content of the dredged material.

Fig. 4.9 shows the 14-day average SPM surface concentration for the simulation with the original and new settings. It is obvious that the SPM levels decrease substantially. From a comparison with observed levels (see Appendix B-6, which also shows detailed mud budgets for both simulations), it is concluded that the modelled SPM concentrations become too low for the new settings, notwithstanding a better (though not yet sufficient) balance between dumping and harbour siltation. The two most likely explanations for this performance loss are:

1. The model is presently calibrated for the situation with an unbalance between harbour siltation and mud dumping; for the situation with an improved balance, other parameter settings may increase the SPM levels towards the observed range.
2. Too much of the released mud is stored on mudflats; too little may remain in suspension and return to the harbour basins. In final 3-month simulations, this has been improved by reducing τ_{crit1} from 0.2 to 0.1 Pa.

As the SPM levels appear to be rather sensitive to the cycle of harbour siltation and dumping, this aspect should be an integral part of the model calibration. Further optimisation is still required.

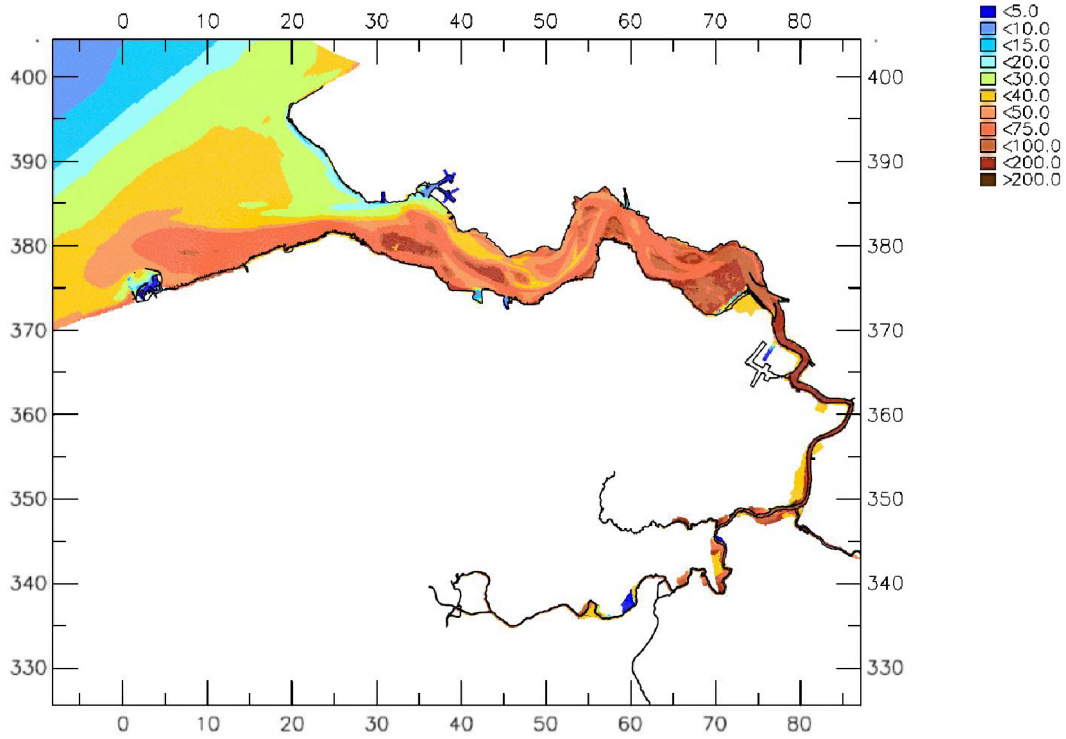

Fig. 4.9a: 14-day winter averaged SPM surface concentration (mg/l), original settings (ws20).

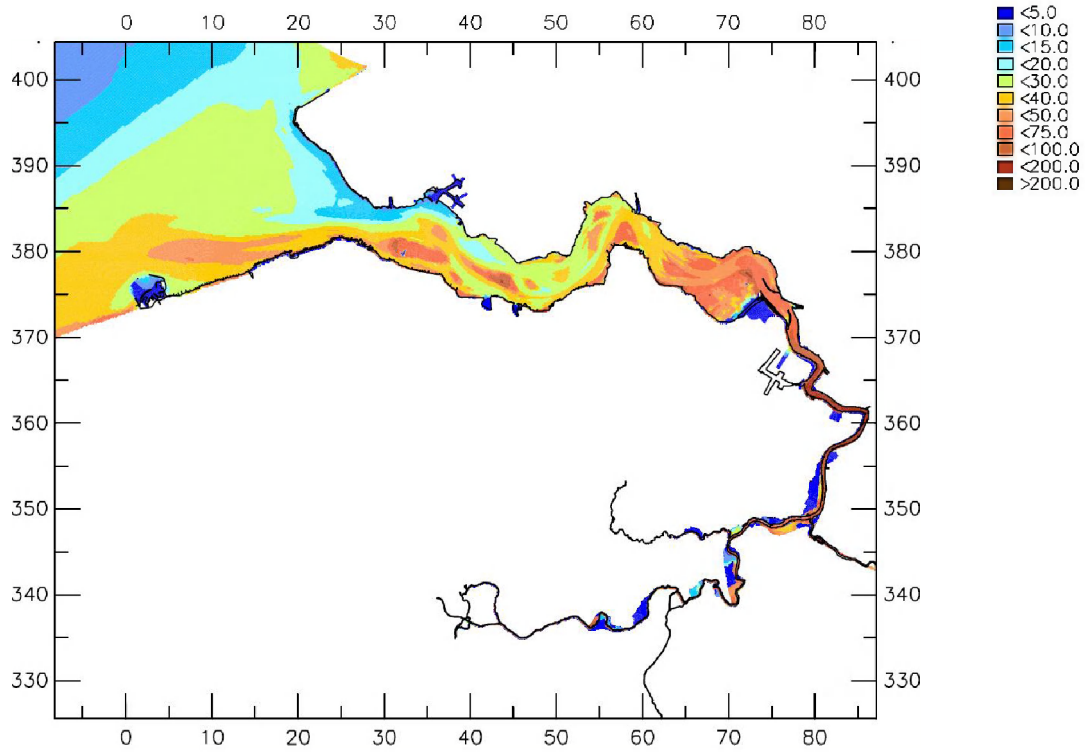

Fig. 4.9b: 14-day winter averaged SPM surface concentration (mg/l), new harbour settings and reduced dumping rate (ws24).

4.7 Effect of shipping traffic

A sensitivity analysis was made on the potential effect of shipping traffic on SPM concentration levels. To this order, two simulations were compared. The first simulation is without the effect of shipping traffic. In the second simulation the effect of shipping traffic was taken into account by increasing the bed shear stress of each grid cell with a value of $\Delta\tau$ Pa and with a probability p. A new draw was made every 15 min for a period of one day. Fig. B.7a in Appendix B-7 shows a typical example of the total bed shear stress including ship movements for $\Delta\tau = 0.5$ Pa and $p = 1\%$. Herein the effect of ships appears through the presence of points with enhanced bed shear stress. Fig. B.7b shows the resulting effect on SPM levels. It is concluded that for the applied settings ($\Delta\tau = 0.5$ Pa and $p = 1\%$) the effect of ship movements is substantial: near Terneuzen, the 14-day average SPM surface concentration increases from 15 to 23 mg/l. However, a more detailed and sophisticated analysis of the navigation density in the Scheldt and its influence on bed shear stress is required to draw more definitive conclusions. Notably, the applied 1% probability of influence of ship movement on the local bed shear stress may not be realistic.

4.8 Comparison between 3-month and 14-day hydrodynamics

Appendix B-8 shows results on a mud transport simulation based on a previous 3-month hydrodynamic period (Jan – Mar 2000). The hydrodynamics used for this simulation (Run11) are described in Van Kessel et *al.* (2007). The figures in Appendix B-8 should be compared with those in Appendix B-4 with variable waves (ws21). Observations based on these model results are:

- Although a number of differences is observed, the results (SPM concentrations) of the simulations do not strongly differ from those based on a 14-day hydrodynamic database (*e.g.* compare Figs. B.8a with B.4b and Figs. B.8d with B.4d);
- The longshore residual mud flux along the Belgian coast is much smaller than for the 14-day simulations. This must be caused by differences in the residual current, as the SPM concentration boundary condition was not changed. The residual currents are steered by the applied boundary conditions. Although the residual longshore flux is much smaller (and is now in much better agreement with other studies), typical SPM levels in the inner estuary do not differ strongly (compare Figs. B.8a with B.4b).
- Computed SPM levels agree quite well with observed levels, although the variability in the 3-month simulation is still smaller than in the available dataset at DOW-jetty. On an intertidal timescale, the computed variations agree well with observed variations.
- The first 3-month simulation does not yet have a good balance between harbour siltation and dredging (=dumping). As a result in the model a sediment surplus of 3.7 MT/y is entering the Scheldt estuary. Part of this material accretes inside the estuary on tidal flats (0.9 MT/y), but most is exported towards the North Sea (2.8 MT/y). This aspects needs attention prior to application of the model for managerial issues.

In chapter 3 of the present report modifications to the hydrodynamic model have been described resulting in an improvement of the reproduction of the tidal amplitude within the estuary. Section 4.9 presents results of the simulations with the mud transport model if use is made of the improved hydrodynamics.

4.9 Validation with improved 3-month hydrodynamics

The hydrodynamic model was modified with respect to the following aspects (see also chapter 3):

- A new set of boundary conditions lowered the M2-amplitude at the downstream boundary;
- The fresh water inflow from the "Bathse Spuikanaal" was included in the fresh water discharge;
- The high fresh water inflow early March was modelled with more data points in the time series.

Subsequently, the mud transport model was run for a 3-month hydrodynamic period (Jan. – March 2000) with the modified hydrodynamics as described above (i.e. run T13 of the hydrodynamic model). Results are analysed in Section 4.9.1 with respect to the reproduction of mud dynamics on the overall scale of the estuary. Section 4.9.2 presents in more detail a

comparison between observed and simulated SPM-concentrations at DOW-jetty near Terneuzen. Results of a modified dredging and dumping methodology, as used in the model, are shown in Section 4.9.3. Note that the time axes of the figures on the SPM variation in time shows mid-April to mid-July 1900. This is caused by a reset of the reference time during the coupling between SIMONA and WAQ. These axes should read January – March 2000.

4.9.1 Comparison with previous 3-month hydrodynamics

Results of the mud transport simulation with improved hydrodynamics are shown in Appendix B-9.1 (run q06). They are compared with results of run q05a, also given in Appendix B, which still makes use of the original hydrodynamics as described by Van Kessel et al. (2007)[1]. The implications of changed hydrodynamics on mud transport are as follows:

- SPM-concentrations have become lower due to the reduced M2-amplitude of the vertical tide. Apparently, less sediment is being resuspended from the bed into the water column. Differences are in the order of 10 mg/l, which follows from (i) the horizontal distribution of the tide-averaged concentrations in the surface layer (Fig. B.9.1b vs. Fig. B.9.1a), (ii) the vertical distribution of the tide-averaged concentrations along the estuary (Fig. B.9.1f vs. Fig. B.9.1e) and (iii) the time series of SPM-concentrations in Doel, Zuidergat, Honte and Wielingen (Fig. B.9.1h vs. Fig. B.9.1g) and at DOW-jetty Terneuzen (Fig. B.9.1j vs. Fig. B.9.1i).
- The net export from the Western Scheldt to the North Sea has reduced with about 40% to 2.9 Mt/y (compare Fig. B.9.1l with Fig. B.9.1k). However, this should be interpreted with care, because during the 3-month balance period with reduced tidal forcing (q06) significant net deposition in the seaward part of the Western Scheldt occurs. This weakens the net mud export towards the North Sea.
- The reproduction of the observed concentrations at Terneuzen DOW-jetty has not changed much (Fig. B.9.1i vs. Fig. B.8e).
- Similar to the first 3-month run this simulation does not have a good balance between harbour siltation and dredging (=dumping). As a result, a sediment surplus of 4.8 MT/y is entering the Scheldt estuary in the model.

4.9.2 Validation with observations at DOW-jetty Terneuzen

Results of the mud transport simulation are shown in Appendix B-9.2 (run q10). Model results on sediment concentrations are compared with observations at DOW-jetty near Terneuzen at three different levels: NAP-4m (model: layer 1), NAP-11m (model: layer 2) and NAP-17m (model: layer 4). The suspended sediment concentrations computed by the model are the sum of both the marine and the fluvial fractions. Time series of suspended sediment concentrations are given in Fig. B.9.2a (full three months of the simulation), Fig.

1. Run q03 as presented in Section 4.8 and run q05a, both with the previous 3-month hydrodynamics, have slightly different parameter settings for the mud properties. This explains why q06 (new hydrodynamics) and q05a are compared to assess the effect of changed hydrodynamics on mud transport; parameter values for these runs are similar.

B.9.2b (neap-spring period of 15 days), Fig. B.9.2c (25 hours during neap tide) and Fig. B.9.2d (25 hours during spring tide). The water depth near Terneuzen during these periods is shown in Fig. B.9.2e and is used for analysis purposes, i.e. to indicate the periods of ebb and flood. It is not at the exact location of DOW-jetty, which explains that the water depth is less than the depths of the sensors for suspended sediment concentrations.

For both marine and fluvial mud a settling velocity of 1 mm/s and a zeroth order resuspension parameter of 1 10^{-4} kg/m^2/s have been applied.

Comparison of the observed suspended sediment concentrations with model results for the full simulation period of three months shows (see Fig. B.9.2a) that in general the magnitude of concentrations is adequately reproduced. This especially holds for the upper level (NAP-4m) and lower level (NAP-17m). At NAP-11m observations are only available for a limited period of time during which the model partly overestimates observed concentrations by about 25 mg/l (during this period concentrations at NAP-4m and NAP-17m are also too high in the model). Variations of suspended sediment concentrations are in phase with variations in the magnitude of the tidal amplitude during the neap-spring tidal cycle. Maximum concentrations are observed during spring tide and minimum concentrations during neap tide, showing the implications of tidal forcing on erosion. Furthermore, observed concentrations appear to be somewhat greater near the bed with a stronger variation during the tide as compared with concentrations at mid depth and near the surface. Both phenomena, greater concentrations and variations near the bed, are reproduced by the mud transport model.

From one selected neap-spring tidal cycle it follows (see Fig. B.9.2b) that on the time scale of 15 days the *variation* of tide-averaged suspended sediment concentrations is more pronounced in the model than according to observations. However, the observed intra-tidal variation is larger for than the modelled intra-tidal variation.

On an intra-tidal time scale of 12.5 hours suspended sediment behaviour is primarily governed by local settling during slack water and local erosion during maximum ebb and maximum flood flow. Concentrations at DOW-jetty are also affected by advection of mud from locations nearby. During neap tide (see Fig. B.9.2c) peaks in the observed concentrations near the surface occur at high water slack, *i.e.* 1-2 hours following high water (for moments of high and low water see Fig. B.9.2e). These concentration peaks, which are not clearly present in the time series at NAP-11 m and NAP-17 m, are possibly the result of resuspension during high water of possibly a very fine sediment fraction at the shallow areas. This phenomena is however not reproduced by the model because that would require more fractions of sediment to be taken into account. Observed concentrations near the bed at NAP-17m show a sharp increase during the first low water and to a lesser extent during the second low water. This may result from settling of sediment from the upper to the lower layers, although one would expect a simultaneous decrease of concentration in the upper layers. During rising tide observed and computed sediment concentrations decrease near the surface as well as near the bed. Apparently this results from advection of relatively sediment-poor water from regions downstream of DOW-jetty. Finally, the model shows an increase of suspended sediment concentrations during maximum ebb flow, which results from erosion either locally or upstream and/or increased vertical mixing. The observations do not show such behaviour.

Analysis of the observed and modelled sediment dynamics during spring tide (see Fig. B.9.2d) also displays an increase of suspended sediment concentrations near the surface at high water slack. Unlike neap tide conditions no concentration increase near the bed is observed during low water. During rising tide measurements indicate a decrease in sediment concentrations near the surface and near the bed (not at mid depth). This is similar to what is observed and computed during neap tide. Model results for spring tide conditions do not show such a trend, which is probably due to erosion of the bed as induced by the stronger tidal forcing. A distinct behaviour of the model is shown by the concentration peaks near the bed during high and low water slack, which is not present in by the observations. Apparently, settling and subsequent accumulation of sediment near the bed is too pronounced in the model.

The detailed description above is summarised as follows:

- Observed levels of suspended sediment concentrations at DOW-jetty between approximately 25 and 200 mg/l are adequately reproduced by the mud transport model. This is the result of the calibration by means of the settling velocity and the resuspension parameter.
- Variation of concentrations on the time scale of subsequent neap–spring tidal cycles is governed by the magnitude of the tidal forcing; greatest concentrations occur during spring tide whereas concentrations during neap tide are less. This is the result of increased erosion rates during spring tides as compared with neap tides. The model reproduces this phenomenon well although concentrations during subsequent spring and neap tides show somewhat greater differences than observed.
- During high water observed peaks in the suspended sediment concentrations may be the result of additional resuspension of very fine-grained sediment present at the shallow areas. These concentration peaks during high water are not reproduced by the model. It may require the inclusion of a very fine-grained sediment fraction and more detailed modelling of sediment dynamics at the intertidal areas.
- It seems that during spring tide the predicted erosion by the model is too pronounced at maximum ebb and flood flow. In addition, settling during slack water in the model results in concentration peaks near the bed. These peaks are absent in the available data set at DOW-jetty. Both phenomena suggest that the magnitude of the vertical sediment fluxes should be reduced in the model. This can be realised by decreasing the settling velocity as well as the resuspension parameter in such a way that the average concentration level remains unchanged. However, a significant reduction of the settling velocity will result in too weak vertical concentration gradients compared to observations.
- Although the magnitude of suspended sediment concentrations and the variation on a time scale of several spring-neap tidal cycles are reproduced by the model, differences remain between observations and model results on the time scale less than one tidal cycle. This has implications for the reproduction of the magnitude as well as the direction (seaward or landward) of the tide-averaged sediment transport.
- Comparison of model results with field data has been focused on one location. In future a more spatial approach is recommended, where for instance satellite data and model output as presented in Fig. B.9.2f is mutually compared. Figures B.9.2f, B.9.2g and B.9.2h are presented in Appendix B as a reference for the simulation with the modified dredging and dumping methodology to be discussed in Section 4.9.3. Figs. B.9.2g

(showing mud percentage in bed) and B.9.2h (showing fraction of marine mud) are compared with field observations in Figs. 4.10 and 4.11, demonstrating that the mud model reproduces the observed spatial distribution of mud in the seabed reasonably well, both regarding the quantity (mud fraction) and quality (marine or fluvial). It is stressed that this distribution is not imposed by the user as initial conditions, but computed by the mud model starting with a uniform mud distribution or even an empty bed.

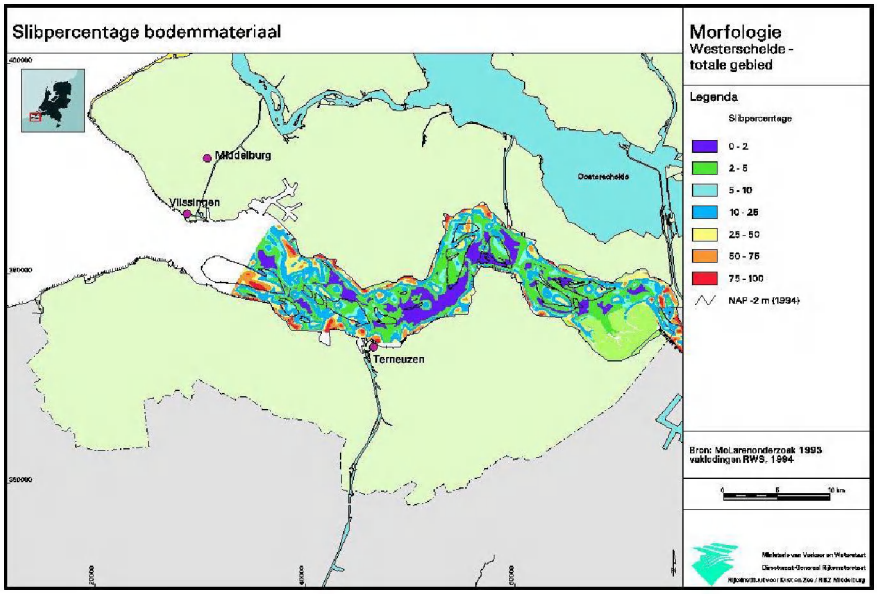

a)

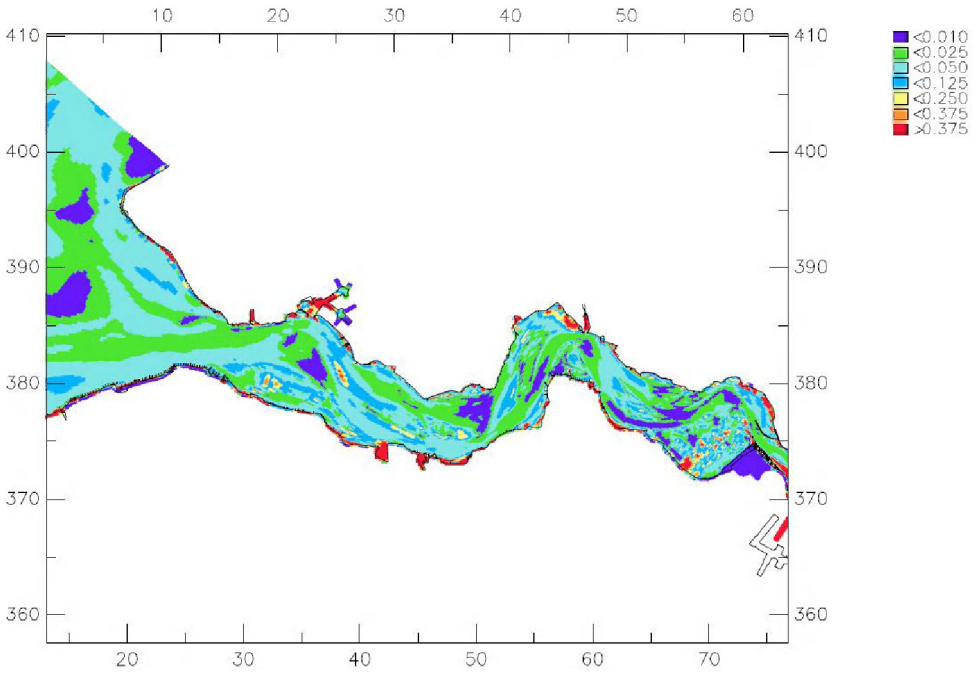

b)

Fig. 4.10: Observed (a) and modelled (b) mud fraction in the bed.

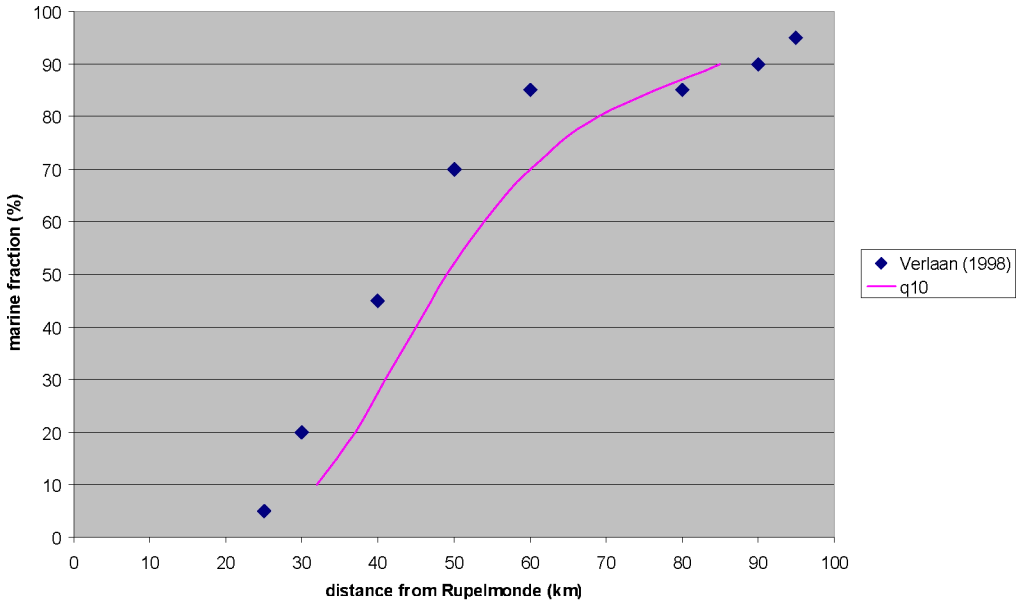

Fig. 4.11: Observed (Verlaan, 1998) and modelled mud origin (fluvial or marine) along the estuary.

Figure B.9.2i shows computed surface concentrations at four stations along the Scheldt estuary: Doel near the Dutch-Belgium border, Zuidergat, Honte and Wielingen. Observed mean levels are indicated with horizontal lines. The 10-percentile level (blue line) and 90-percentile level (dashed black line) enclose the observed range in suspended sediment concentrations. Furthermore mean summer and mean winter levels are given with green and red horizontal lines; the simulated period from January-March reflects winter conditions[2]. At Doel the variation of suspended sediment concentrations between the 10- and 90-percentile levels is reproduced by the model. The computed mean suspended sediment concentrations are between observed mean levels for winter and summer conditions. The variation of suspended sediment concentrations at Zuidergat appears to be underestimated although the computed average concentration is between mean levels for summer and winter conditions. The variation of concentrations at Honte is too large in the model whereas at Wielingen the agreement between measurements and computed values is reasonable. In the latter case the model concentrations appear to decrease gradually.

The mud balance for the Scheldt-estuary is shown in Fig. B.9.2j. Similar to Table 4.1 the net sedimentation in harbours according to the model and the total volume of dumped material in the model, as based on field data, are given in Table 4.2.

Location	siltation (kT/y)		dumping (kT/y)	
		q10		q10
Zeebrugge + Western Scheldt		3551		5556
Sea Scheldt		1660		2120
TOTAL		5211		7676

Table 4.2 Siltation and dumping rates for validation run (q10).

For simulation q10, harbour siltation amounts to 5.2 MT/y, whereas sediment dumping amounts to 7.7 MT/y (number based on dumping permits). Note that the automated dredging and dumping module has not been used for simulation q10.

Fig. B.9.2j also shows that 5.5 MT/y of mud is exported from the Western Scheldt to the North Sea. The export is exaggerated as 2.5 MT/y of sediment originating from the harbour of Zeebrugge is dumped in the Western Scheldt close to the boundary separating the estuary from the North Sea. Therefore, the net export amounts 3.0 MT/y rather than 5.5 MT/y.

According to Verlaan (1998) the amount of mud entering at the mouth of the estuary is unknown; estimated values range from 0.05 to 0.35 MT/y. The net transport is the difference between a large sediment flux in ebb direction and a large sediment flux in flood direction. Assuming a characteristic suspended sediment concentration of 50 mg/l and a flood and ebb volume of 2 10^9 m^3 in a reach in the estuary mouth (approximately 15 km west of Vlissingen) the annual sediment flux in both directions is in the order of 70 MT/y. If tidal asymmetry increases the total transport in ebb direction by only 10% an export of 7 MT/y follows, showing the sensitivity of the net transport to the asymmetry of the tide. Dronkers (2005), amongst others, discusses various conditions for net import or net export of fine sediment such as maximum currents during ebb and flood, the duration of high water slack versus low water slack, presence of waves etc. For specific characteristics of the bathymetry, such as intertidal area relative to total area, channel depth compared to tidal range, tidal asymmetry results in an export or import of fine sediment.

From this simulation, two conclusions can be drawn:

1. Modelled siltation rates agree reasonably well with observed siltation rates. As the observed siltation rates vary considerably in time and also include coarser material (this has been taken into account, but the sand fraction is not always measured, but sometimes estimated), a perfect agreement between the computed and estimated siltation (based on dredged volume) would be coincidental. The computed volume is 2/3 of the estimated volume, which may be considered as satisfactory.
2. The surplus of dumping with respect to siltation is 2.5 MT/y, most of which is exported from the Scheldt estuary towards the North Sea. Although this residual flux is quite small compared to instantaneous sediment fluxes, it has a major influence on the overall long-term mud balance.

4.9.3 Modified dredging and dumping methodology in the model

If dredging of harbours is not accounted for in the model then these areas along the estuary will act as a sink in the model, where accumulation of sediment occurs. In reality the harbours are dredged on a regular basis and on average the amount of dredged material equals net sedimentation. The dredged material is dumped at specific sites in the estuary and the material adds up to the suspended sediment concentration.

2. The figures show a time axis for the 3-month period between mid April-mid July. The reason is that the model results are shown for the latter 3-months of a 6-month simulation period, this to minimize the effects of the initial conditions.

Up to now dredging and dumping activities have been modelled by means of forcing functions derived from historic dredging data. In this way volumes of sediment were removed and added at specific dredging and dumping locations. However, the problem is that these removals and discharges are independent of the *actual* net sedimentation in the model. If the computed net sedimentation in the harbour is too large then dredging based on field data will be insufficient to remove all sediment from the harbour basins. On the long term net accumulation of sediment will occur so that the harbour acts as a sink for the mud transport in the estuary. This will result in computed suspended sediment concentrations in the estuary which are too low. Vice versa, if the computed net sedimentation in the harbour is too small then dredging based on field data results in too large dumping volumes. The harbours will be a source of sediment for the estuary while on average erosion due to dredging takes place within the harbour. Consequently, in the estuary suspended sediment concentrations will be too high.

To avoid these problems a new module was added to the mud transport model, which guarantees that the material removed from the harbours equals the computed net sedimentation. The module accounts for dredging of a harbour basin at a specific frequency and all material which exceeds a certain threshold in the thickness of the bed layer is removed from the water bed. Simultaneously, this material is added to the (water) concentration of the model at a specific dumping location within the estuary with a specified rate representative for the actual dredging. The module can be used simultaneously for several harbour basins, each with there own threshold for dredging, frequency of dredging, dumping rate and dumping site.

A simulation was performed with the implemented dredging and dumping methodology as described above. Because this resulted in too low suspended sediment concentrations the settling velocity for both the marine and fluvial sediment fraction was reduced from 1 mm/s to 0.75 mm/s while the resuspension parameter was increased from 1 10^{-4} kg/m^2/s to 2 10^{-4} kg/m^2/s. The time series of suspended sediment concentrations at DOW-jetty, see Figures B.9.3a-d, indicate that observed concentrations are still underestimated by the model due to the lower dumping volumes. Computed concentrations gradually decrease which indicates that the model has not reached a dynamic equilibrium. See also Fig. B.9.3e for computed concentrations at Doel, Zuidergat, Honte and Wielingen showing a significant decrease of concentrations with time as compared with Fig. B.9.2i for validation run q10.

Table 4.3 shows the rate of siltation and dumping for two simulations with 2007 settings: simulation q10 with user-defined dumping rates (see also Section 4.9.2) and simulation q09 with the automated dredging module balancing dredging with siltation.

Location	siltation (kT/y)		dumping (kT/y)	
	q09	q10	q09	q10
Zeebrugge + Western Scheldt	2995	3551	3173	5556
Sea Scheldt	719	1660	741	2120
TOTAL	3714	5211	3914	7676

Table 4.3 Siltation and dumping rates for run with modified dredging and dumping methodology (q09) compared with validation run (q10).

For simulation q10, harbour siltation amounts to 5.2 MT/y, whereas sediment dumping amounts to 7.7 MT/y. For simulation q09, the difference between harbour siltation and sediment dumping is only 5%. The computed harbour siltation is 3.7 MT/y, whereas sediment dumping amounts to 3.9 MT/y. The small difference may be explained by the presence of older deposits in harbour basins and the limited duration of the simulation (3 months). The equilibrium aimed at is realised indeed with the automated dredging module developed for Delwaq. However, typical concentration levels in the Scheldt estuary are significantly reduced to levels well below observed levels (see Figs. B.9.3a and B.9.3e, notably towards the end of the 3 month simulation period), down to a SPM concentration level that results in long-term mud balance with 2.5 MT/y less export from the Scheldt estuary towards the North Sea or, to a lesser extent, accumulation on mudflats.

The computed net harbour siltation of 3.7 MT/y for the simulation with the automated dredging module (run q09) is approximately 50% of observed dredge volumes. Similar remarks can be made as given earlier in Section 4.9.2: the observed siltation rates vary considerably in time and also include coarser material. The total volume of dredged mud is derived from the total dredged sediment volume using a sand fraction which is not always measured and thus sometimes estimated. Given these uncertainties the agreement between observed and computed maintenance dredge volumes can be considered as reasonable. However, more analysis is required on the modelled large export of SPM towards the North Sea.

5 Application to Dutch management issues

In Chapter 4 is was concluded that the mud transport model for the Scheldt in its present state of development meets most requirements defined at the start of the LTV-mud project:

1. global spatial concentration distribution (e.g. location of ETM's): mean Western Scheldt ca. 50 mg/l
2. intra-tide SPM concentration fluctuations: factor 2 to 5
3. neap/spring SPM concentration fluctuations: factor 1.5 to 2
4. vertical concentration gradients: factor 2 to 10
5. a proper overall mud balance, including a sensible mass of 'active' mud in the system
6. the spatial distribution of sandy and muddy areas (conform McLaren soil data)
7. seasonal SPM concentration fluctuations, including response time of freshwater discharge peaks and storms: factor 2
8. siltation rate of intertidal areas and salt marshes (order 1 – 2 cm/y), siltation rate in harbours (up to 1 cm/day)
9. ratio between fluvial and marine mud according to Verlaan (1998)
10. available mass of sediment (Van Maldegem, 1997):
    - 13 MT in the bed
    - 0.1 – 0.4 MT suspended
    - load from sea and upstream: 0.2 MT/y
    - load from dumping: 1.5 MT/y
11. long-term equilibrium between dumping from harbour maintenance and harbour siltation

Of these points, only point 5 in combination with point 11 does not yet meet the requirements. Also, point 7 has yet to be validated, as a full year hydrodynamic simulation has not yet been made.

Although a long-term equilibrium between harbour siltation and dumping (requirement 11) is automatically achieved with the new dredging module in Delwaq, this results in too low equilibrium SPM levels in the Scheldt estuary because of a net export of SPM in the order of 2 MT/y towards the North Sea, which is unrealistically high and therefore in violation of requirement 5. However, a surplus of dumping of about 2 MT/y in comparison with harbour siltation maintains the SPM concentration at realistic levels and may act temporarily as a 'quick fix'.

Notwithstanding, it is judged that the present model is fit for a first application for the support of managerial issues. The focus for 2007 with regard to these issues is on the sediment release of dredged material from the Sloe harbour near Vlissingen. Starting from present day's practice, how does the dredging volume and SPM concentration increase change as a function of release location or release frequency and rate? The location change may be both in longshore and cross-shore direction.

In total six simulations have been carried out to investigate the effect of various dumping locations on suspended sediment concentrations and harbour siltation:

- Reference simulation with a release of dredged material from the Sloe harbour in the Western Scheldt according to the present day`s practice (run q10).
- Dumping of dredged material at location Sloe (run q10Sloe);
- Dumping of dredged material 12 km East of the Sloe harbour (run q10O12km);
- Dumping of dredged material 6 km East of the Sloe harbour (run q10O6km);
- Dumping of dredged material 12 km West of the Sloe harbour (run q10W12km);
- Dumping of dredged material 6 km West of the Sloe harbour (run q10W6km).

The values for the settling velocity and resuspension parameter of both mud fractions are identical to those of calibration run q10. The sediment load from Sloe harbour released in the model is 638 kT/y (fines only).

The original locations for dumping of sediment originating from the harbour of Vlissingen are given in Fig. 5.1. The new dumping locations for the subsequent five runs are presented in Fig. 5.2.

The total net sedimentation in the harbour of Vlissingen is summarised in Table 5.1. Differences between the suspended sediment concentrations as computed for the relocated dumping locations according to Fig. 5.2 and the original locations according to Fig. 5.1 are given in Fig. B.11a-c in App. B.

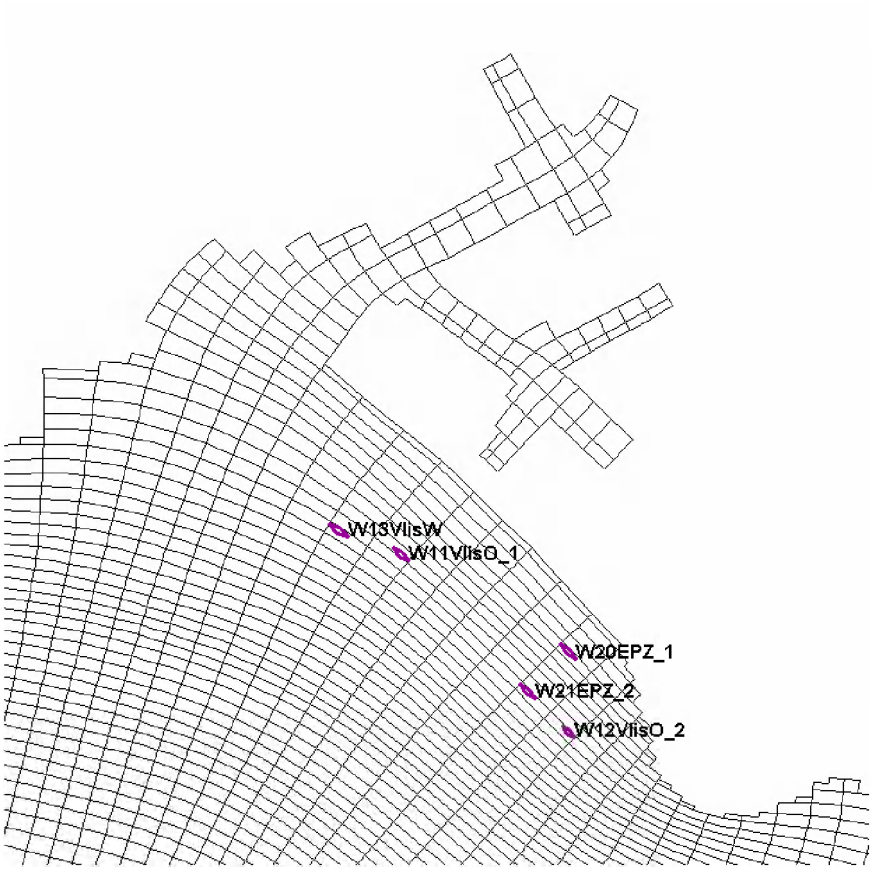

Fig. 5.1: Original dumping locations for run q10.

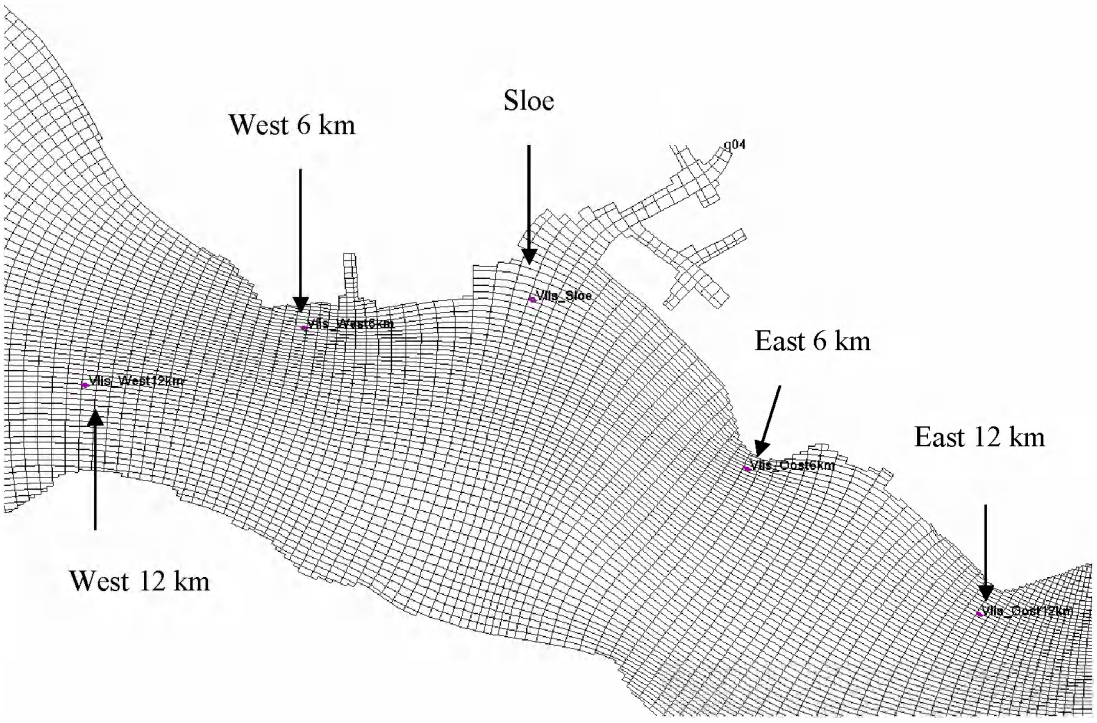

Fig. 5.2: New dumping locations

Location	harbour siltation (kT/y)					
Vlissingen	**q10**	**12 km W**	**6 km W**	**Sloe**	**6 km E**	**12 km E**
Absolute:	480.5	449.4	477.0	491.1	481.9	475.0
Rel. difference	-	-6.5%	-0.7%	+2.2%	+0.3%	-1.1%

Table 5.1 Siltation in Vlissingen harbour for runs on release of dredged material from Vlissingen harbour in various locations (q10, q10O12km, q10O6km, q10W12km, q10W6km). Note: fines only.

From Table 5.1 and Figs. B.11a-c the sensitivity of both harbour siltation and SPM levels to the location of sediment release can be determined. Typical changes in SPM levels are a few mg/l, or less than 10% of the background concentration. A shift of the release location to the west results in a concentration reduction in the east and vice versa. Harbour siltation is reduced for release locations farther from the harbour mouth. A shift to the west results in a stronger siltation reduction in Sloe harbour than an equal shift to the east (6.5 and 1.1% reduction a 12 km shift, respectively). A release location west of the harbour mouth tends to be more favourable as more sediment is transported towards the North Sea. Furthermore, dumping farther away from the estuary banks may have reduced the return transport to the harbour for location West 12 km.

The computed changes in SPM levels and siltation rate are quite small with respect to the natural variability of SPM levels and the accuracy of the dredging volumes. However, as the simulations are mutually compared, the computed *changes* in SPM levels and siltation rate are significant. Typically, the computed changes are quite insensitive to changes in model settings (within reasonable limits).

A cost-benefit analysis could reveal the optimal distance for sediment release from an economical point of view. However, from an ecological point of view the optimal release location may be located elsewhere.

In this analysis, only the fine sediment release from Sloe harbour is considered, which amounts to approximately 10% of the total fine sediment release at Zeebrugge, Antwerp and in the Western Scheldt combined. If other release locations are changed as well, the combined impact on the SPM distribution is expected to increase.

6 Conclusions and recommendations

6.1 Conclusions

At a technical level, all model improvements scheduled for 2007 have been implemented. The most important developments are: longer hydrodynamic simulation period (3 month), more accurate concentration boundary conditions, variable wave effects and biological effects. Based on first results the following conclusions are drawn.

6.1.1 On hydrodynamics

In this report three actions have been identified to improve the reproduction of the observed hydrodynamics by the model:

- The high fresh water inflow event in the beginning of March has been modelled more accurately by adding locally more data points in the time series of fresh water inflow in order to increase the volume of fresh water contained in the peak.
- Furthermore, the time series of fresh water inflow of the Bathse Spuikanaal was included in the model.
- Finally, a different set of boundary conditions, consisting of a combination of water levels and velocities obtained from the ZUNO-model improved the reproduction of water levels in the estuary.

The following conclusions on hydrodynamics are drawn:

1. Tidal analysis of modelled and predicted water levels shows that the amplitude of the tidal signal is predicted well throughout the modelling domain. There is probably a 5° phase lag of M2 and a 10° phase lag of M4 in the boundary condition. In the current modelling set-up, the boundaries are read-in as time series out of a larger model (ZUNO) which makes phase corrections of separate harmonic components a tedious task.
2. Upstream Antwerp the model predicts a drop in M2 and M4 amplitudes that is not represented in the measurements. This difference is considered important for possible future applications of the model in the region upstream of Antwerp (such as GOG's), and is under current investigation at WL Borgerhout.
3. Plots of horizontal components of the residual velocity vectors in the lowest layer show a convergent pattern close to the mouth of the estuary, and between Deurganckdok and Kallo sluice. At these locations the measurements show enhanced SPM concentrations.

6.1.2 On mud transport

In this report a number of improvements to the mud transport model have been investigated, following the recommendations from the previous phase of the LTV project (Van Kessel et al., 2006). The following conclusions on mud transport are drawn:

4. A minor shift of two dumping locations near Antwerp improves significantly the proper modelling of the estuarine turbidity maximum (ETM).
5. New concentration boundary conditions at sea based on SeaWiFs satellite images result in more realistic SPM concentrations at sea and more realistic longshore SPM fluxes. The turbidity maximum near Zeebrugge is well reproduced.
6. The difference between simulations with 5 and 10 horizontal layers is minor.
7. Variable waves temporarily enhance the SPM concentration in the western part of the Western Scheldt during storms. Towards Antwerp, the computed SPM time series are tide-dominated, but higher concentrations may occur after storms by advection from sea direction.
8. With biological settings taken from a Wadden Sea model, the biological impact on large-scale SPM concentrations in the Scheldt estuary appears to be minor. However, locally the SPM concentration and mud content of the bed can be affected significantly.
9. The SPM levels appear to be rather sensitive to the cycle of harbour siltation and dumping. Net sedimentation in the harbours is computed by the model, whereas dumping of dredged material from harbours is based on actual data. An unbalance between both quantities introduces an artificial withdrawal or discharge of sediment affecting computed suspended sediment concentrations. Therefore this aspect should be an integral part of model calibration to prevent that adjustment of model parameters are biased by the inclusion of inconsistent dumping loads due to harbour siltation.
10. A first sensitivity analysis suggests that shipping traffic may have a significant impact on SPM levels in the Scheldt estuary, but a more detailed analysis of actual ship movements in the Scheldt and their influence on the bed shear stress is required to prove this.
11. A mud transport simulation based on a 3-month instead of a 14-day hydrodynamic period results in a number of changes, but still does show a similar behaviour and does not lead to strongly different results on SPM concentrations. Computed alongshore SPM fluxes are in better agreement with values found in literature.
12. The 3-month simulation with improved hydrodynamics results in suspended sediment concentrations, which are decreased by approximately 10 mg/l as compared with the original 3-month run. This is mainly caused by the reduced tidal forcing resulting from the modification of the boundary conditions at the seaward model boundaries.
13. Validation of the mud transport model against observed suspended sediment concentrations at DOW-jetty results in the following conclusions:
    - Levels of suspended sediment concentrations at DOW-jetty between approximately 25 and 200 mg/l are adequately reproduced by the mud transport model. This is accomplished by means of adjustment of the settling velocity and the resuspension parameter.
    - Variation of concentrations on the time scale of subsequent neap–spring tidal cycles is governed by the magnitude of the tidal forcing; greatest concentrations occur during spring tide whereas concentrations during neap tide are less. This is the result of increased erosion rates during spring tides as compared with neap tides. The

model reproduces this phenomena well although the observed concentration fluctuation during a tidal cycle is somewhat greater.

- During high water observed peaks in the suspended sediment concentrations may be the result of additional resuspension of very fine-grained sediment present at the shallow areas. These concentration peaks during high water are not reproduced by the model. It may require the inclusion of a very fine-grained sediment fraction and more detailed modelling of sediment dynamics at the intertidal areas.
- It appears that during spring tide erosion in the model is too pronounced during maximum ebb and flood flow. In addition, settling during slack water results in near-bed concentration peaks in the model. These peaks are absent in the available data set at DOW-jetty. Both phenomena suggest, that the magnitude of the vertical sediment fluxes should be reduced in the model by decreasing the settling velocity as well as the resuspension parameter in such a way that the average concentration level remains unchanged.
- Although the variation of suspended sediment concentrations on a time scale of subsequent spring-neap tidal cycles is reproduced by the model, differences between observations and model results on the time scale of one tidal cycle remain. This has implications for the reproduction of the magnitude as well as the direction (seaward or landward) of the tide-averaged sediment transport.
- The unbalance between net harbour siltation, as computed by the model, and dumping of dredged material according to field data amounts to 2.3 MT/y. Due to this unbalance mud is added to the model by means of artificial dumping which may enhance the export of mud.

14. Computed net sedimentation in the harbours along the Sea Scheldt and the Western Scheldt amounts to 2/3 of actual dredge volumes. This can be considered satisfactorily given the natural variability of total dredge volumes and uncertainties in the sand content of dredged material.
15. The net export as computed by the model for the validation run amounts to 3.0 MT/y if corrected for the dumping of harbour mud from Zeebrugge in the estuary mouth. This is about one order of magnitude larger than the net *import* following from mud balances. Exact figures from observations are unknown but estimates range from an import of 0.05 to 0.35 MT/y. However, mud balances based on observations involve large uncertainties. Nonetheless an import from the North Sea to the Western Scheldt is expected given the observed gradual accumulation of muddy sediment on tidal flats. It is known from literature that import or export of fine sediment depends on the asymmetry of the tide. Further investigation of conditions that relate to the tidal asymmetry is needed to explain the discrepancy between observations and model results.
16. The new dredging and dumping simulation methodology used by the model has almost balanced the computed dredging volumes from the harbours and the applied dumping volumes in the estuary. However, typical concentration levels in the Scheldt estuary are significantly reduced to levels well below observed levels, down to a SPM concentration level that results in long-term mud balance with 2.5 MT/y less export from the Scheldt estuary towards the North Sea.

6.1.3 On management issues

It is concluded that the sensitivity of both harbour siltation and SPM levels to the location of sediment release is limited. Typical changes in SPM levels are a few mg/l, or less than 10% of the background concentration. Harbour siltation is reduced for release locations farther from the harbour mouth. A release location west of the harbour mouth tends to be more favourable as more sediment is transported towards the North Sea, but also the distance of the release location from the estuary banks may play a part herein. A cost-benefit analysis could reveal the optimal distance for sediment release from an economical point of view. However, from an ecological point of view the optimal release location may be located elsewhere.

6.2 Recommendations for future research

The following recommendations are listed in order of suggested priority.

1. A major aspect that requires further research concerns the computed export of mud from the Western Scheldt to the North Sea. Although exact figures on the actual net sediment transport in the mouth of the estuary are not available it seems that computed values are one order of magnitude larger than estimates retrieved from mud balances. Net transport of sediment is intricately related to the asymmetry of the tide. Comparison of model results with (available) point measurements regarding flow velocity and suspended concentration of mud during a tidal cycle is recommended, to study in detail processes associated with tidal asymmetry and their effect on net sediment transport.
2. Simulations for longer periods (at least one year) are recommended to investigate the model behaviour on the long term, *i.e.* including seasonal fluctuations and its effect on computed net sediment transport from or to the North Sea. Also the present 3 month period can be analysed further, *e.g.* by analyzing the weekly and monthly variability of the residual sediment flux.
3. Further validation of the model by means of point measurements, as recommended above, should be combined with the use of satellite images of the Scheldt estuary to allow for a more spatial comparison between observed and computed suspended sediment concentrations.
4. The model can be made operational for turbidity modelling by inclusion of appropriate routines on light extinction thus broadening the scope of the model for application on ecological management issues. This may also require in addition of a very fine fraction. Such extension facilitates the application of the model for ecological modelling, which will also be a part of the LTV project in 2008.
5. Further comparison of the observed and computed ratio of marine and fluvial mud in the bed may give further information on the reproduction of the estuarine mixing processes by the model.
6. Further analysis of biological effects on mud transport is recommended. This includes the incorporation of more species than currently used and application of dedicated functions for the Scheldt estuary.
7. A more detailed and sophisticated analysis of the navigation density in the Scheldt and its influence on bed shear stress is required to draw more definitive conclusions on the effect of shipping traffic on suspended sediment concentrations. Notably, the applied 1%

probability of influence of ship movement on the local bed shear stress may not be realistic.

8. A number of fundamental processes on mud dynamics have not been included in the mud transport model. This holds for the settling velocity of mud flocs which is assumed to be constant in time but in reality depends on several factors such as turbulence, suspended sediment concentration, water and sediment properties. Furthermore, the sediment dynamics in the Scheldt estuary is also governed by the transport of sand. Interaction between the non-cohesive sand and cohesive mud, especially in the bed, is not yet accounted for by the present model. It implicitly requires the modelling of the consolidation process including effects on bed shear strength.

The model development will also benefit from ongoing application for the support of managerial issues. Detected strengths and weaknesses may also steer further developments and their prioritisation.

7 References

Aubrey, D.G., P.E. Speer, 1985, A study of non-linear tidal propagation in shallow inlet / estuarine systems, Part I: observations, Estuarine, Coastal and Shelf Science, Vol. 21, pp. 185-205.

Borsje, B.W., S.J.M.H Hulscher, M.B. de Vries, G.J. de Boer (2007). Modelling large scale cohesive sediment transport by including biological activity. *Submitted to:*

Bruens, A., J. Vanlede, T. van Kessel (2006). Notitie beheersvragen LTV-slibmodel. WL | Delft Hydraulics report Z4210.75 (in Dutch).

Chen, M.S., S. Wartel, S. Temmerman (2005). Seasonal variation of floc characteristics on tidal flats, the Scheldt estuary. *Hydrobiologia* 540, pp. 181–195.

Doxaran, D., P. Castaing, S.J. Lavender (2006). Monitoring the maximum turbidity zone and detecting fine-scale turbidity features in the Gironde estuary using high spatial resolution satellite sensor (SPT HRV, Landsat ETM+) data. *International Journal of Remote Sensing*, Vol. 27, No. 11, pp. 2303 – 2321.

Dronkers, Job (2005). Dynamics of coastal systems. Advanced Series on Ocean Engineering – Volume 25. World Scientific. ISBN 981-256-207-9.

Fettweis, M., Nechad, B. & Van den Eynde, D (2007). An estimate of the suspended particulate matter (SPM) transport in the southern North Sea using SeaWiFS images, in-situ measurements and numerical model results. Continental Shelf Research (submitted).

Jong, D.J. de, V.N. de Jonge (1995). Dynamics and distribution of microphytobenthic chlorophyll-a in the Western Scheldt estuary (SW Netherlands). *Hydrobiologia* 311, pp. 21–30.

Kessel, T. van, J. Vanlede, A. Bruens (2006). Development of a mud transport model for the Scheldt estuary in the framework of LTV. WL | Delft Hydraulics & WL Borgerhout report Z4210.

Kessel, T. van, J. Vanlede, J. de Kok (2007). Development of a mud transport model for the Scheldt estuary in the framework of LTV. Phase 1. WL | Delft Hydraulics & WL Borgerhout report Z4375..

McManus, J.P. and D. Prandle (1997). Development of a model to reproduce observed suspended sediment distributions in the North Sea using Principle Component Analysis and Multiple Linear Regression. Continental Shelf Research, Vol. 17, No. 7, pp. 761–778.

Smith and Bank (1975). Variation of the sea surface drag coefficient with wind speed. *Quart. J. Roy. Meteorol. Soc.* Vol. 101, pp. 665–673.

Suijlen, J.M. and Duin, R.N.M. (2001). Variability of near-surface total suspended matter concentrations in the Dutch coastal zone of the North Sea. Climatological study on the suspended mater concentrations in the North Sea. Report RIKZ/OS/2001.150X.

Verlaan, P.A.J. (1998). Mixing of marine and fluvial particles in the Scheldt estuary. Ph.D. thesis Delft University of Technology, The Netherlands.

Wang, Z.B., M.C.J.L. Jeuken, H. Gerritsen, H.J. de Vriend, B.A. Kornman, 2002, Morphology and asymmetry of the vertical tide in the Westerschelde estuary, Continental Shelf Research, 22, pp. 2599-2609.

Winterwerp, J.C. en De Kok, J. (2006). Plan van aanpak LTV-slib: modelinstrumentarium t.b.v. beheersproblematiek slib. Intern document no. Z4210.95 – M756/01.

A Figures on hydrodynamic model

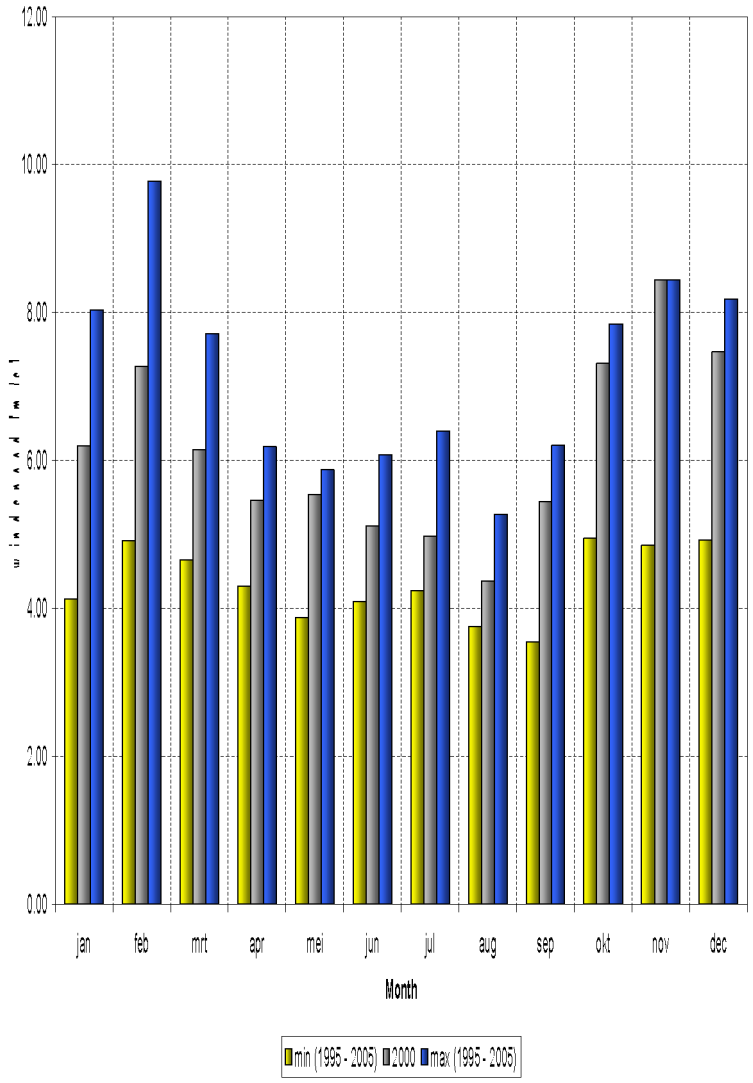

Figure A-1: Monthly averaged wind at Vlissingen	**M.756/02**
FLANDERS HYDRAULICS RESEARCH / DELFT HYDRAULICS	

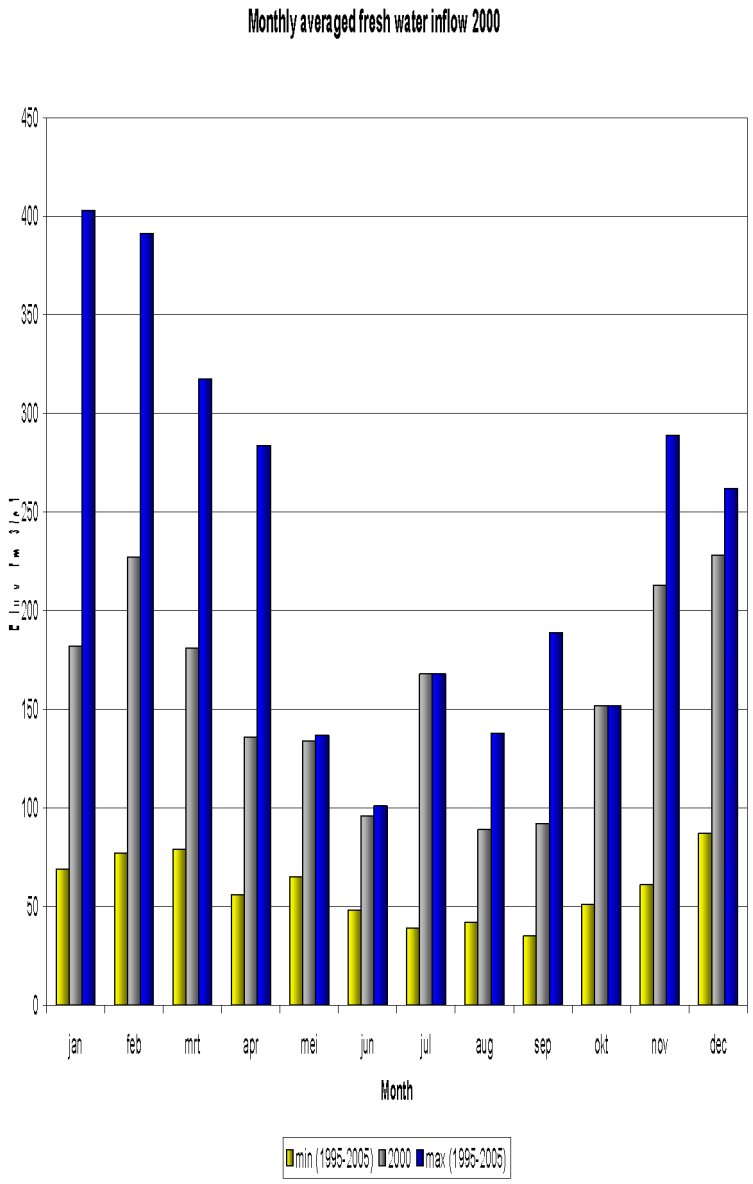

Figure A-2: Monthly averaged fresh water inflow	**M.756/02**
FLANDERS HYDRAULICS RESEARCH / DELFT HYDRAULICS	

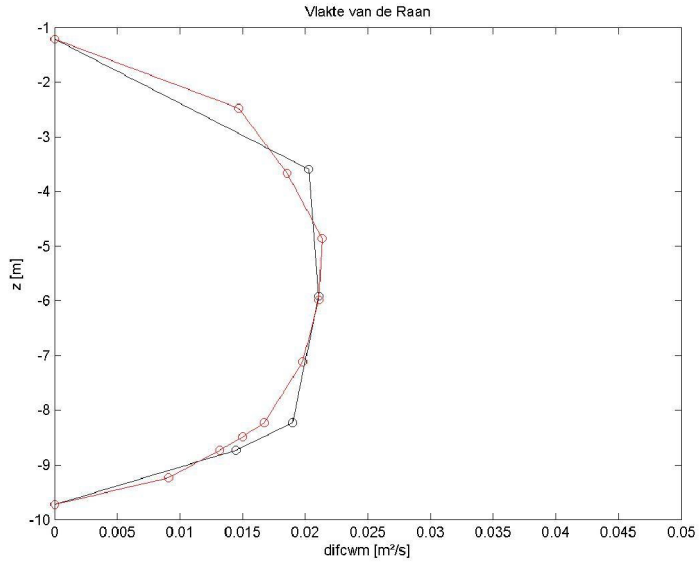

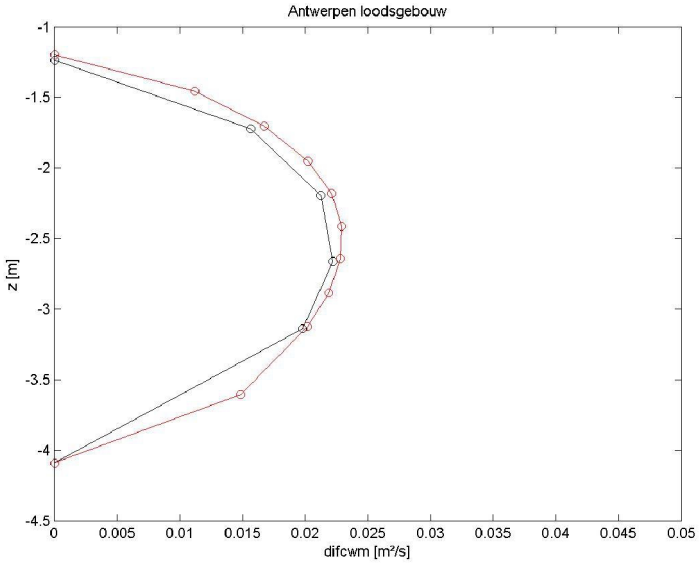

Figure A-3: Profiles of diffusivity: 5 layer model and 10 layer model	**M.756/02**
FLANDERS HYDRAULICS RESEARCH / DELFT HYDRAULICS	

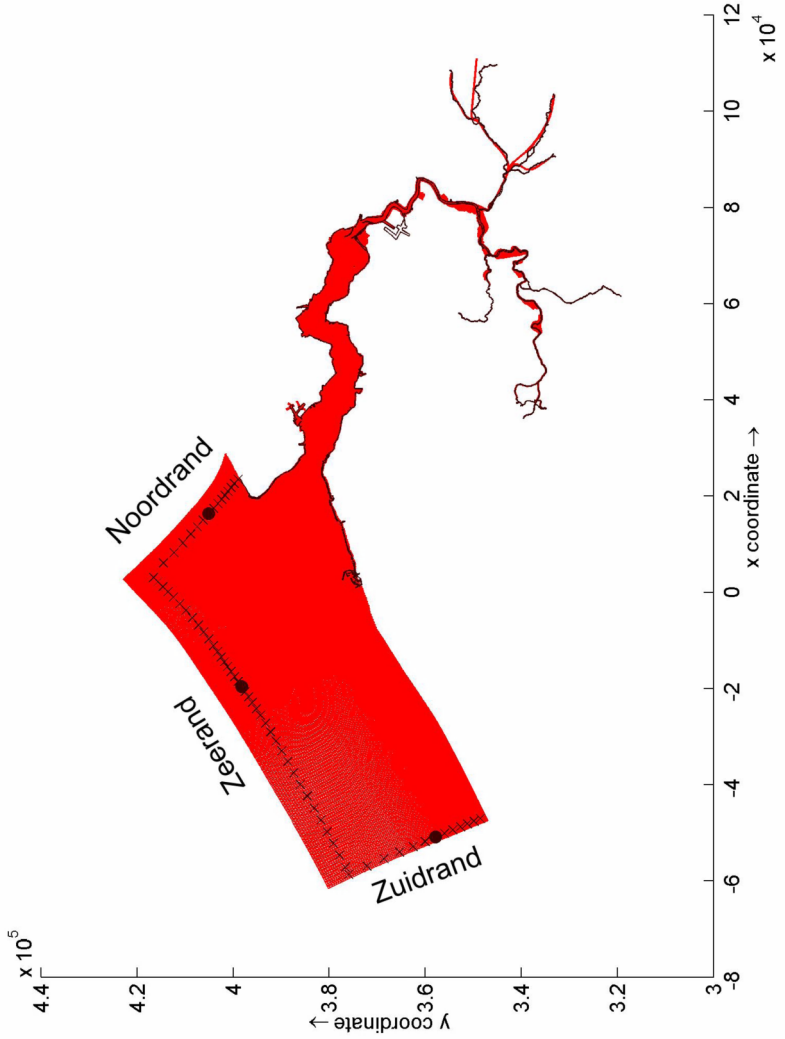

Figure A-4: Downstream boundaries of the model
"+" indicates the boundary of the 2007 model. The 2006 HD model covered the entire red area.

M.756/02

FLANDERS HYDRAULICS RESEARCH / DELFT HYDRAULICS

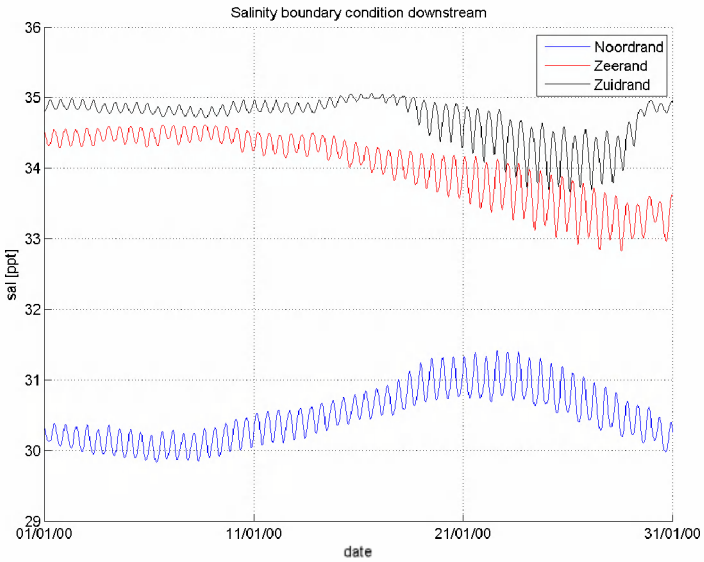

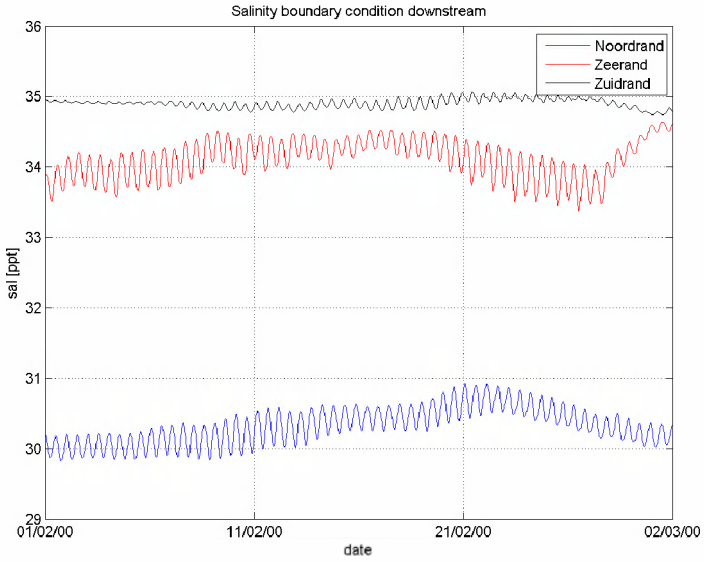

Figure A-5: Salinity boundary condition	**M.756/02**
FLANDERS HYDRAULICS RESEARCH / DELFT HYDRAULICS	

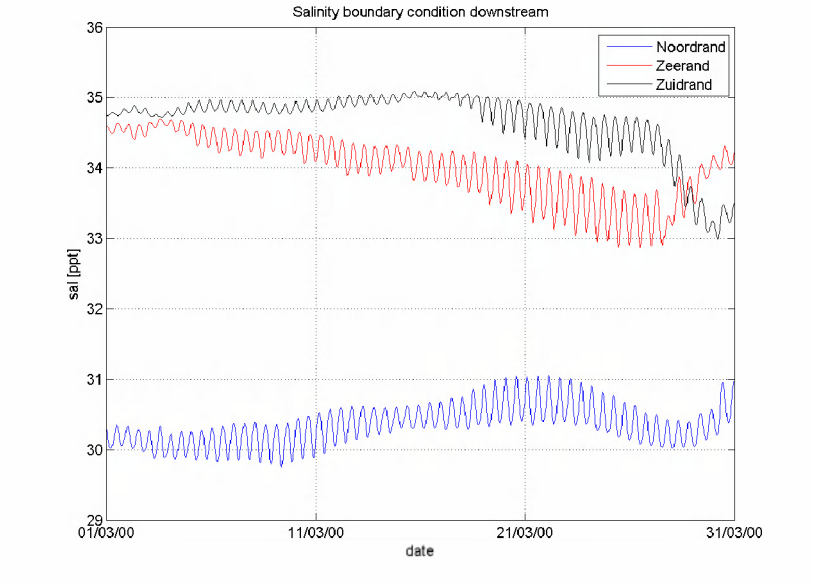

Figure A-6: Salinity boundary condition	**M.756/02**
FLANDERS HYDRAULICS RESEARCH / DELFT HYDRAULICS	

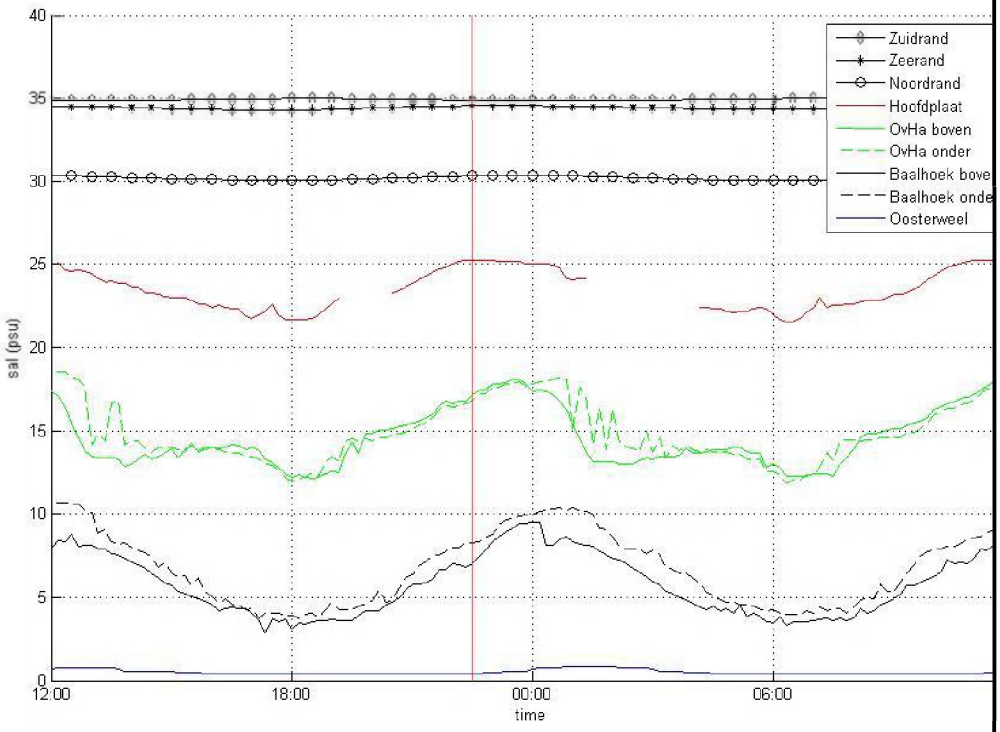

Figure A-7: Selection of initial salinity values	**M.756/02**	
FLANDERS HYDRAULICS RESEARCH / DELFT HYDRAULICS		

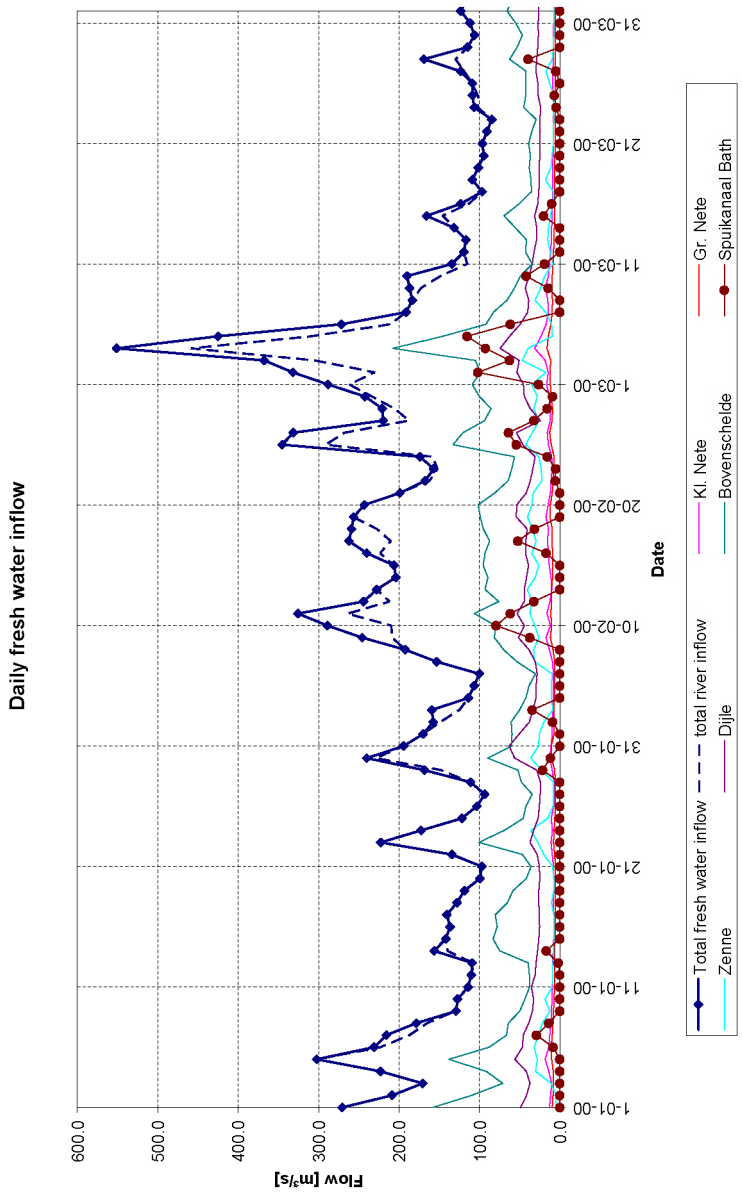

Figure A-8: Total daily fresh water inflow	**M.756/02**
FLANDERS HYDRAULICS RESEARCH / DELFT HYDRAULICS	

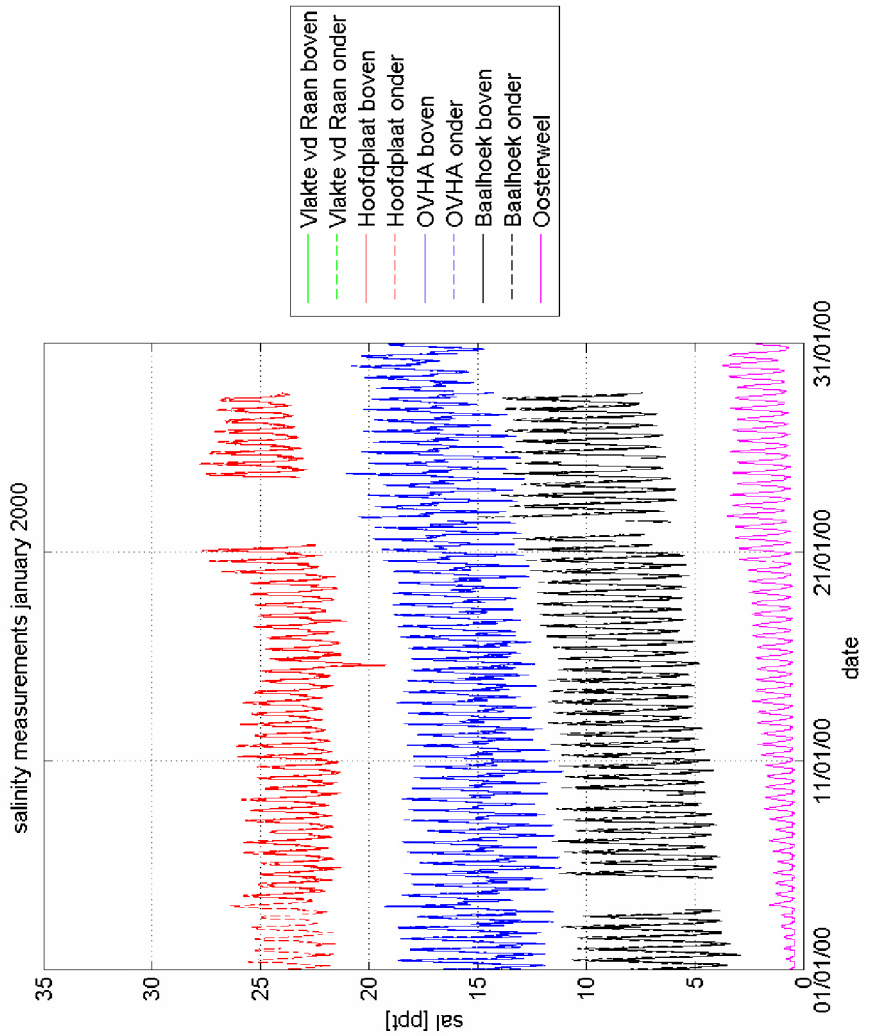

Figure A-9: Salinity measurements January

M.756/02

FLANDERS HYDRAULICS RESEARCH / DELFT HYDRAULICS

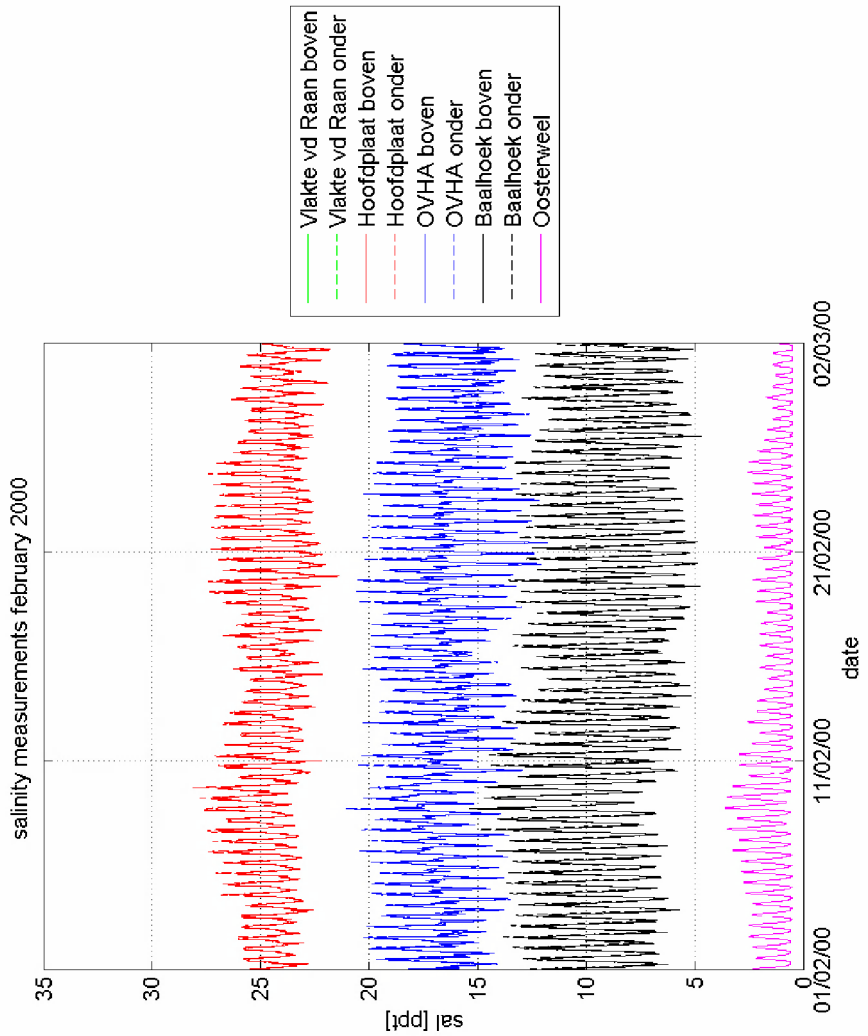

Figure A-10: Salinity measurements February	**M.756/02**
FLANDERS HYDRAULICS RESEARCH / DELFT HYDRAULICS	

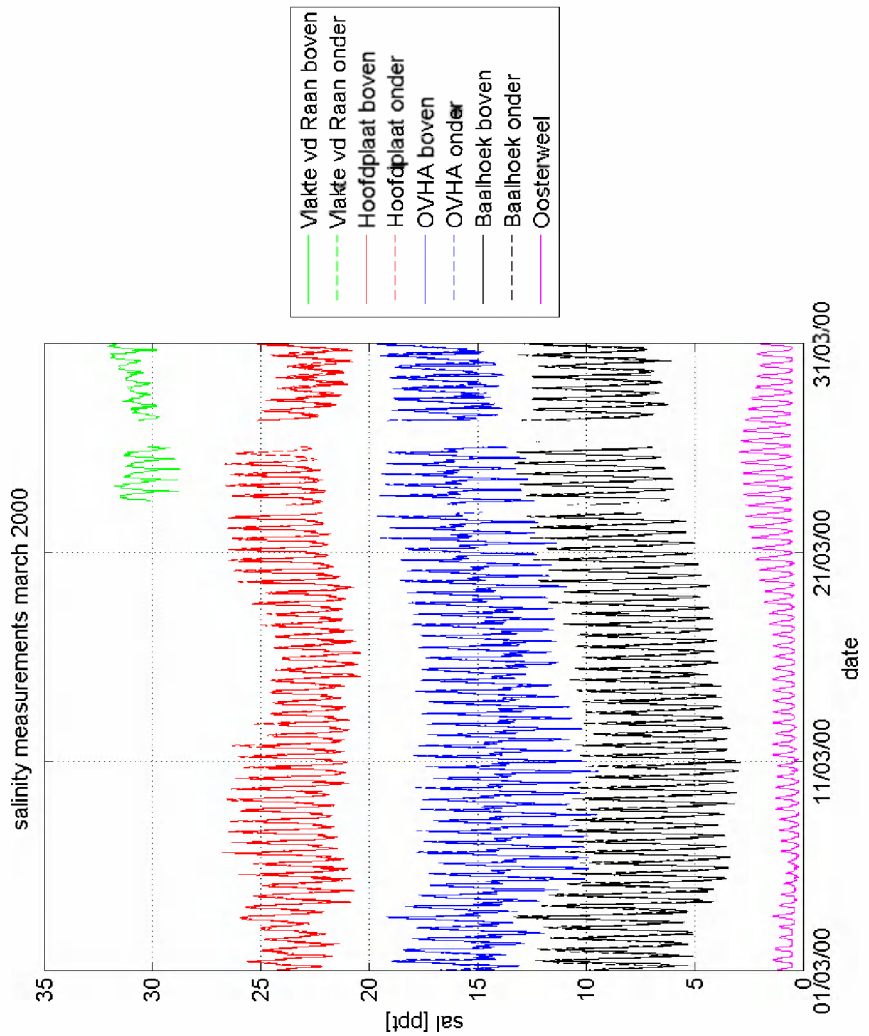

Figure A-11: Salinity measurements March	**M.756/02**
FLANDERS HYDRAULICS RESEARCH / DELFT HYDRAULICS	

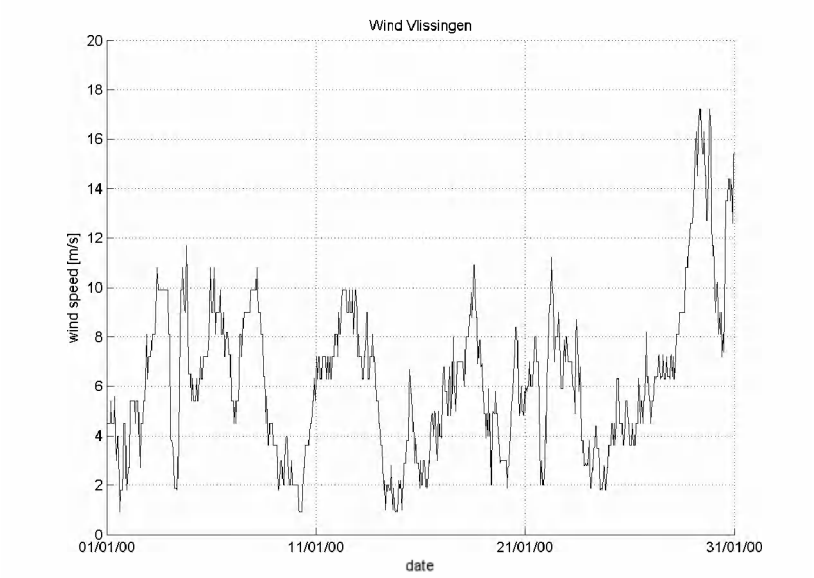

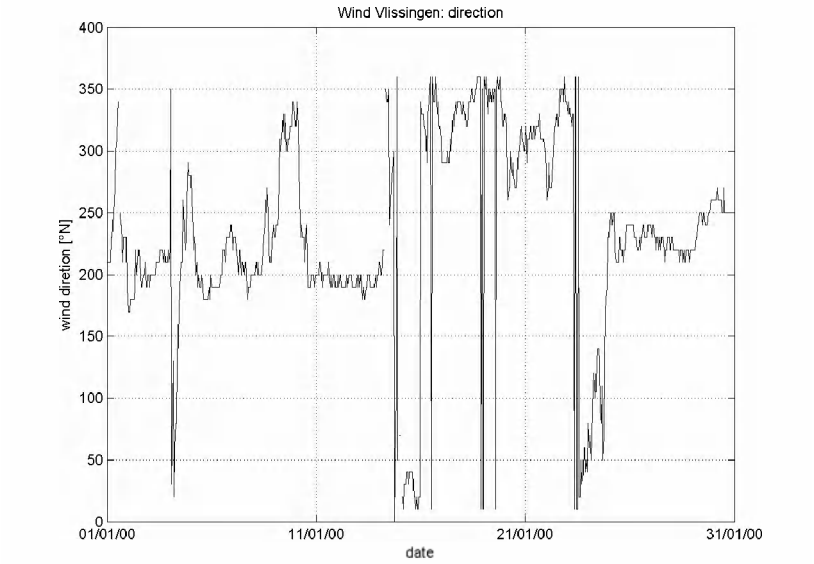

Figure A-12: Wind Vlissingen January
10 minute mean windspeed (top) and direction (bottom)

M.756/02

FLANDERS HYDRAULICS RESEARCH / DELFT HYDRAULICS

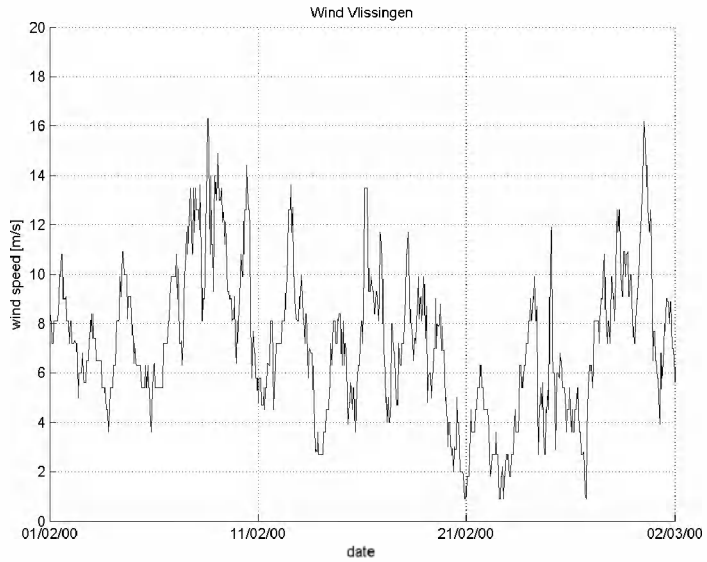

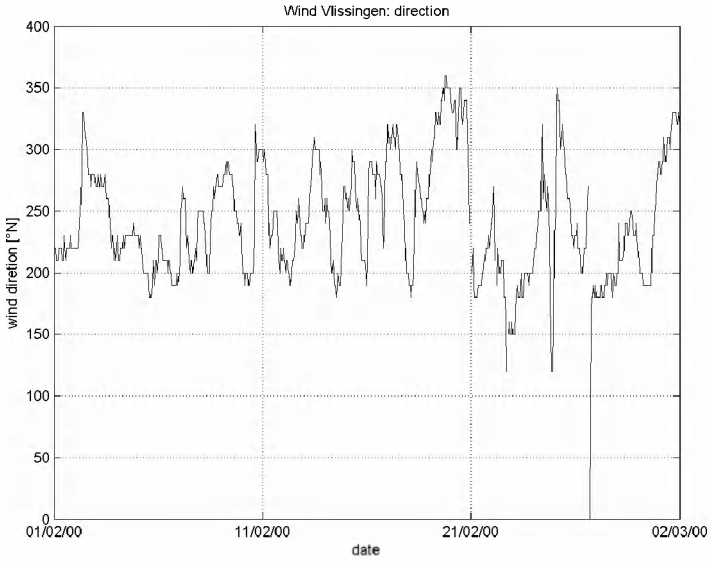

Figure A-13: Wind Vlissingen February.
10 minute mean windspeed (top) and direction (bottom)

M.756/02

FLANDERS HYDRAULICS RESEARCH / DELFT HYDRAULICS

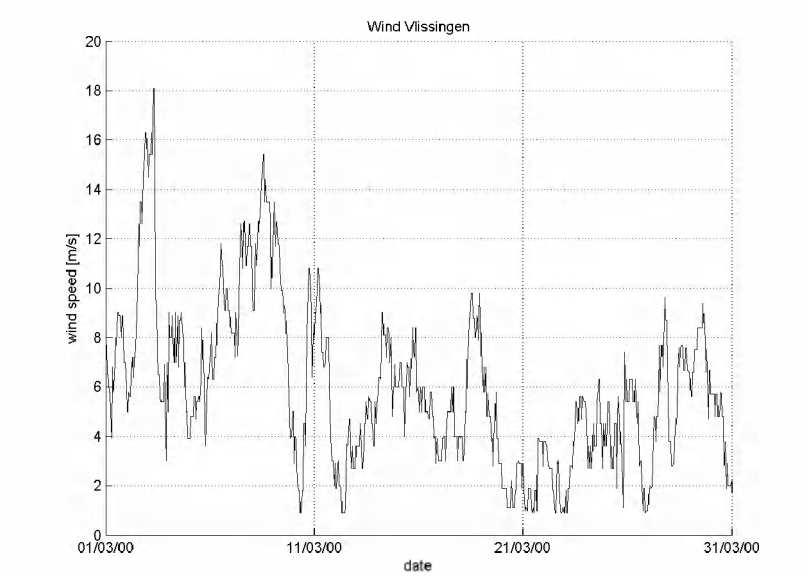

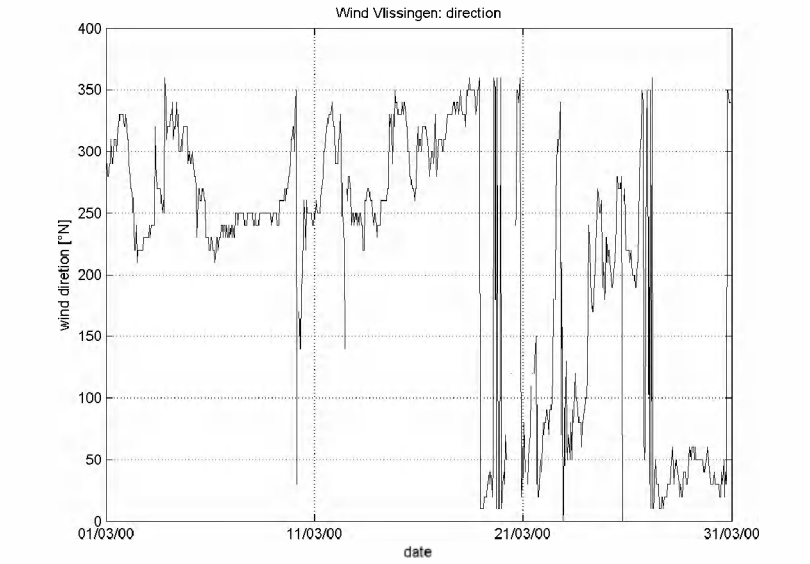

Figure A-14: Wind Vlissingen March.
10 minute mean windspeed (top) and direction (bottom)

M.756/02

FLANDERS HYDRAULICS RESEARCH / DELFT HYDRAULICS

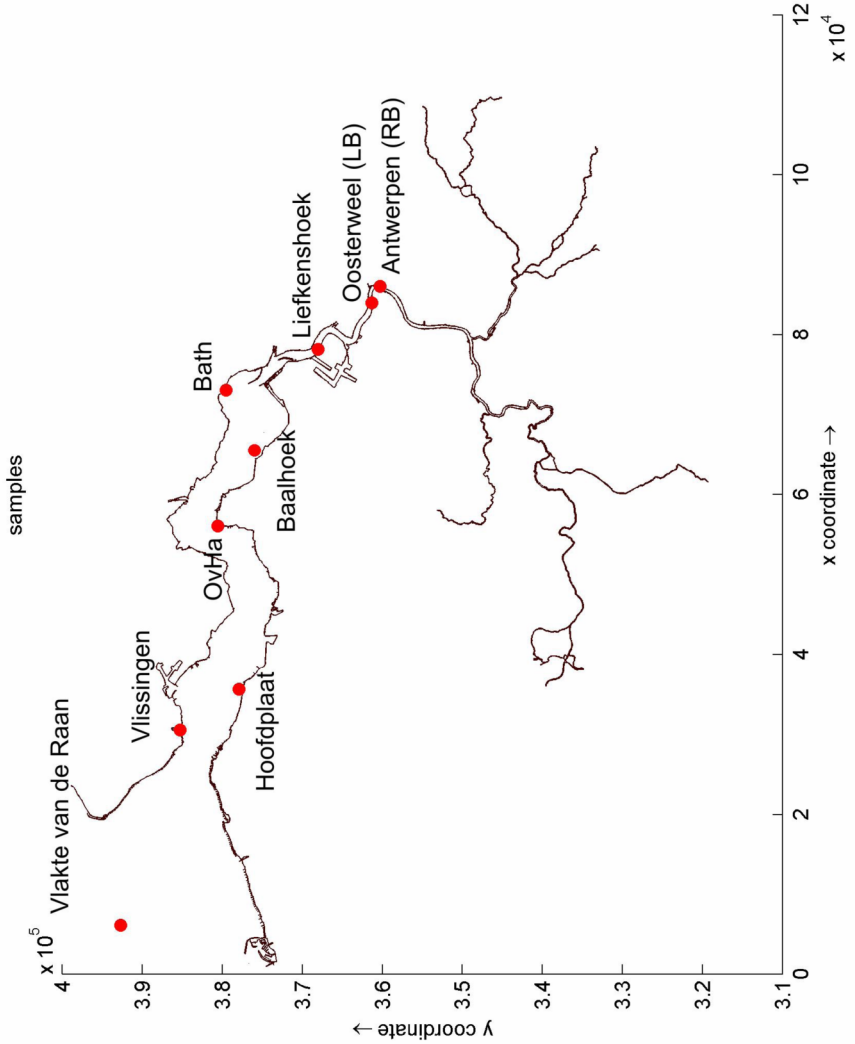

Figure A-15: Output locations	**M.756/02**
FLANDERS HYDRAULICS RESEARCH / DELFT HYDRAULICS	

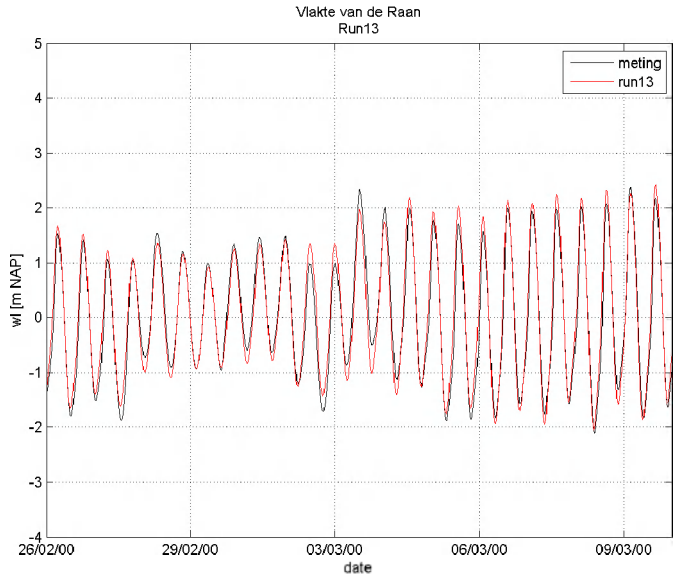

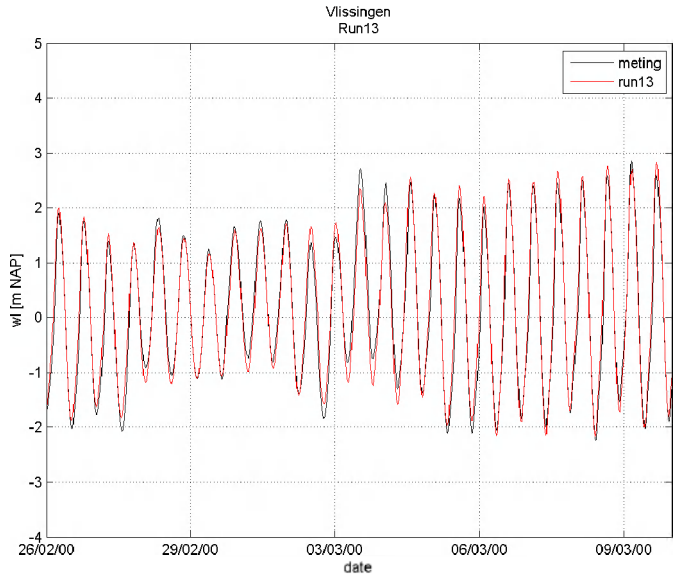

Figure A-16: Water level: computed results and measurements (26/02 to 09/03)

M.756/02

FLANDERS HYDRAULICS RESEARCH / DELFT HYDRAULICS

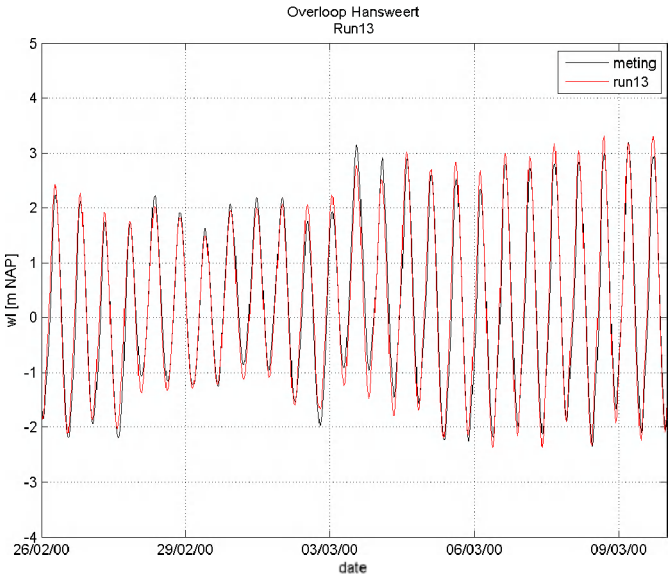

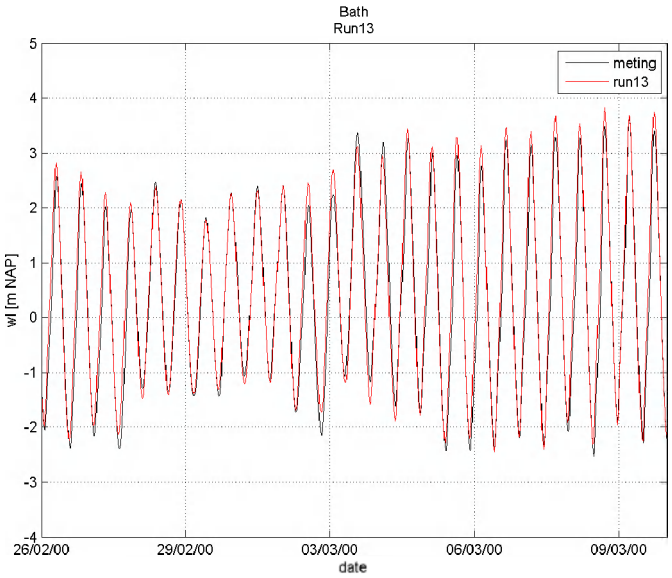

Figure A-17: Water level: computed results and measurements (26/02 to 09/03)

M.756/02

FLANDERS HYDRAULICS RESEARCH / DELFT HYDRAULICS

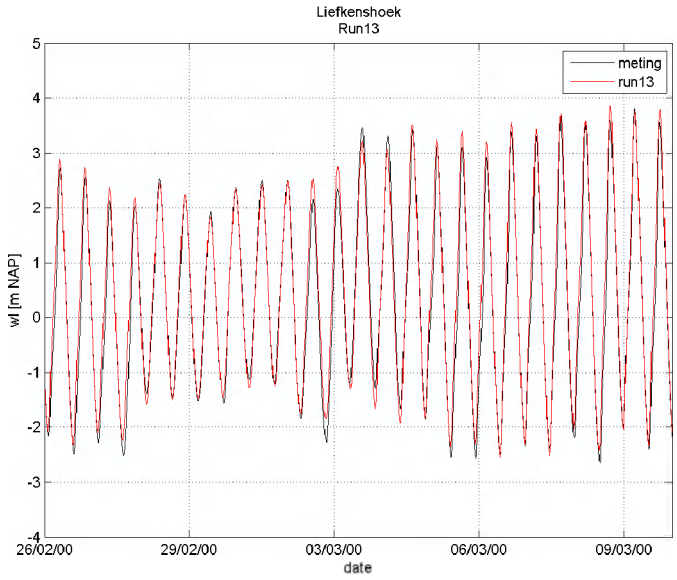

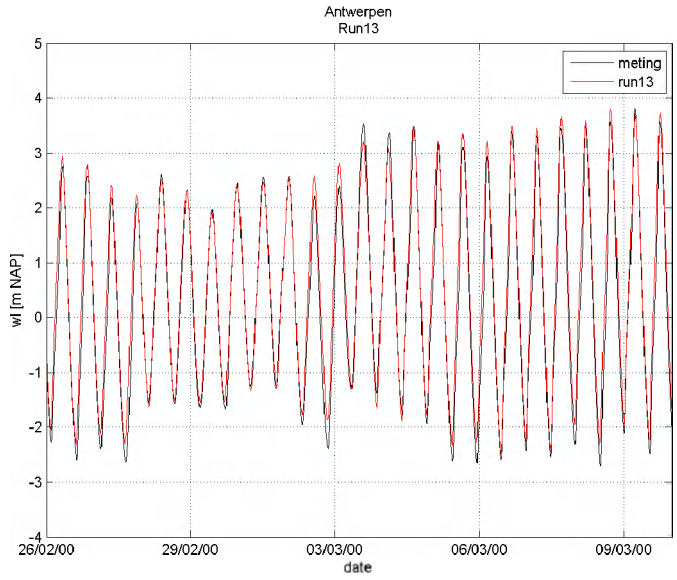

Figure A-18: Water level: computed results and measurements (26/02 to 09/03)	**M.756/02**
FLANDERS HYDRAULICS RESEARCH / DELFT HYDRAULICS	

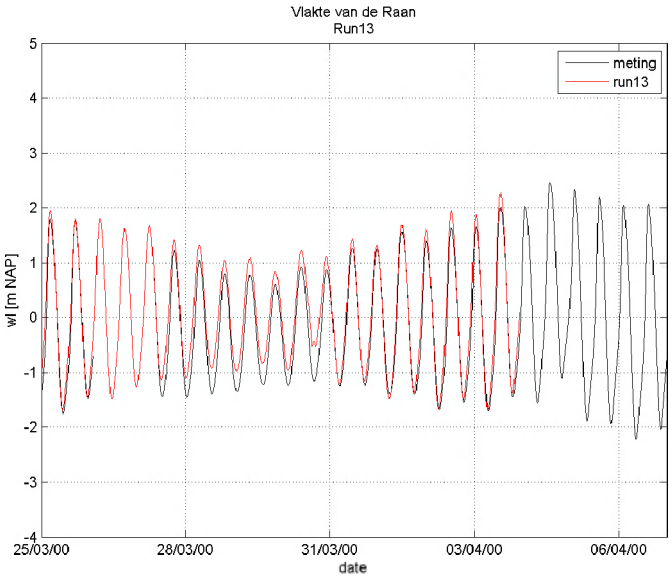

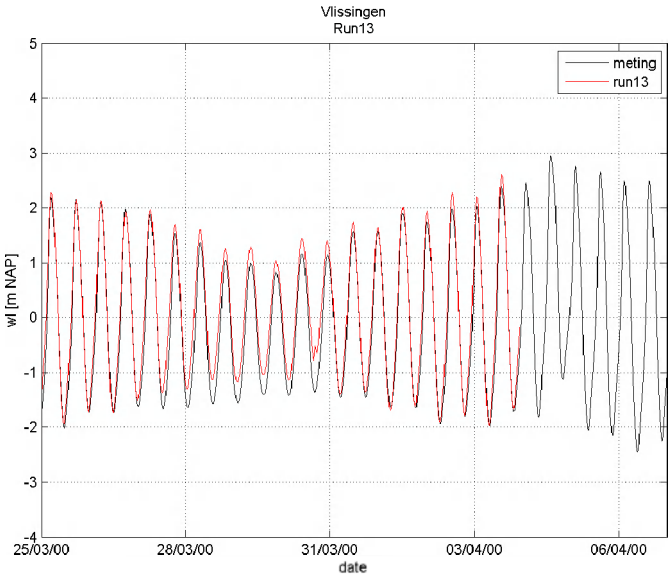

Figure A-19: Water level: computed results and measurements (25/03 to 06/04)

M.756/02

FLANDERS HYDRAULICS RESEARCH / DELFT HYDRAULICS

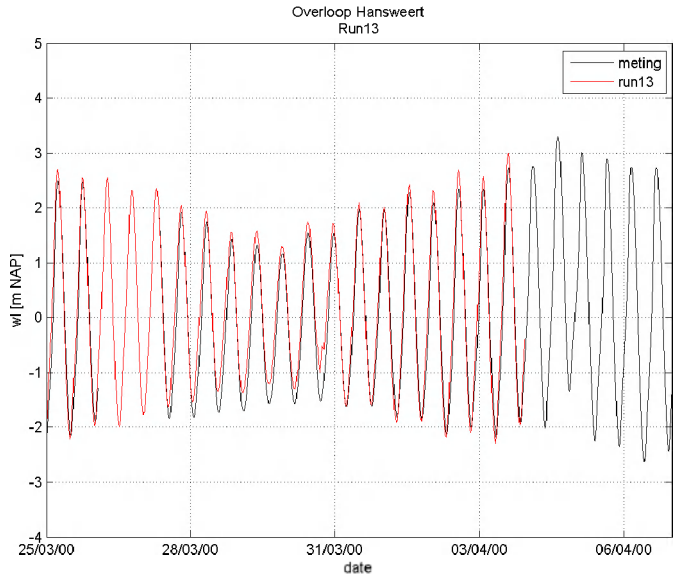

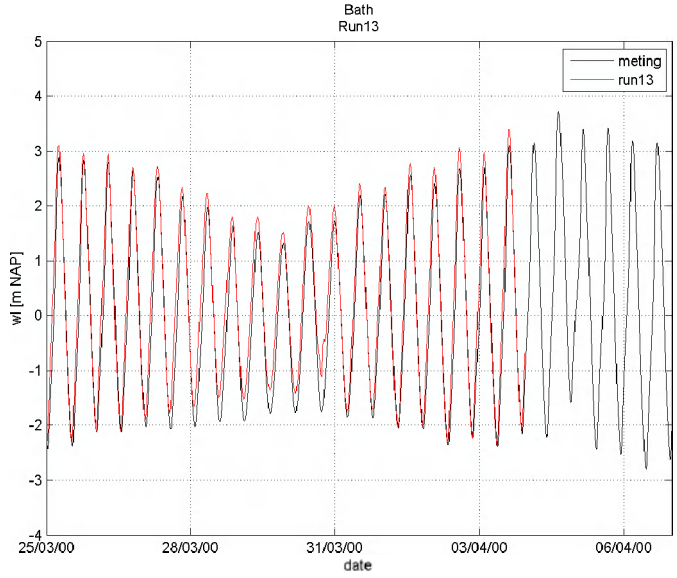

Figure A-20: Water level: computed results and measurements (25/03 to 06/04)	**M.756/02**
FLANDERS HYDRAULICS RESEARCH / DELFT HYDRAULICS	

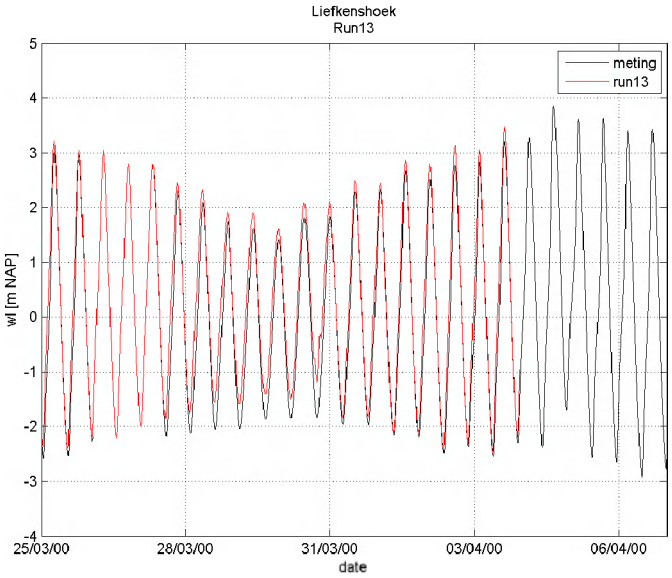

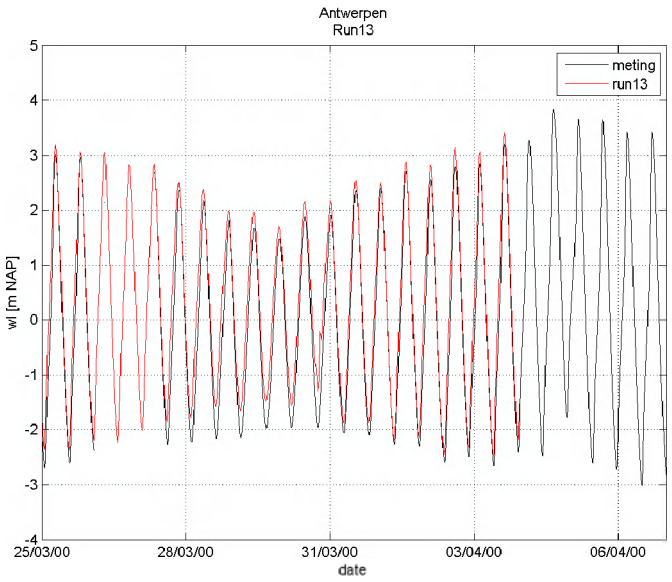

Figure A-21: Water level: computed results and measurements (25/03 to 06/04)

M.756/02

FLANDERS HYDRAULICS RESEARCH / DELFT HYDRAULICS

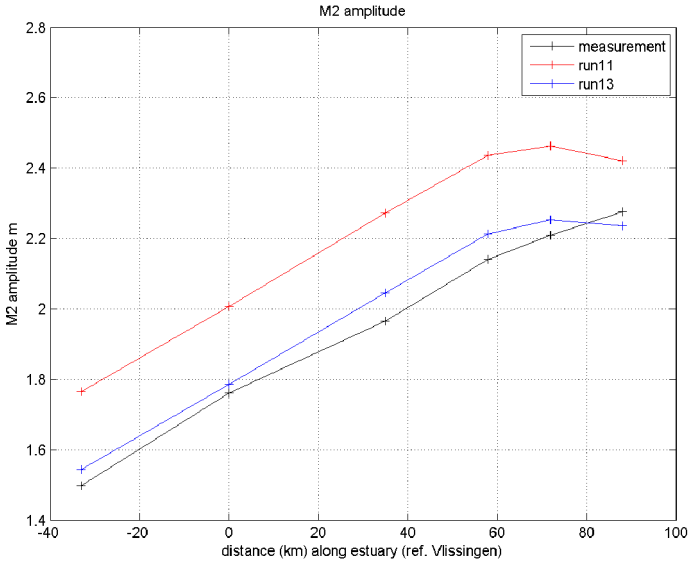

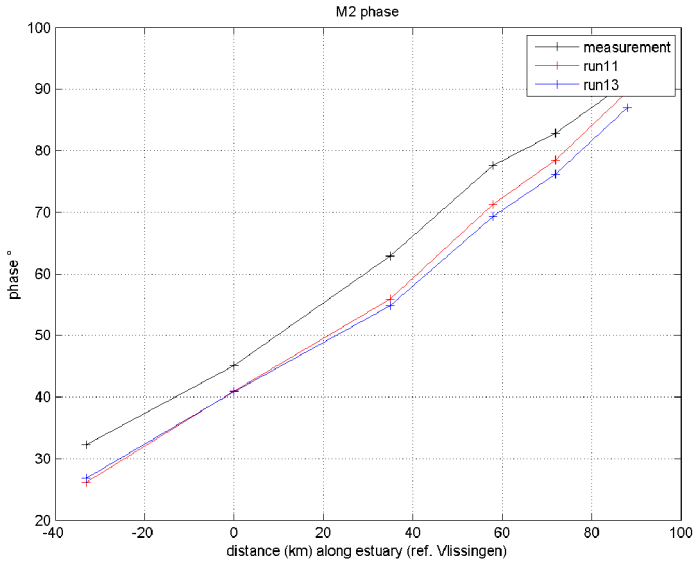

Figure A-22: Harmonic analysis of computed water levels: M2 amplitude and phase	**M.756/02**
FLANDERS HYDRAULICS RESEARCH / DELFT HYDRAULICS	

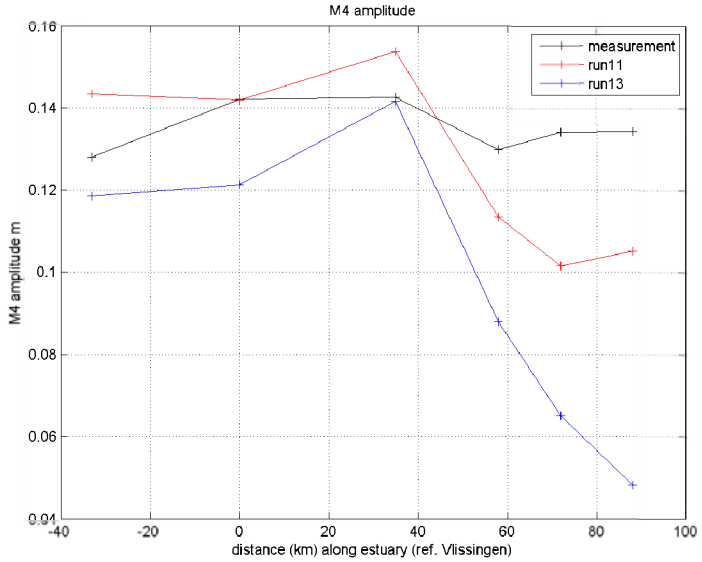

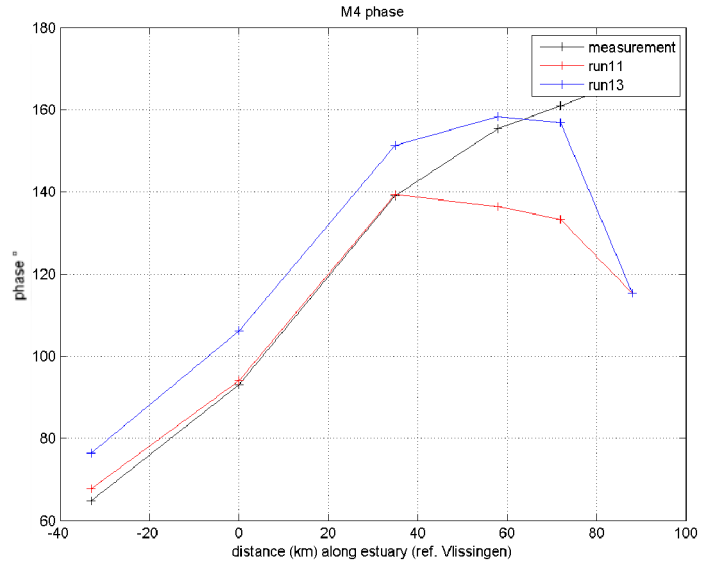

Figure A-23: Harmonic analysis of computed water levels: M4 amplitude and phase

M.756/02

FLANDERS HYDRAULICS RESEARCH / DELFT HYDRAULICS

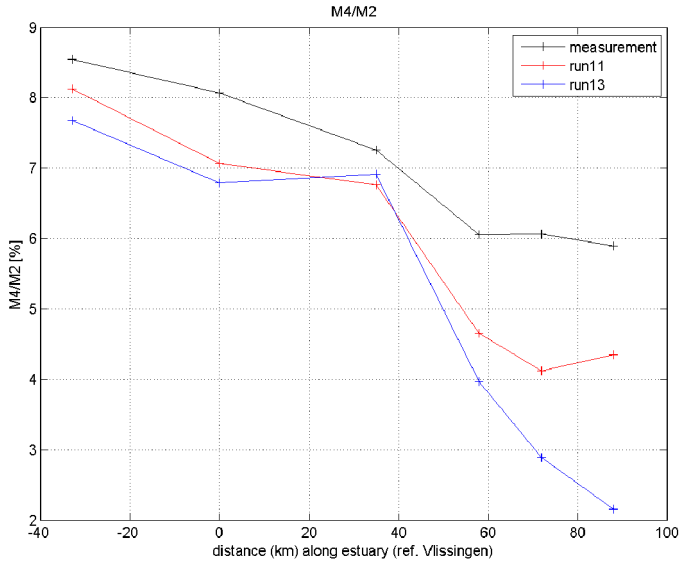

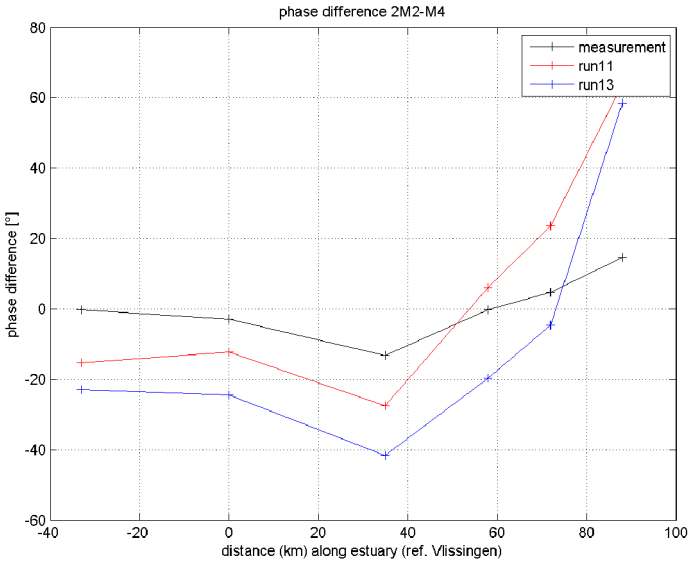

Figure A-24: Harmonic analysis of computed water levels. Ratio of M4 amplitude to M2 ampltude (top) and phase difference (2M2 - M4) (bottom)	**M.756/02**
FLANDERS HYDRAULICS RESEARCH / DELFT HYDRAULICS	

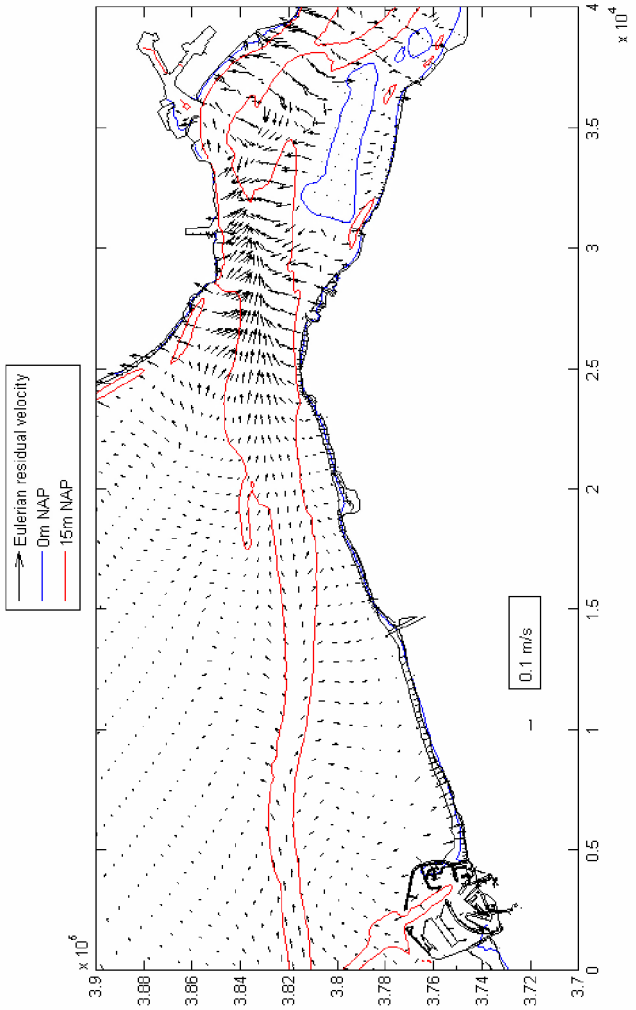

Figure A-25: Eulerian residual bottom velocity field over 1 tidal cycle.
Vlissingen – Zeebrugge

M.756/02

FLANDERS HYDRAULICS RESEARCH / DELFT HYDRAULICS

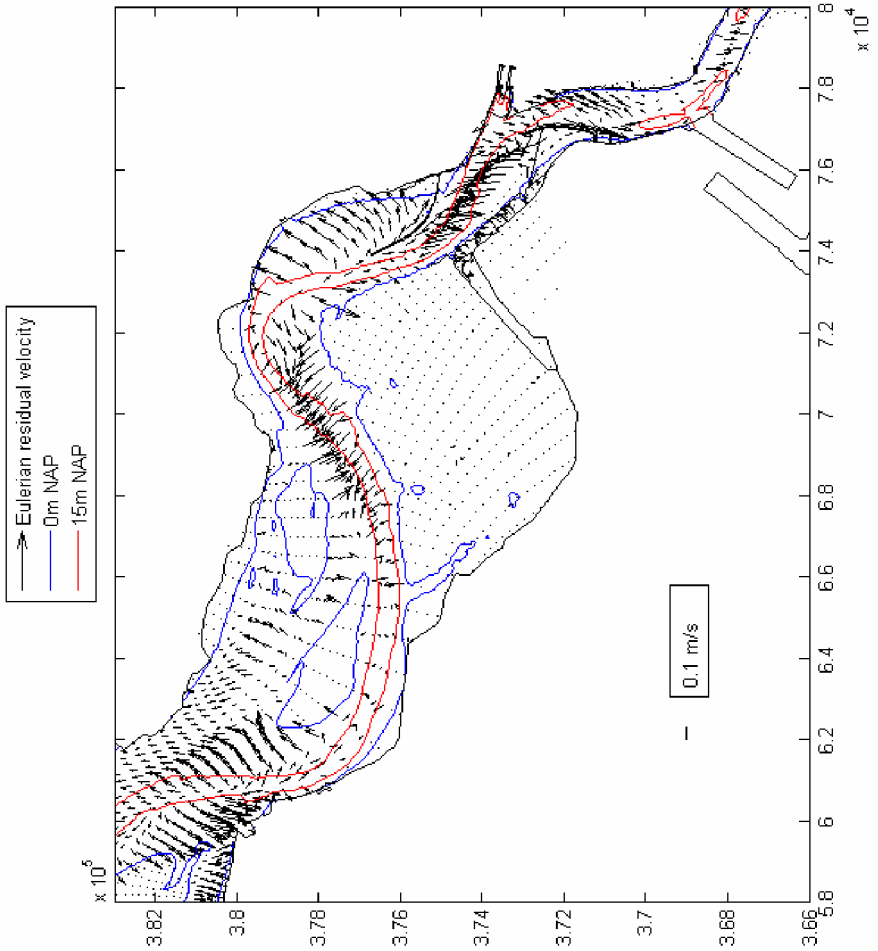

Figure A-26: Eulerian residual bottom velocity field over 1 tidal cycle.
Liefkenshoek – Overloop Hansweert

M.756/02

FLANDERS HYDRAULICS RESEARCH / DELFT HYDRAULICS

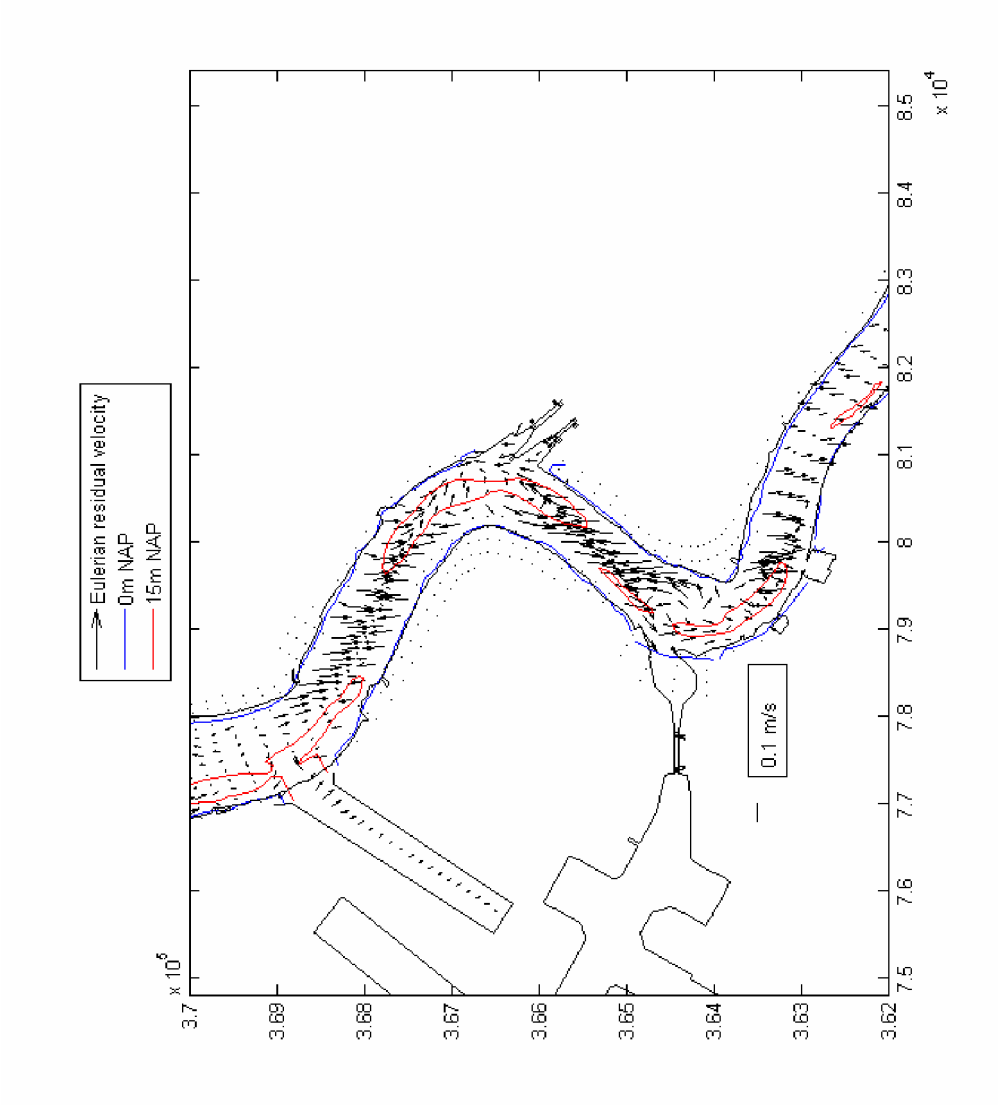

Figure A-27: Eulerian residual bottom velocity field over 1 tidal cycle.
Deurganckdok – Kallo sluis

M.756/02

FLANDERS HYDRAULICS RESEARCH / DELFT HYDRAULICS

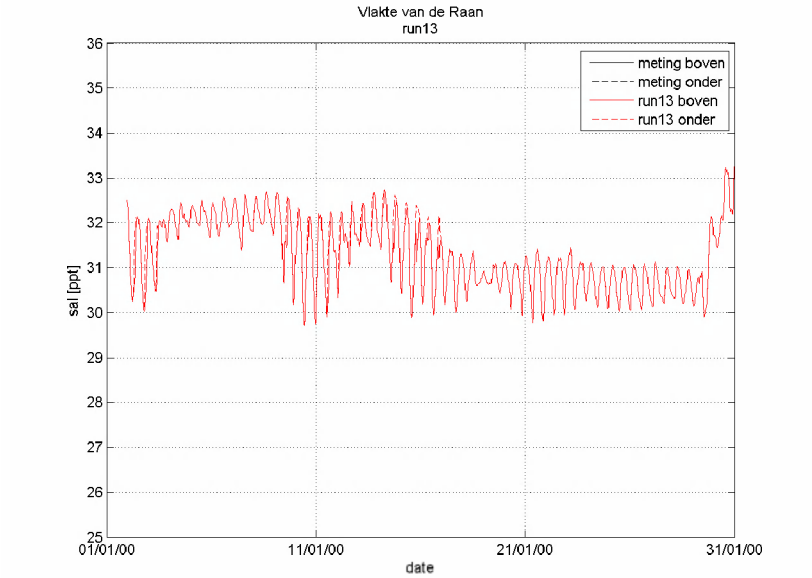

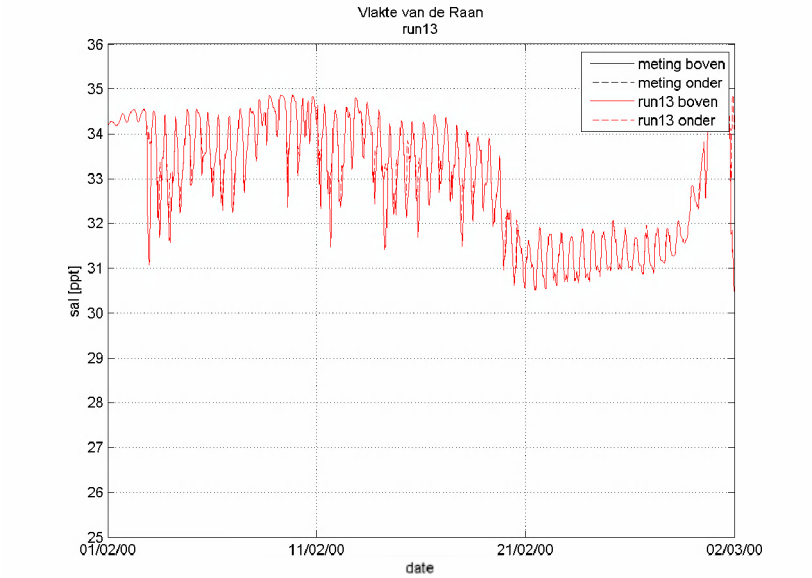

Figure A-28: Salinity: computed results and measurements	**M.756/02**
FLANDERS HYDRAULICS RESEARCH / DELFT HYDRAULICS	

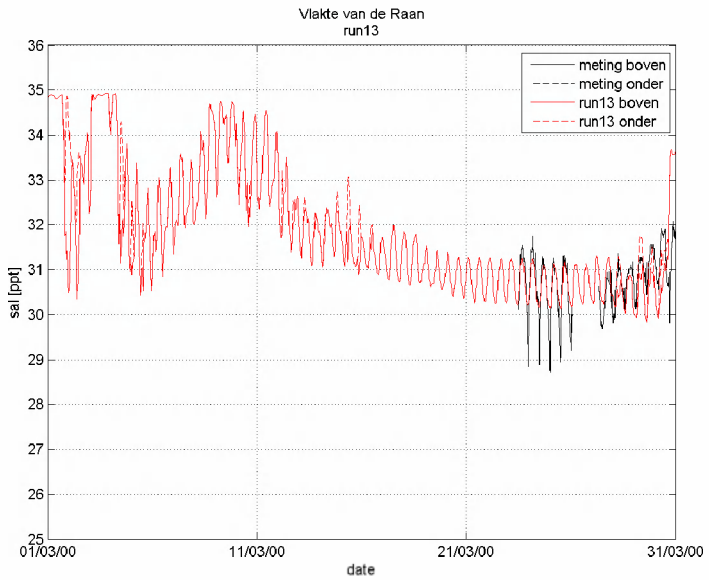

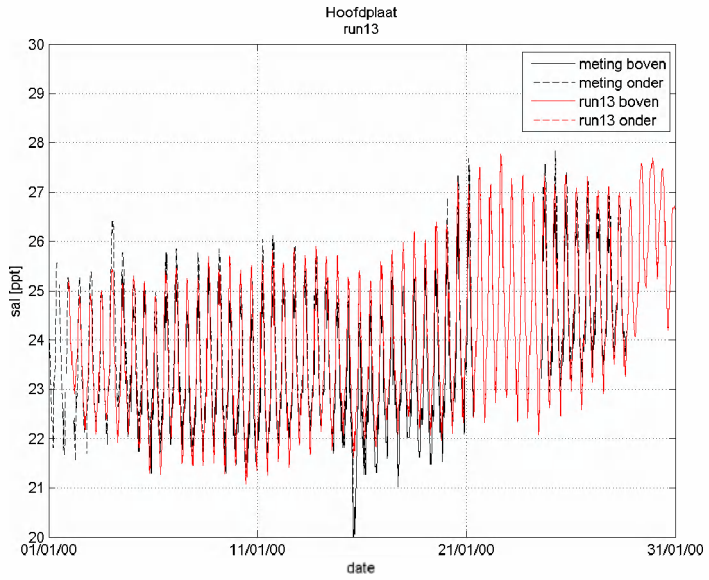

Figure A-29: Salinity: computed results and measurements

M.756/02

FLANDERS HYDRAULICS RESEARCH / DELFT HYDRAULICS

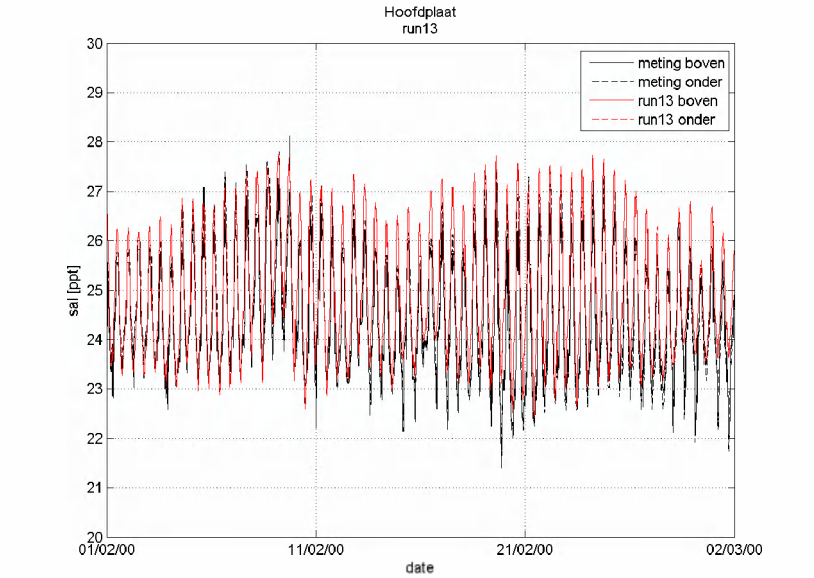

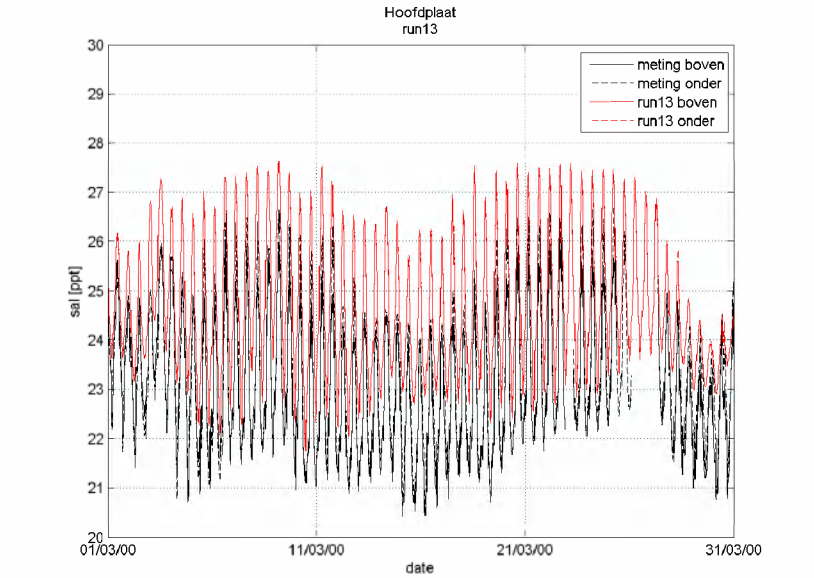

Figure A-30: Salinity: computed results and measurements	**M.756/02**
FLANDERS HYDRAULICS RESEARCH / DELFT HYDRAULICS	

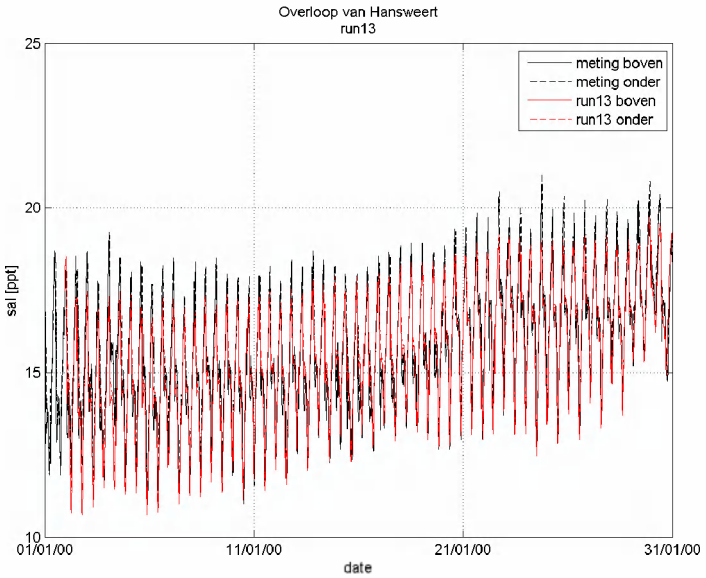

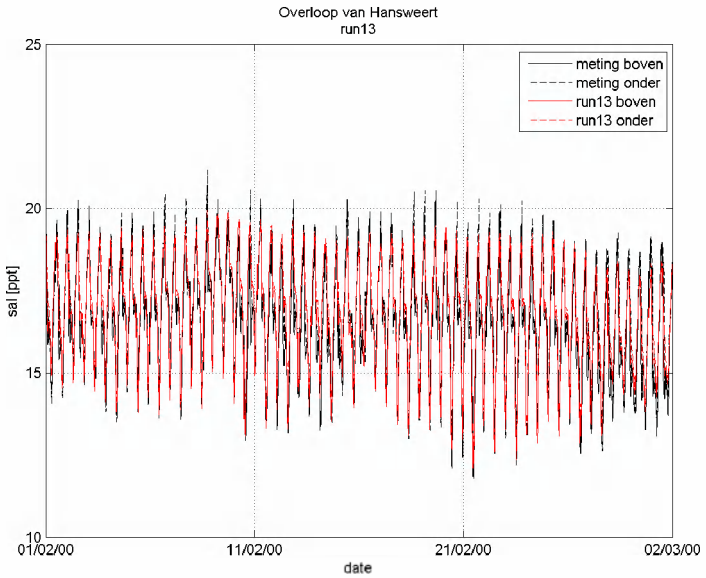

Figure A-31: Salinity: computed results and measurements

M.756/02

FLANDERS HYDRAULICS RESEARCH / DELFT HYDRAULICS

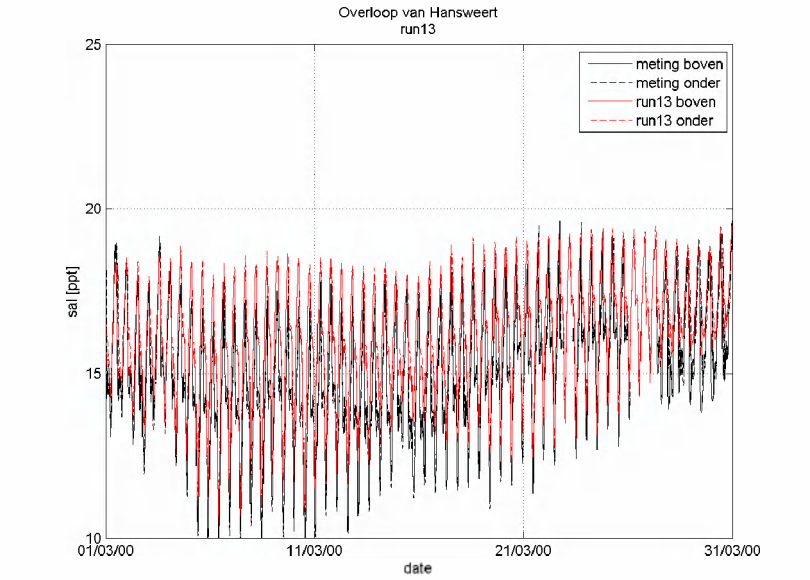

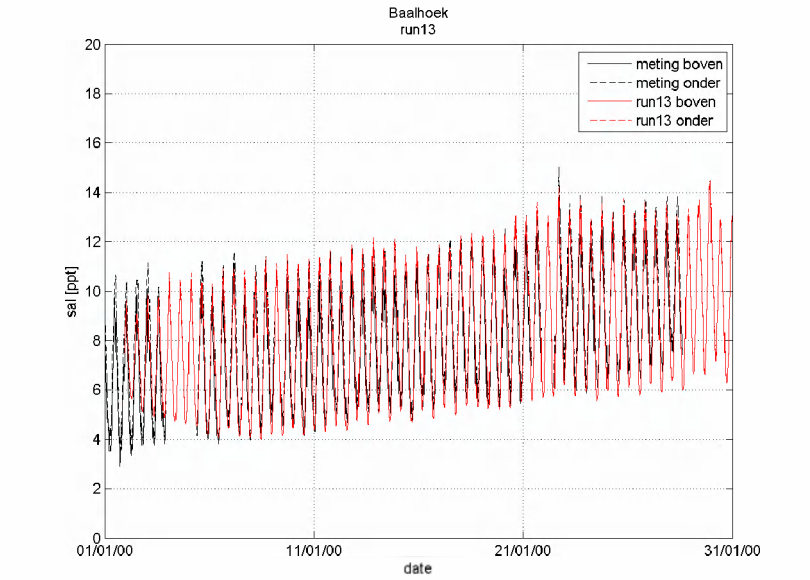

Figure A-32: Salinity: computed results and measurements	**M.756/02**
FLANDERS HYDRAULICS RESEARCH / DELFT HYDRAULICS	

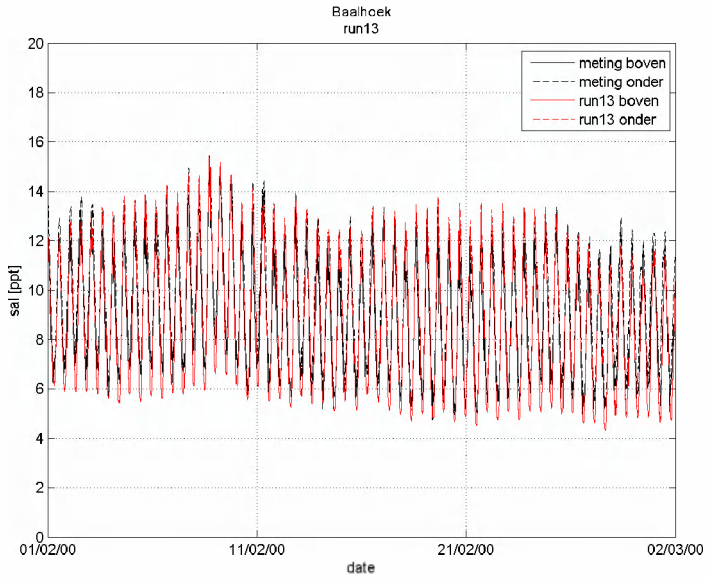

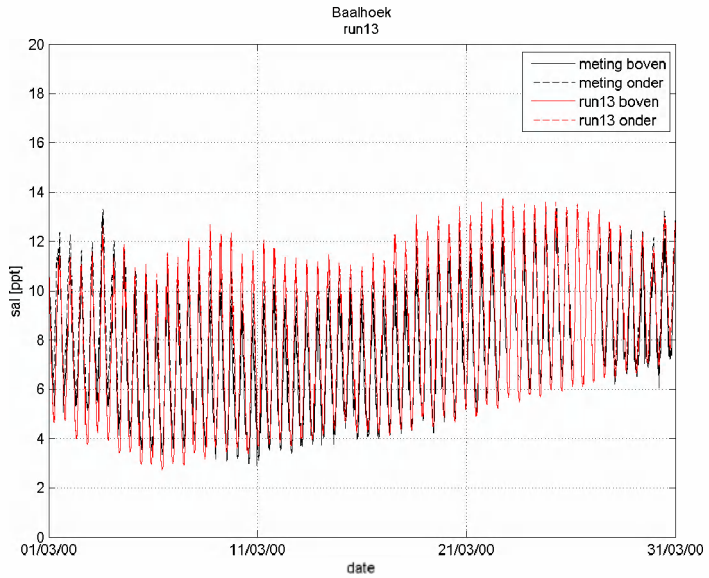

Figure A-33: Salinity: computed results and measurements

M.756/02

FLANDERS HYDRAULICS RESEARCH / DELFT HYDRAULICS

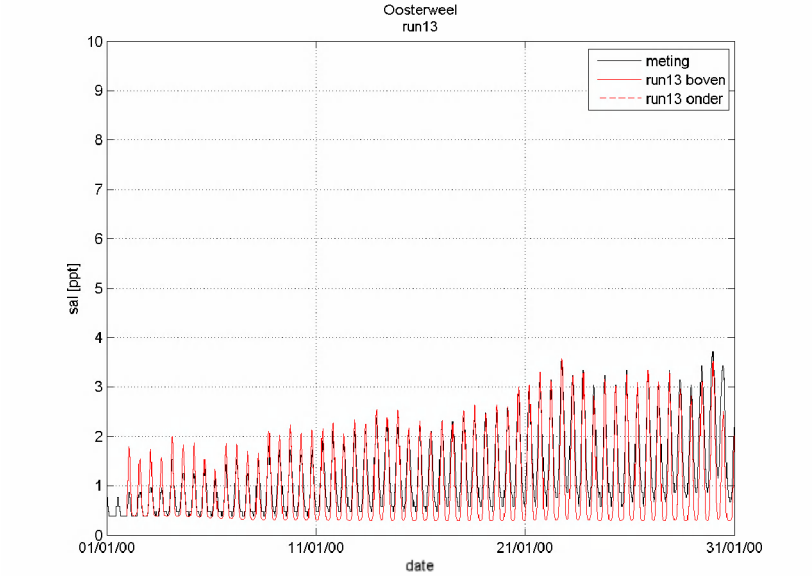

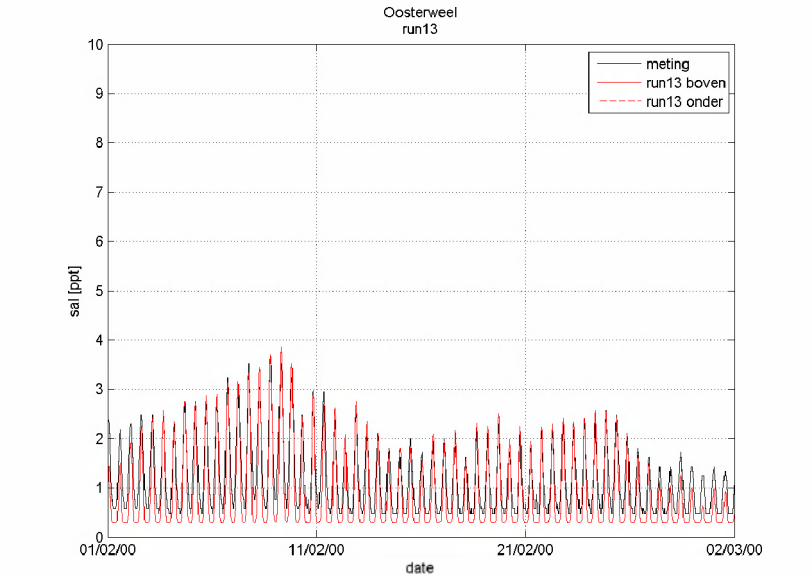

Figure A-34: Salinity: computed results and measurements	**M.756/02**
FLANDERS HYDRAULICS RESEARCH / DELFT HYDRAULICS	

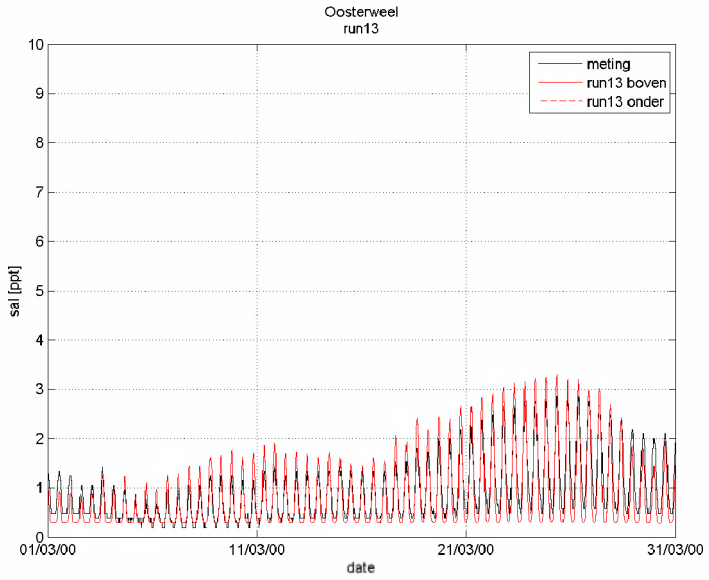

Figure A-35: Salinity: computed results and measurements	**M.756/02**
FLANDERS HYDRAULICS RESEARCH / DELFT HYDRAULICS	

B Figures on mud transport model

B.1 New dumping locations near Antwerp

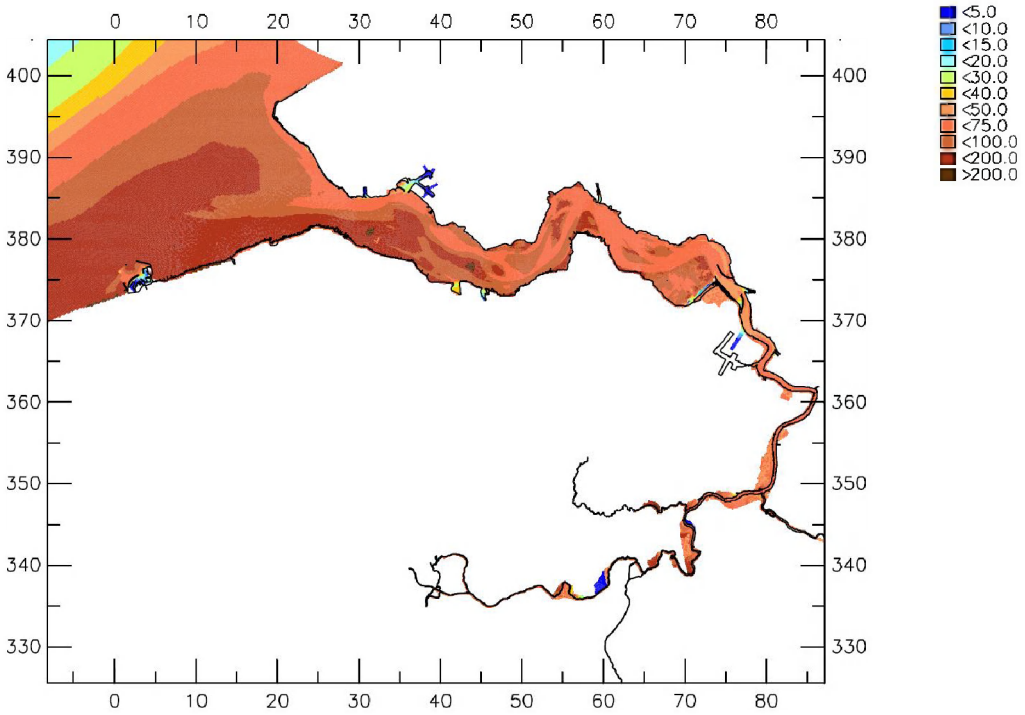

Fig. B.1a: 14-day winter averaged SPM surface concentration (mg/l), original dumping locations (ws15)

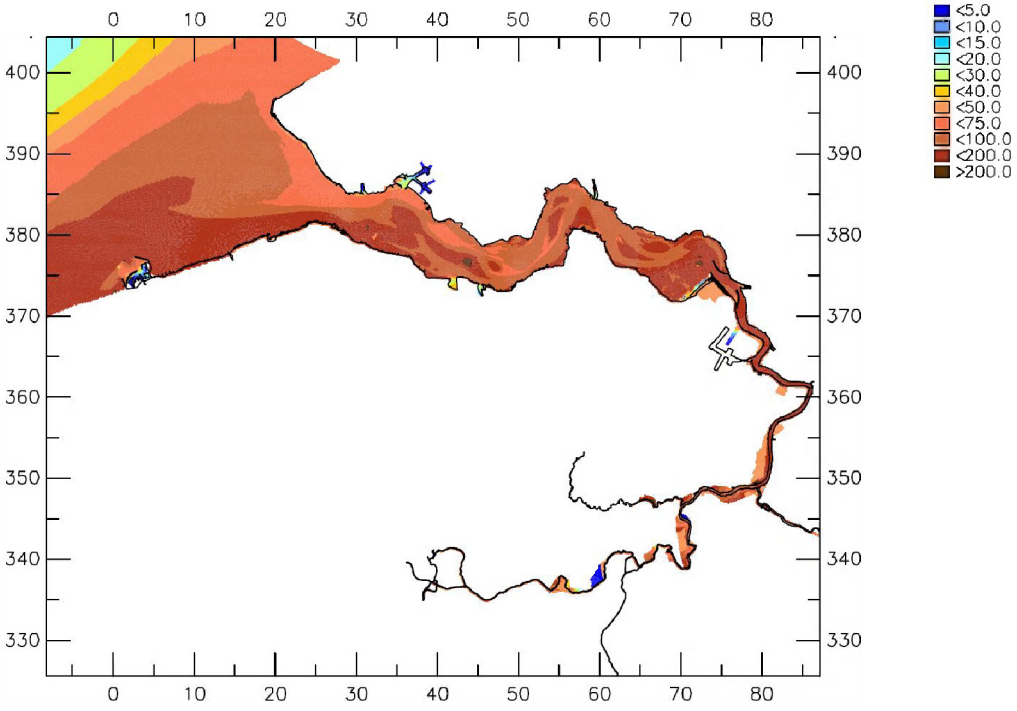

Fig. B.1b: 14-day winter averaged SPM surface concentration (mg/l), new dumping locations (ws15new)

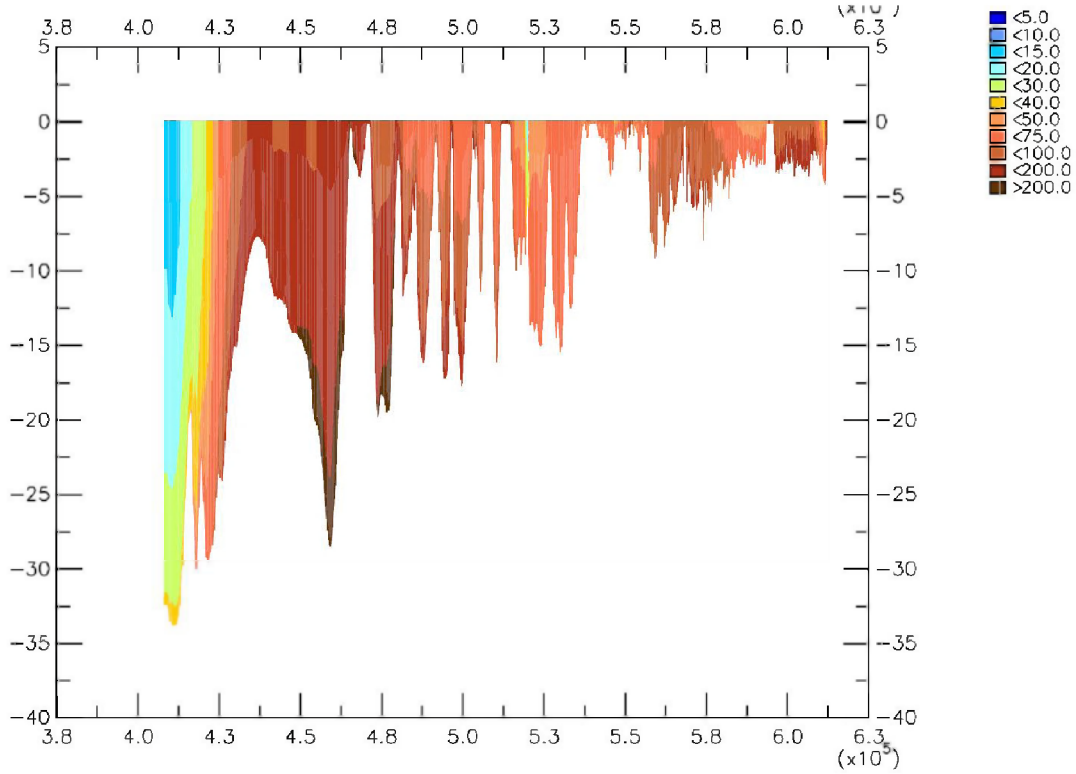

Fig. B.1c: 14-day winter averaged vertical SPM concentration transect (mg/l) along the estuary (left = sea), original dumping locations (ws15)

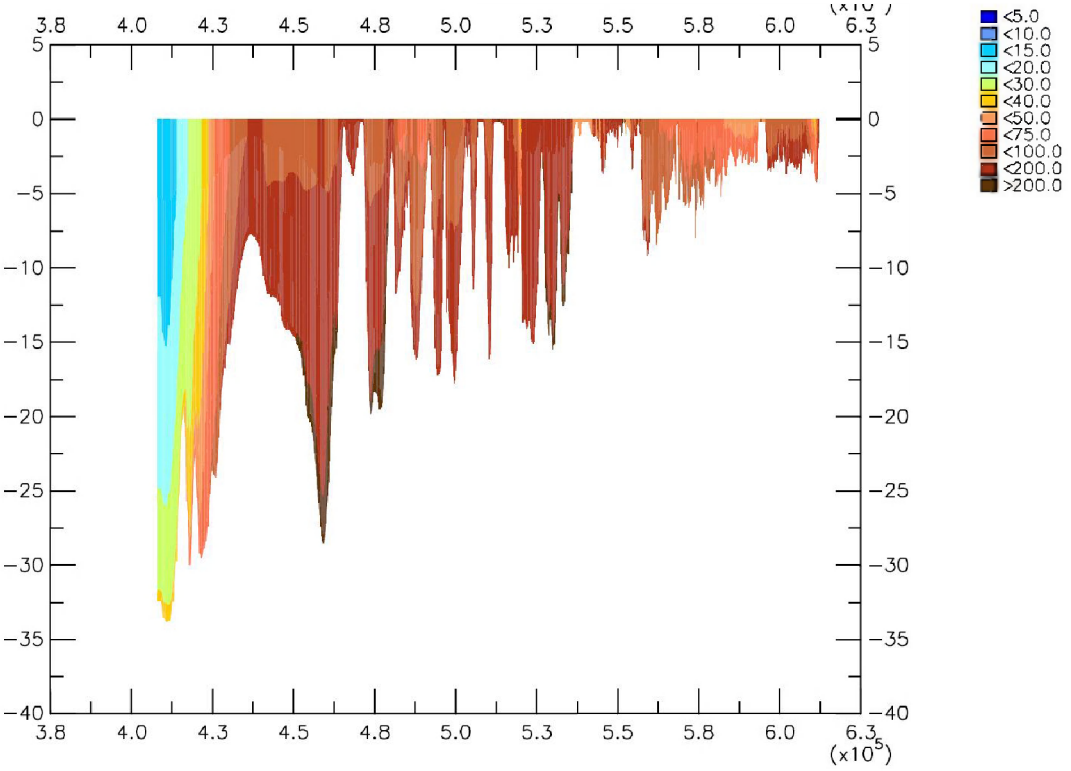

Fig. B.1d: 14-day winter averaged vertical SPM concentration transect (mg/l) along the estuary (left = sea), new dumping locations (ws15new)

B.2 Effect of new SeaWiFs boundary conditions

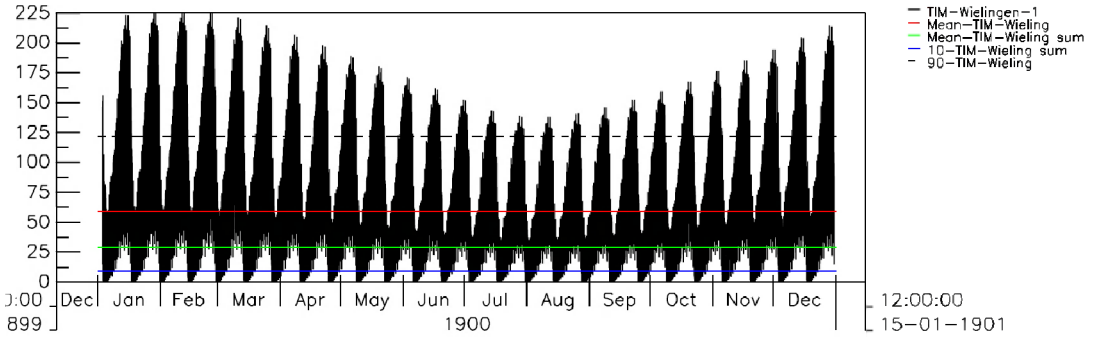

a)

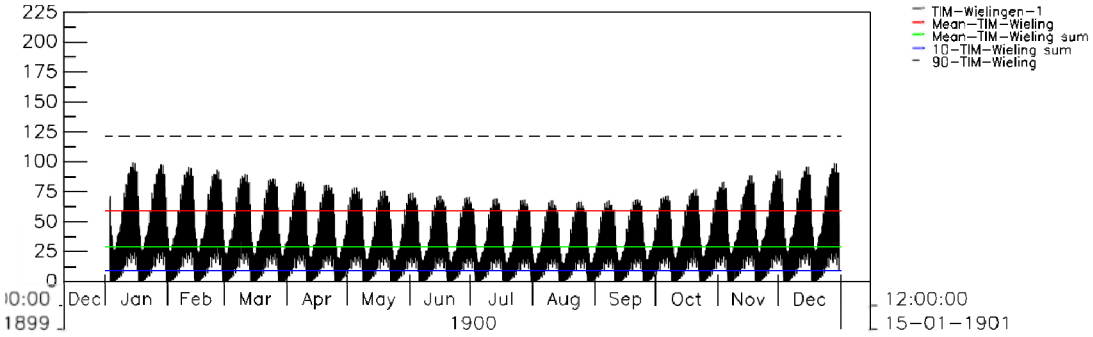

b)

Figure B.2: Computed SPM surface concentration at Wielingen. a) original boundary conditions; b) new boundary conditions based on SeaWiFs images. Observed mean levels are indicated with horizontal lines. In blue: 10-percentile level; in green: mean summer level; in red: mean winter level; dashed black: 90-percentile level.

B.3 Comparison between 5L and 10L

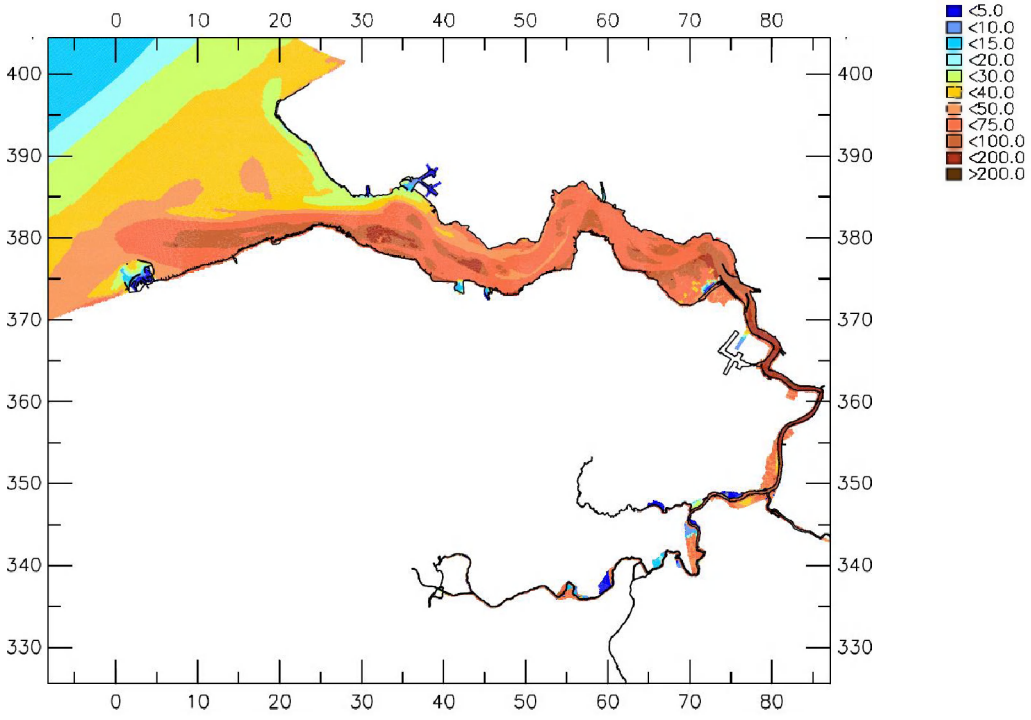

Fig. B.3a: 14-day winter averaged SPM surface concentration (mg/l), 5 horizontal layers (05L01).

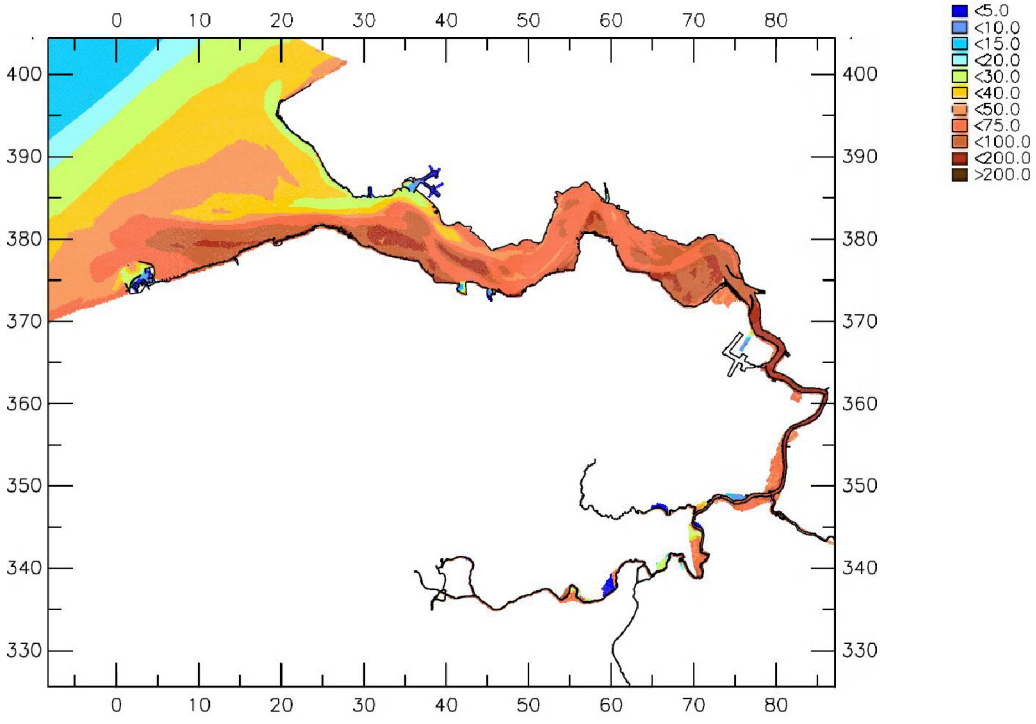

Fig. B.3b: 14-day winter averaged SPM surface concentration (mg/l), 10 horizontal layers (10L01).

B.4 Comparison between constant and variable wave forcing

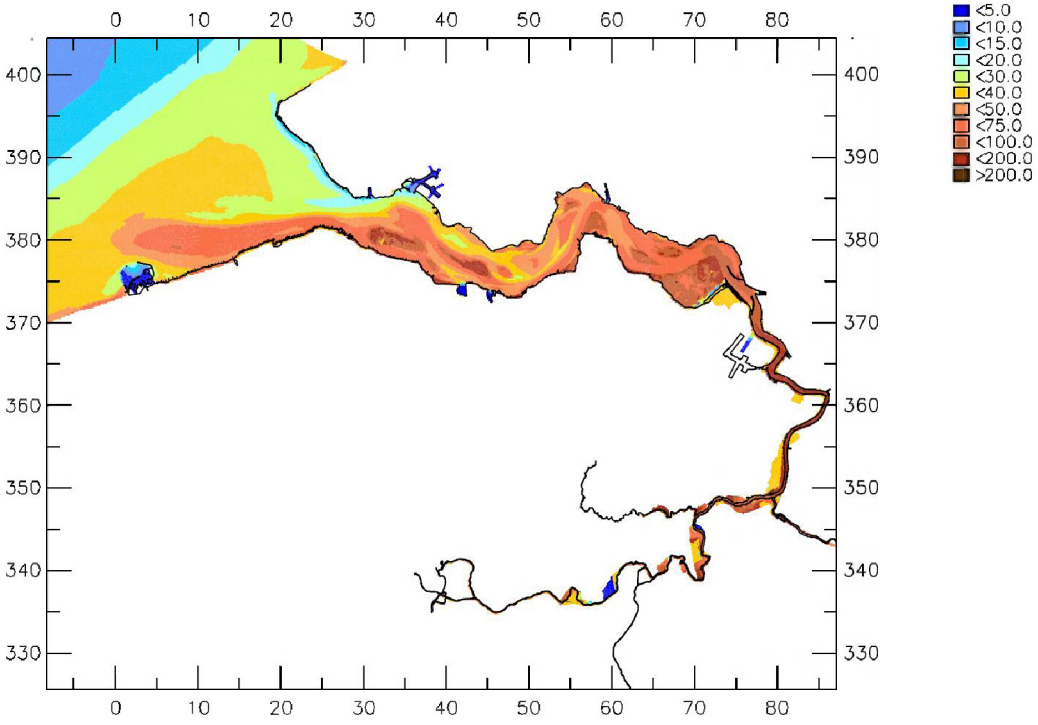

Fig. B.4a: 14-day winter averaged SPM surface concentration (mg/l), constant waves (ws22).

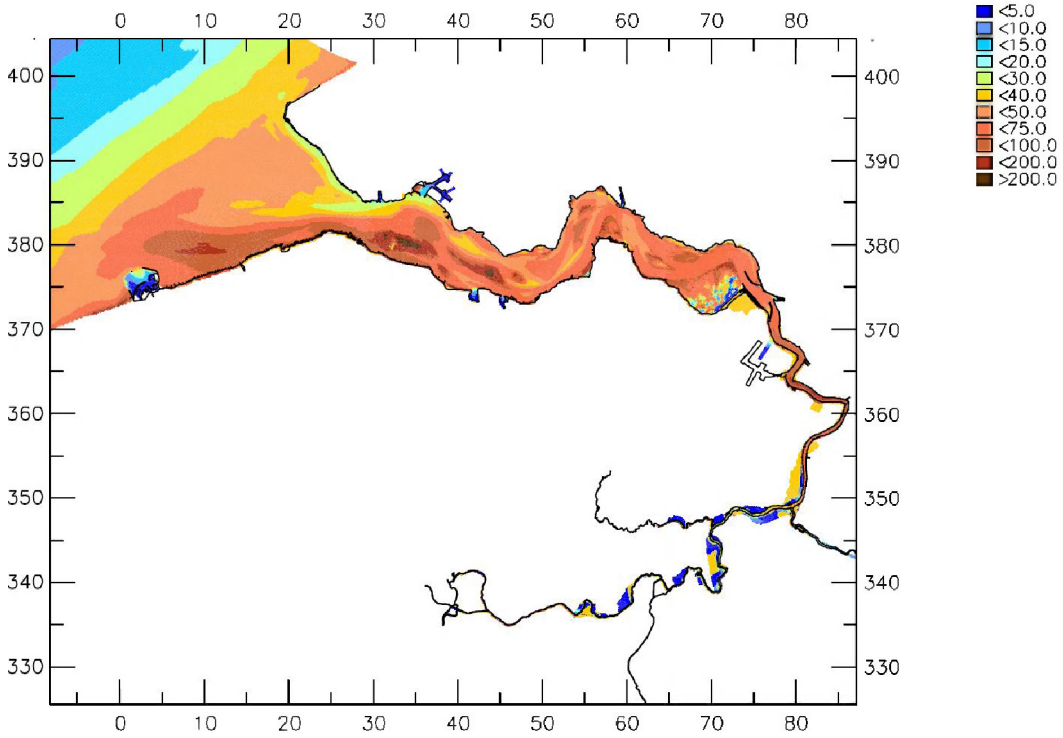

Fig. B.4b: 14-day winter averaged SPM surface concentration (mg/l), variable waves (ws21).

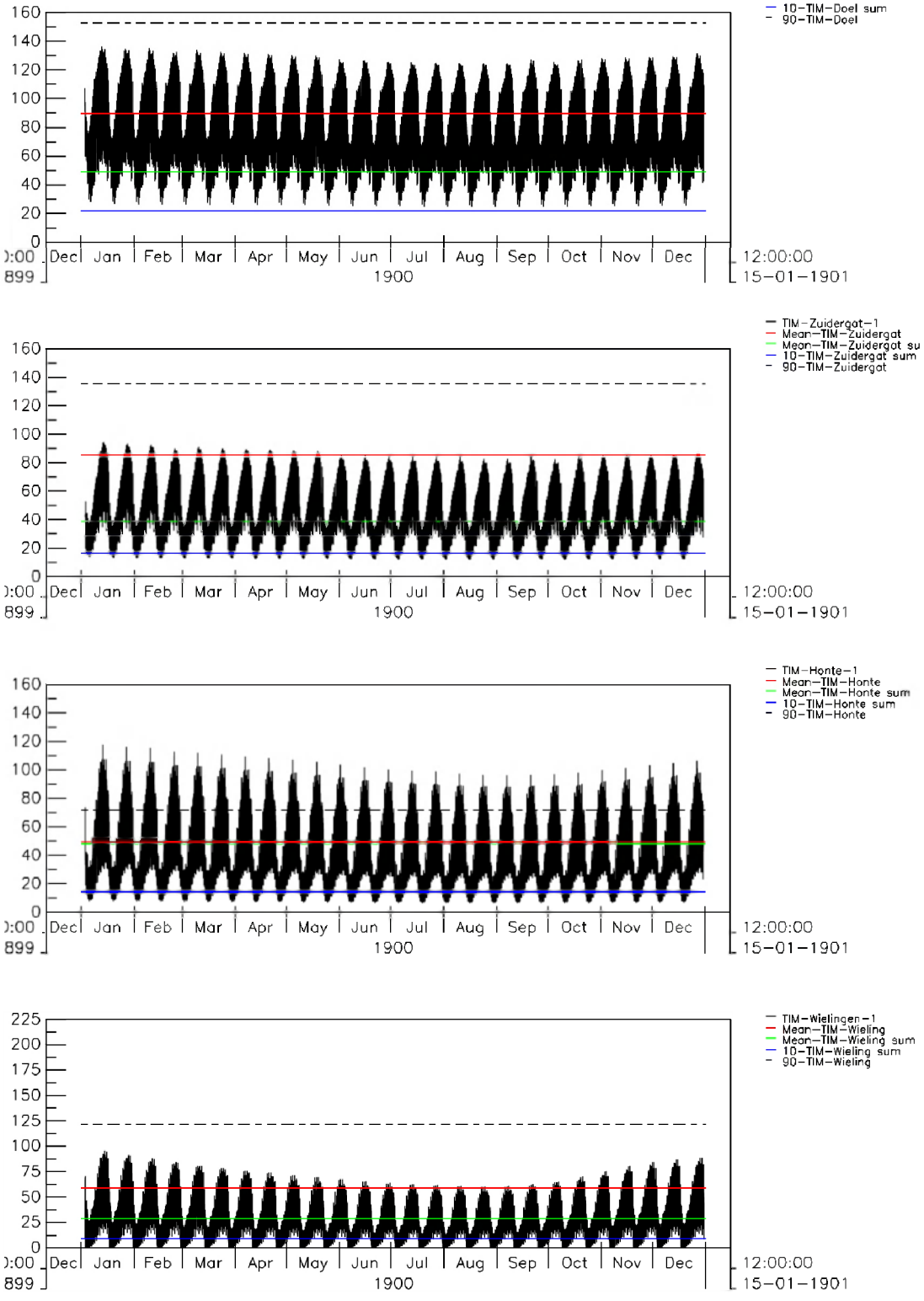

Figure B.4c: Computed SPM surface concentration at 4 stations along the Scheldt estuary for a simulation with constant waves (**ws22**). Observed mean levels are indicated with horizontal lines. In blue: 10-percentile level; in green: mean summer level; in red: mean winter level; dashed black: 90-percentile level.

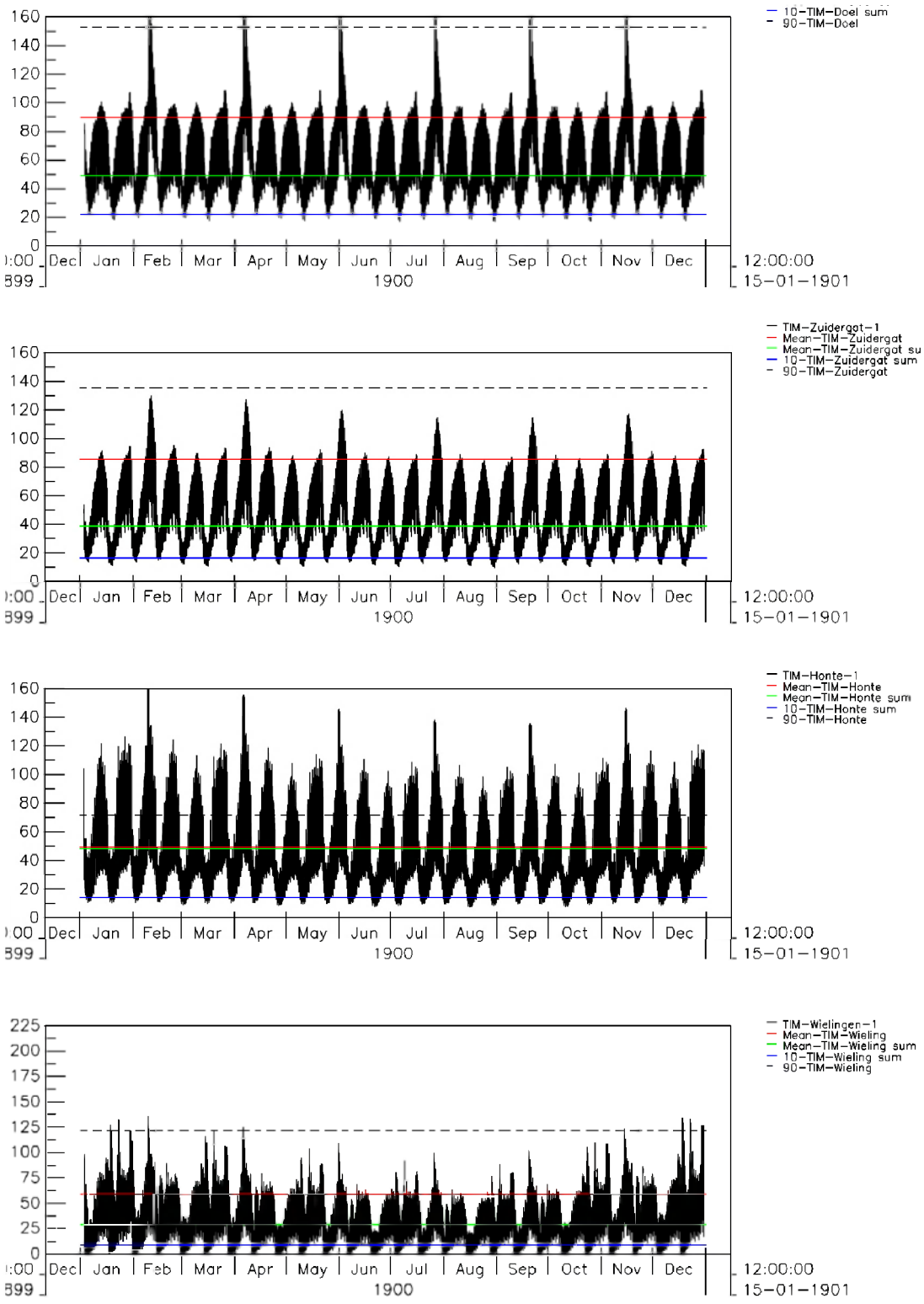

Figure B.4d: Computed SPM surface concentration at 4 stations along the Scheldt estuary for a simulation with variable waves (ws21). Observed mean levels are indicated with horizontal lines. In blue: 10-percentile level; in green: mean summer level; in red: mean winter level; dashed black: 90-percentile level.

B.5 Influence of biology

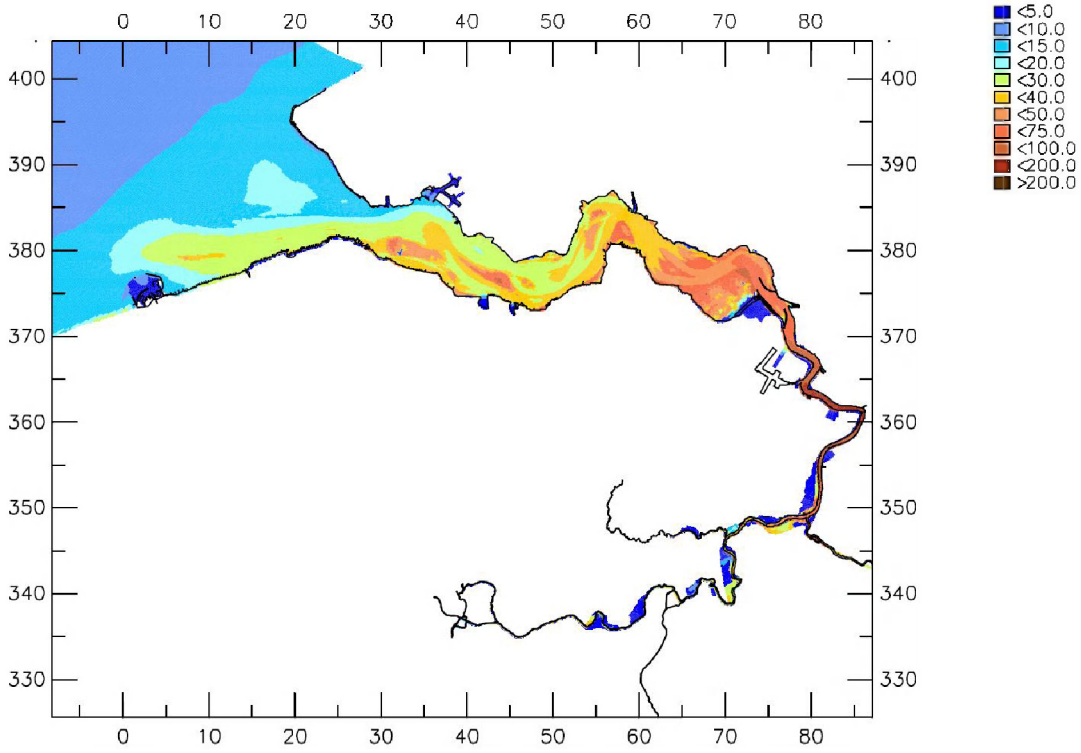

Fig. B.5a: 14-day summer averaged SPM surface concentration (mg/l), with biology, (ws26).

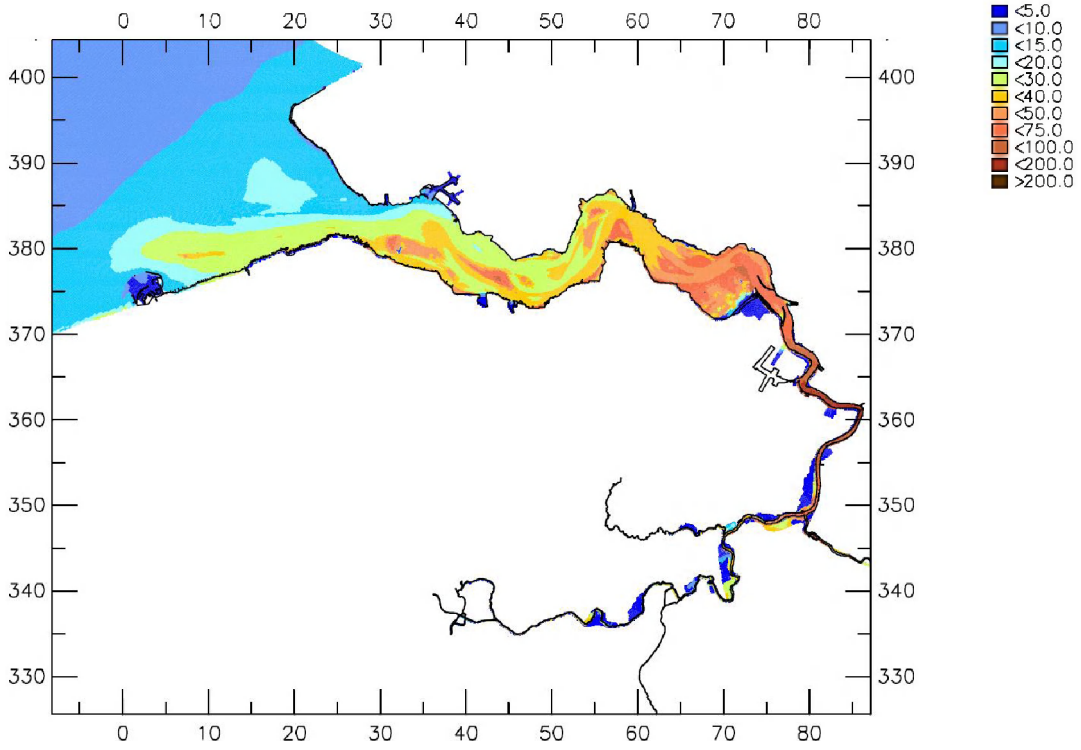

Fig. B.5b: 14-day summer averaged SPM surface concentration (mg/l), without biology, (ws27).

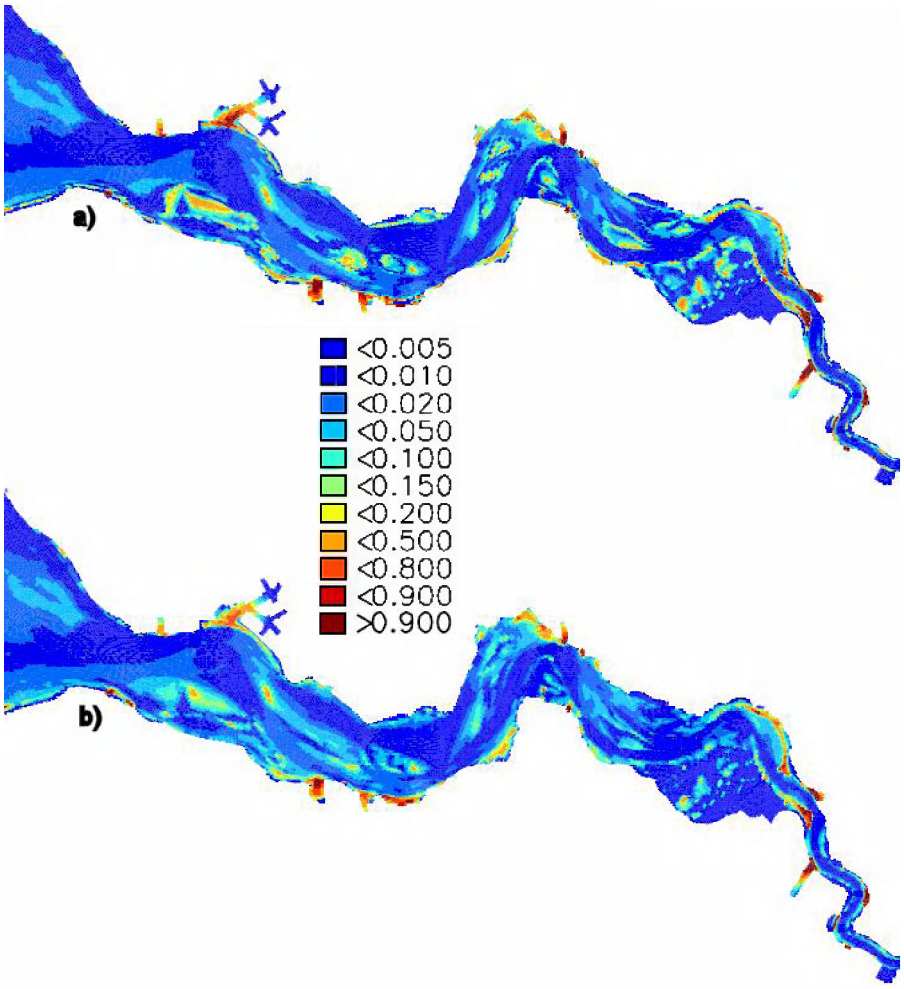

Fig. B.5c: Mud fraction in seabed in summer a) with biology; b) without biology.

B.6 Matching siltation and dumping flux

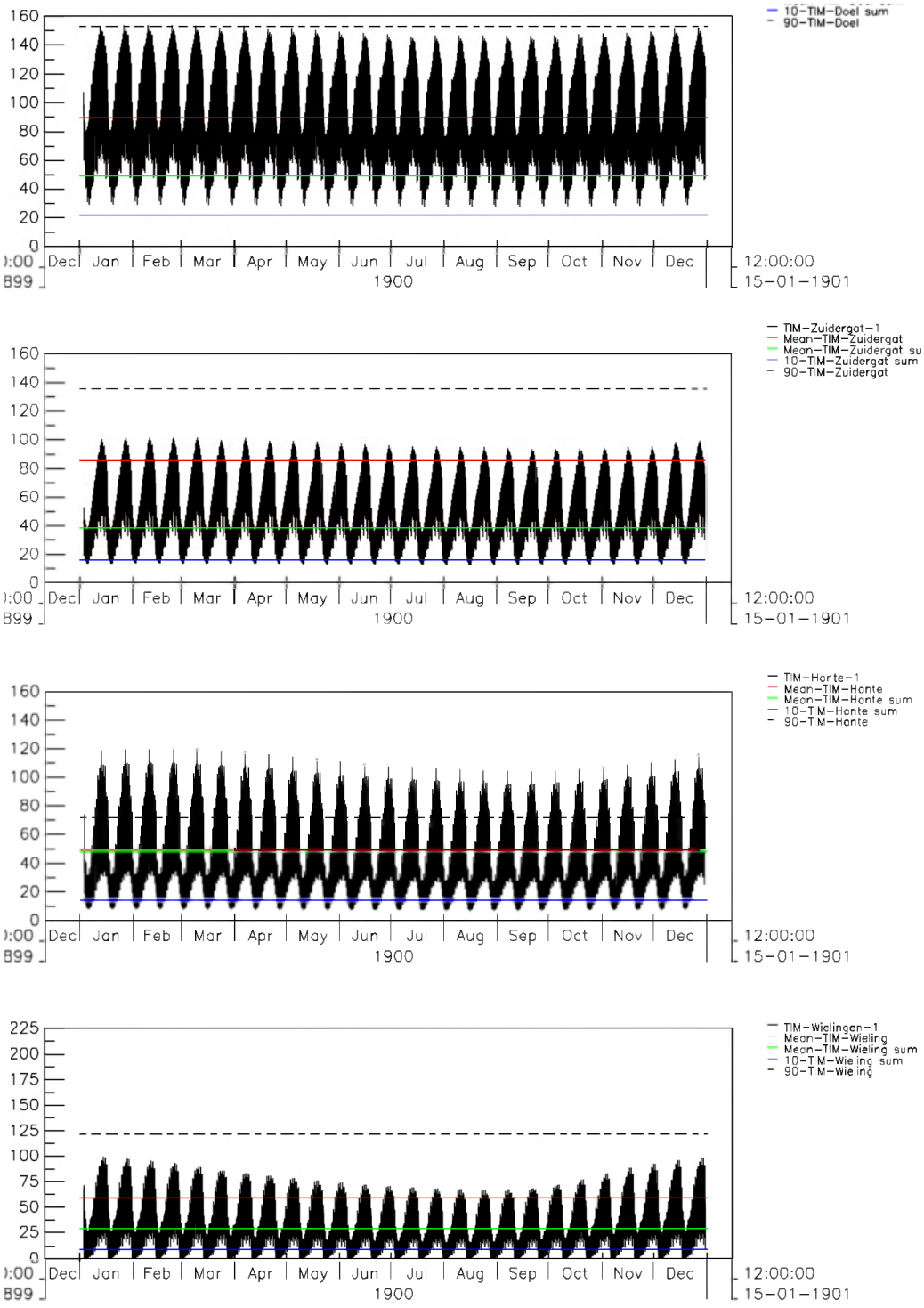

Figure B.6a: Computed SPM surface concentration at 4 stations along the Scheldt estuary for a simulation with original sediment loads (ws20). Observed mean levels are indicated with horizontal lines. In blue: 10-percentile level; in green: mean summer level; in red: mean winter level; dashed black: 90-percentile level.

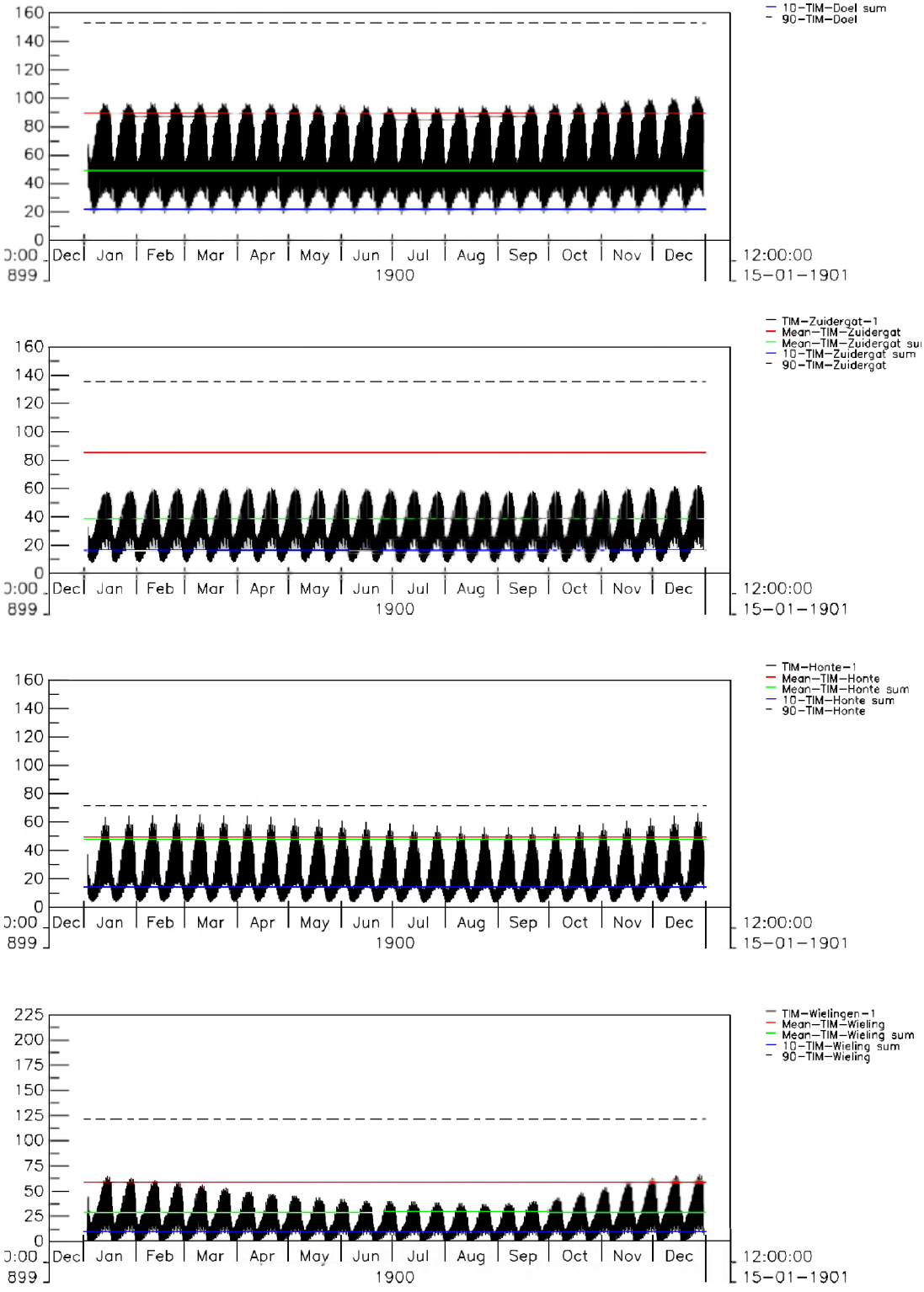

Figure B.6b: Computed SPM surface concentration at 4 stations along the Scheldt estuary for a simulation with reduced sediment loads and enhanced harbour siltation (ws24). Observed mean levels are indicated with horizontal lines. In blue: 10-percentile level; in green: mean summer level; in red: mean winter level; dashed black: 90-percentile level.

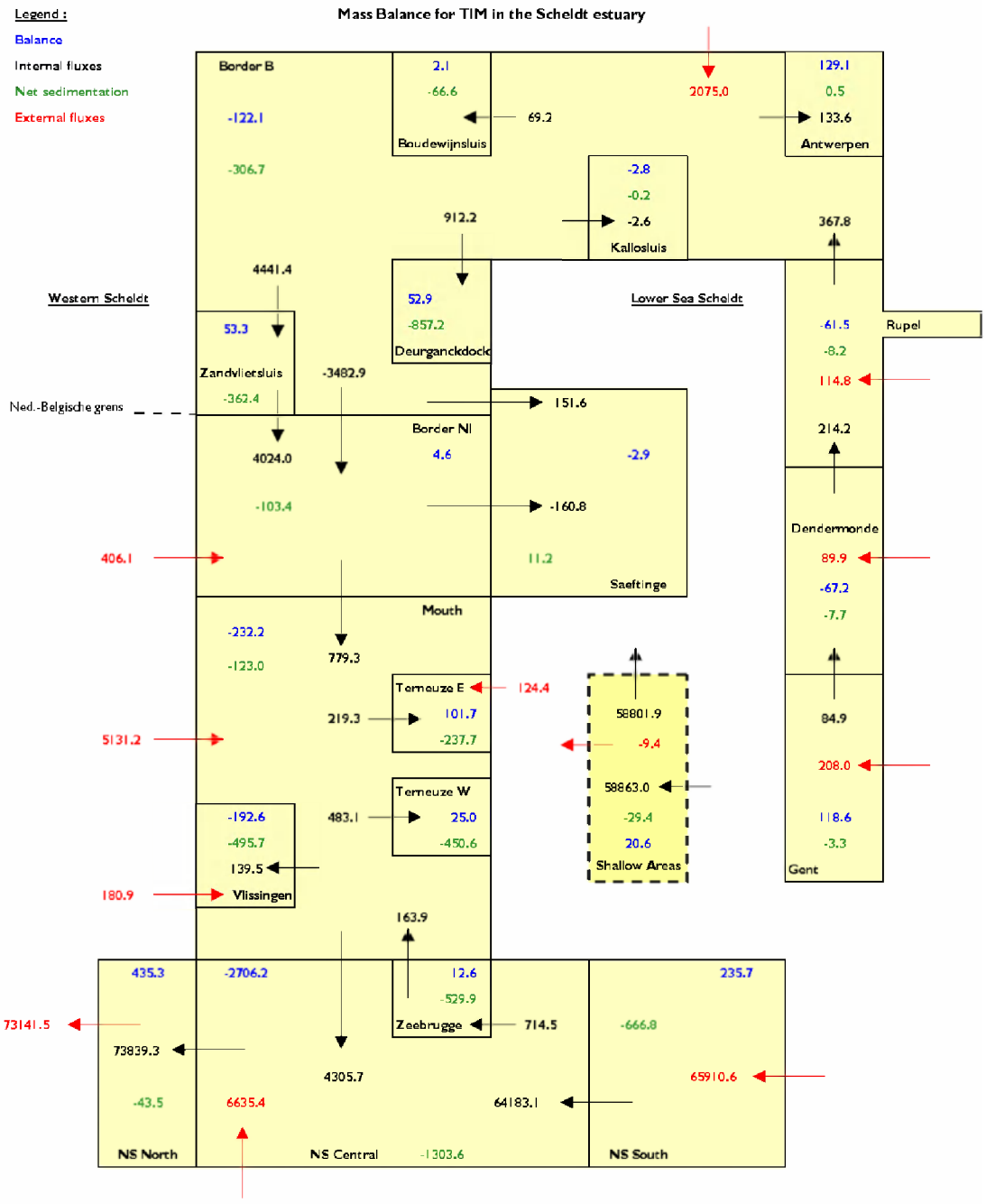

Figure B.6c: Mud balance (in kton/year) for simulation with original loads (ws20, winter conditions).

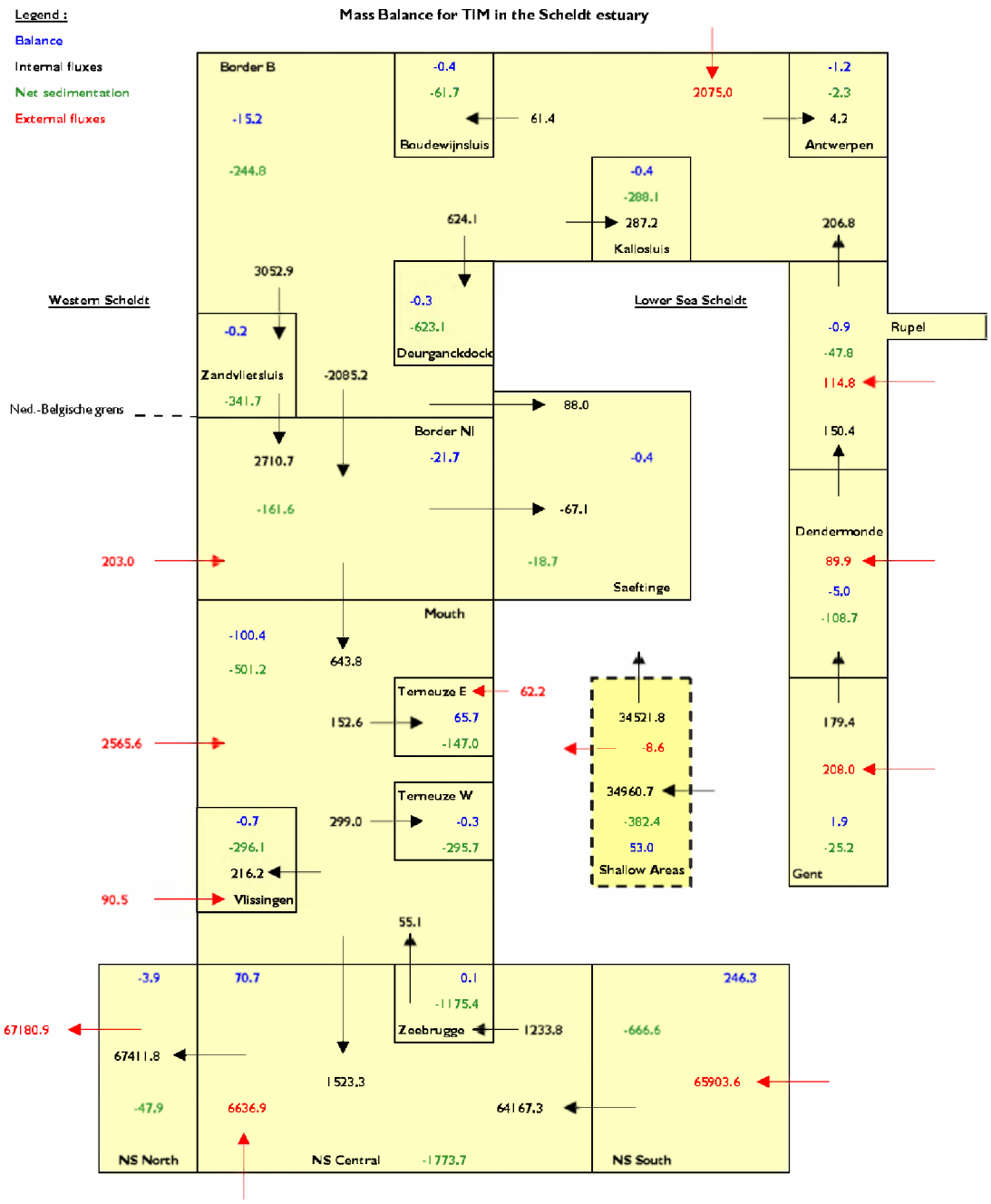

Figure B.6d: Mud balance (in kton/year) for simulation with reduced loads and enhanced harbour siltation (ws24, winter conditions)

B.7 Potential effect of shipping traffic

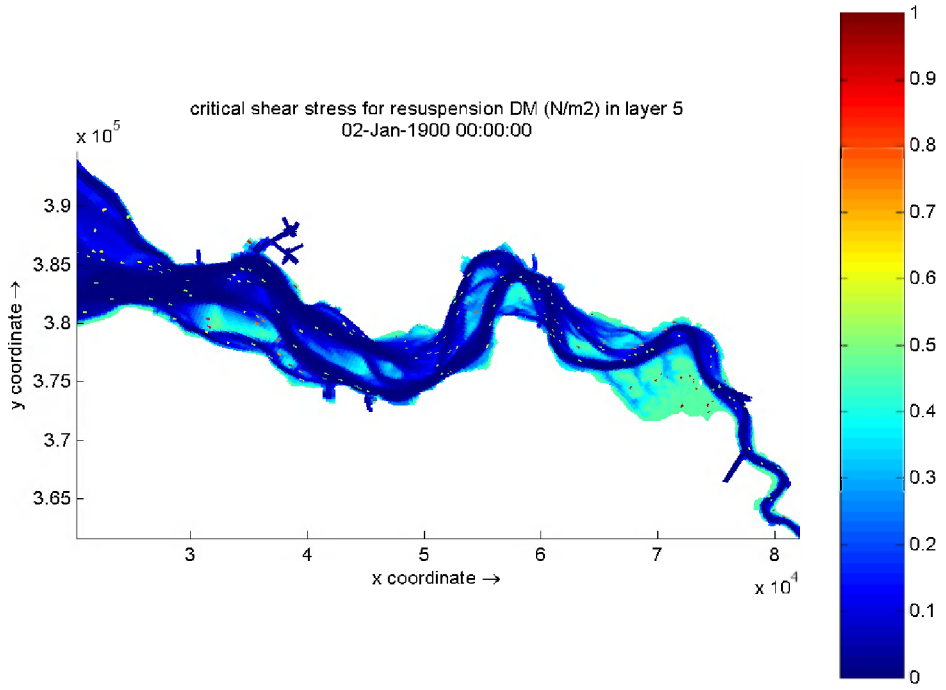

Fig. B.7a: Example of the actual total bed shear stress including ship movements (**ws27**). Dots signify the presence of ships (distributed randomly). $\Delta\tau$ = 0.5 Pa and p = 1%.

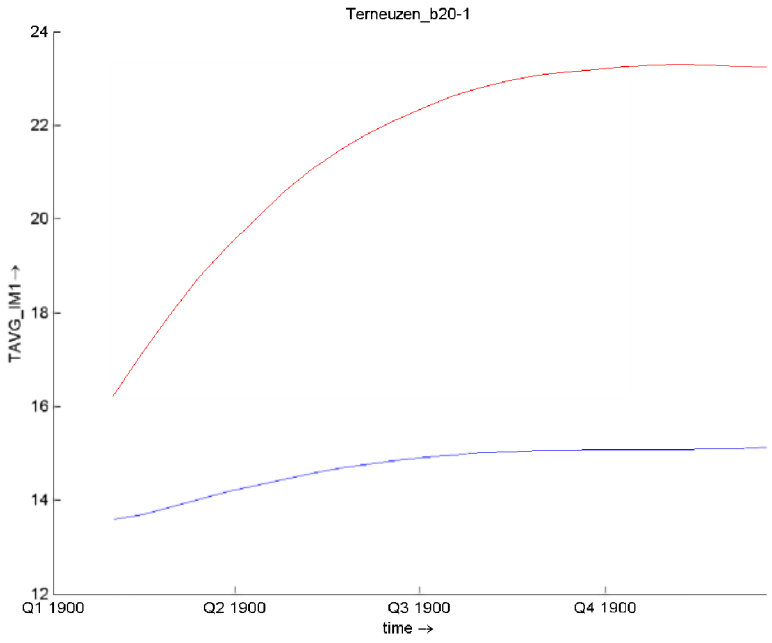

Fig. B.7b: 14-day average SPM surface concentration levels at DOW jetty, Terneuzen for a simulation without (**ws36**, blue line) and with (**ws37**, red line) ship movement (. $\Delta\tau$ = 0.5 Pa and p = 1%).

B.8 Comparison between 3-month and 14-day hydrodynamics

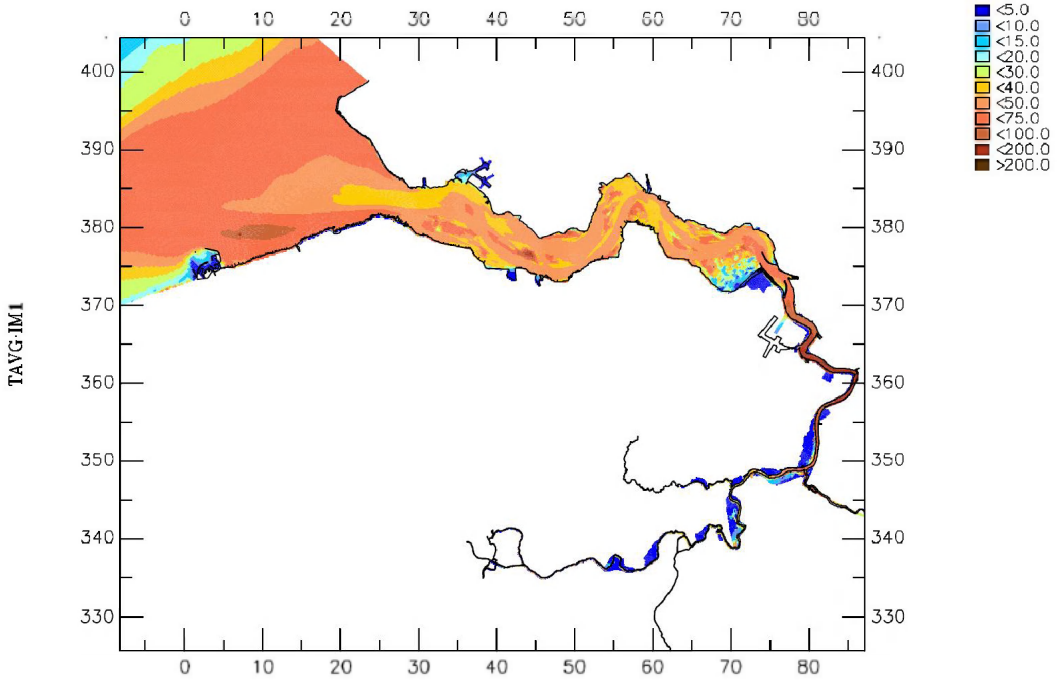

Figure B.8a: 14-day averaged SPM surface concentration (mg/l) at end of 3-month simulation (q03).

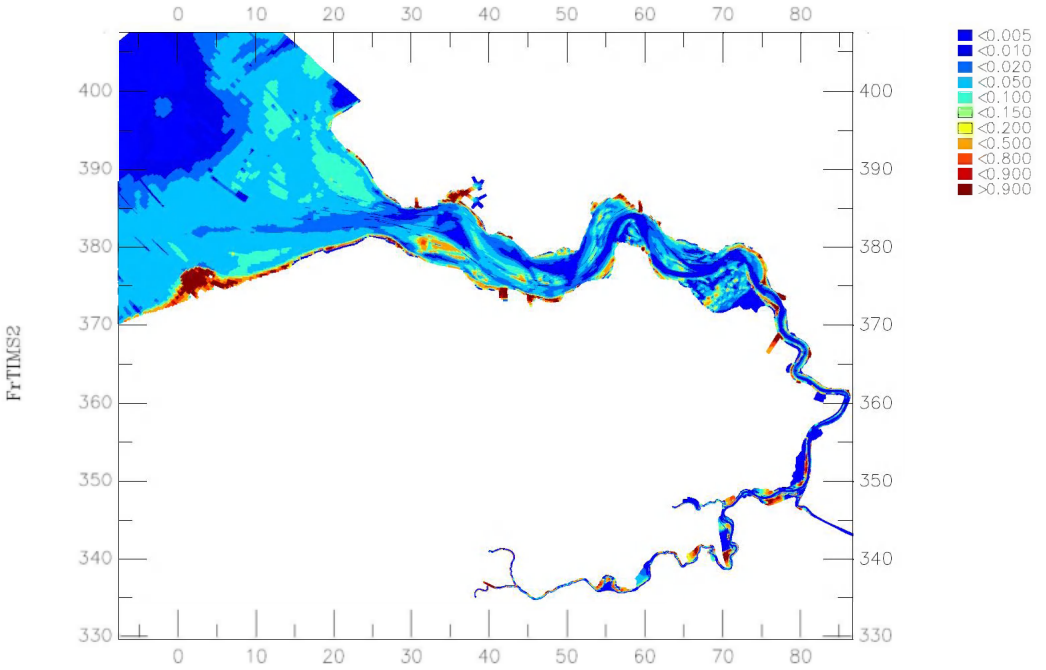

Figure B.8b: Mud fraction in sediment bed for 3-month simulation (q03).

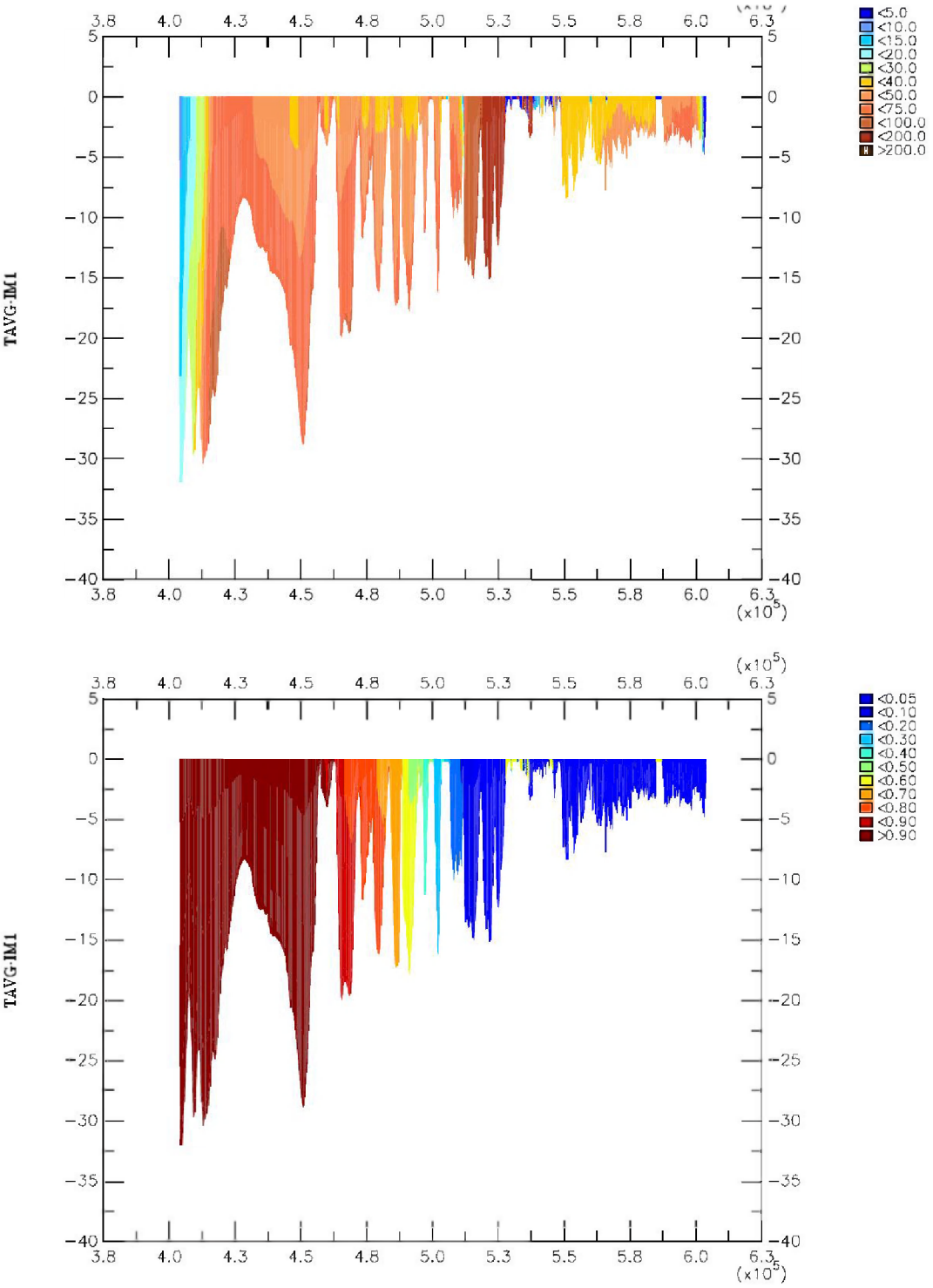

B.8c: surface: 14-day winter averaged vertical SPM concentration transect (mg/l) along the estuary (left = sea) for 3-month simulation (q03); bottom: fraction marine mud.

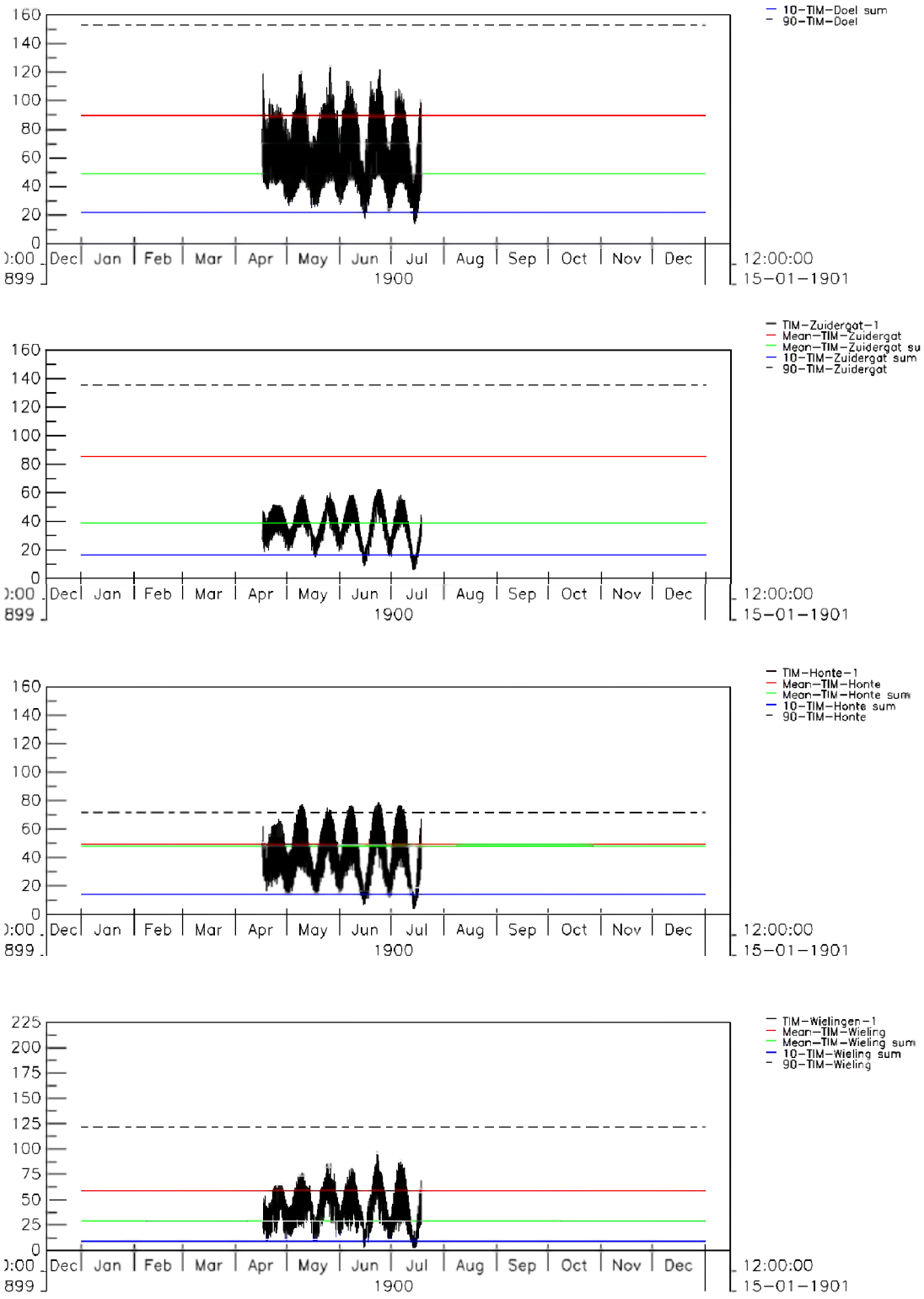

Figure B.8d: Computed SPM surface concentration at 4 stations along the Scheldt estuary for a 3-month simulation (q03). Observed mean levels are indicated with horizontal lines. In blue: 10-percentile level; in green: mean summer level; in red: mean winter level; dashed black: 90-percentile level..

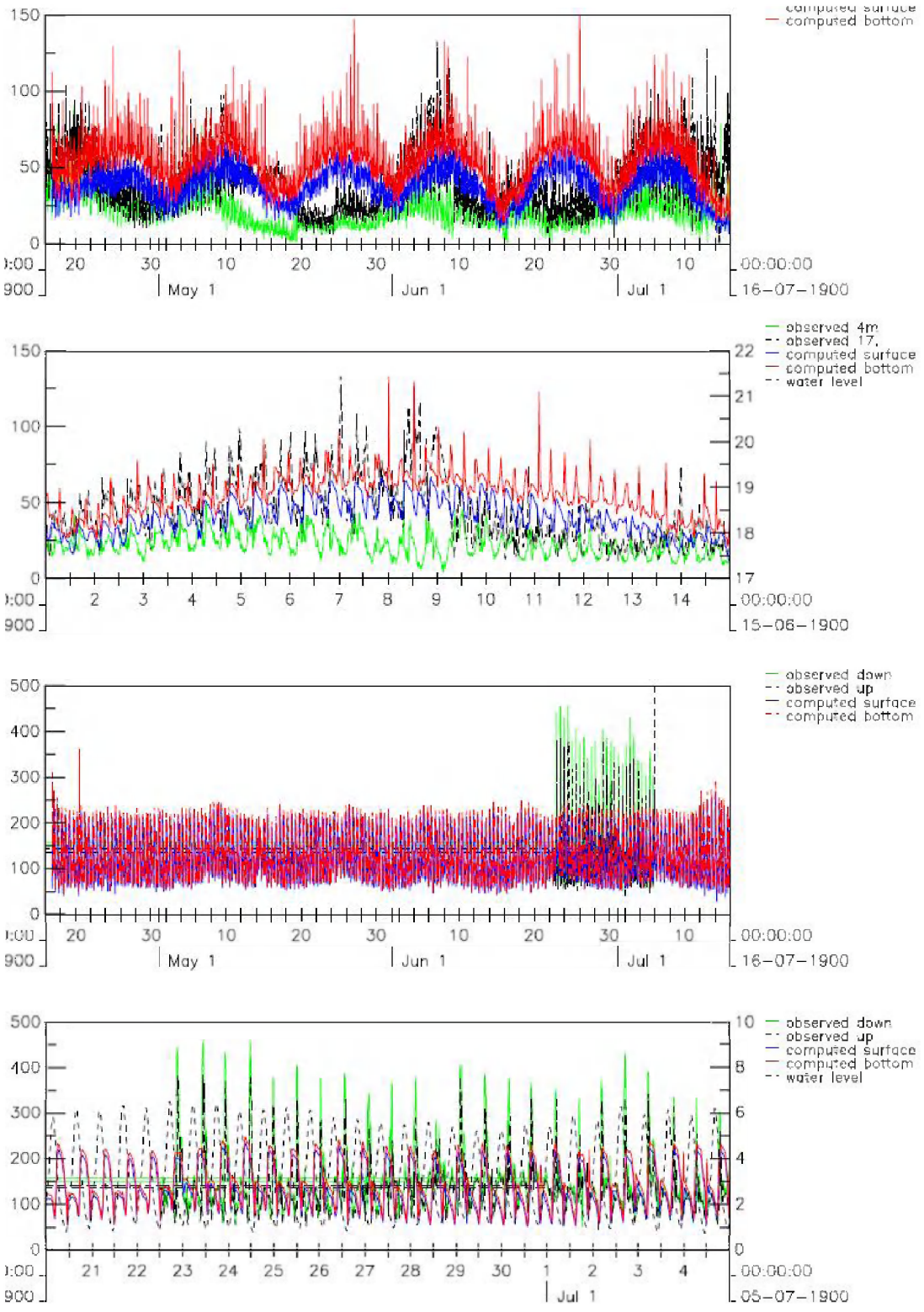

Figure B.8e: Mud : Computed SPM surface concentration at 2 stations along the Scheldt estuary for a 3-month simulation (q03). Upper two panels: at DOW-jetty; lower two panels: at Oosterweel. Observations are included in green (surface) and black (bottom).

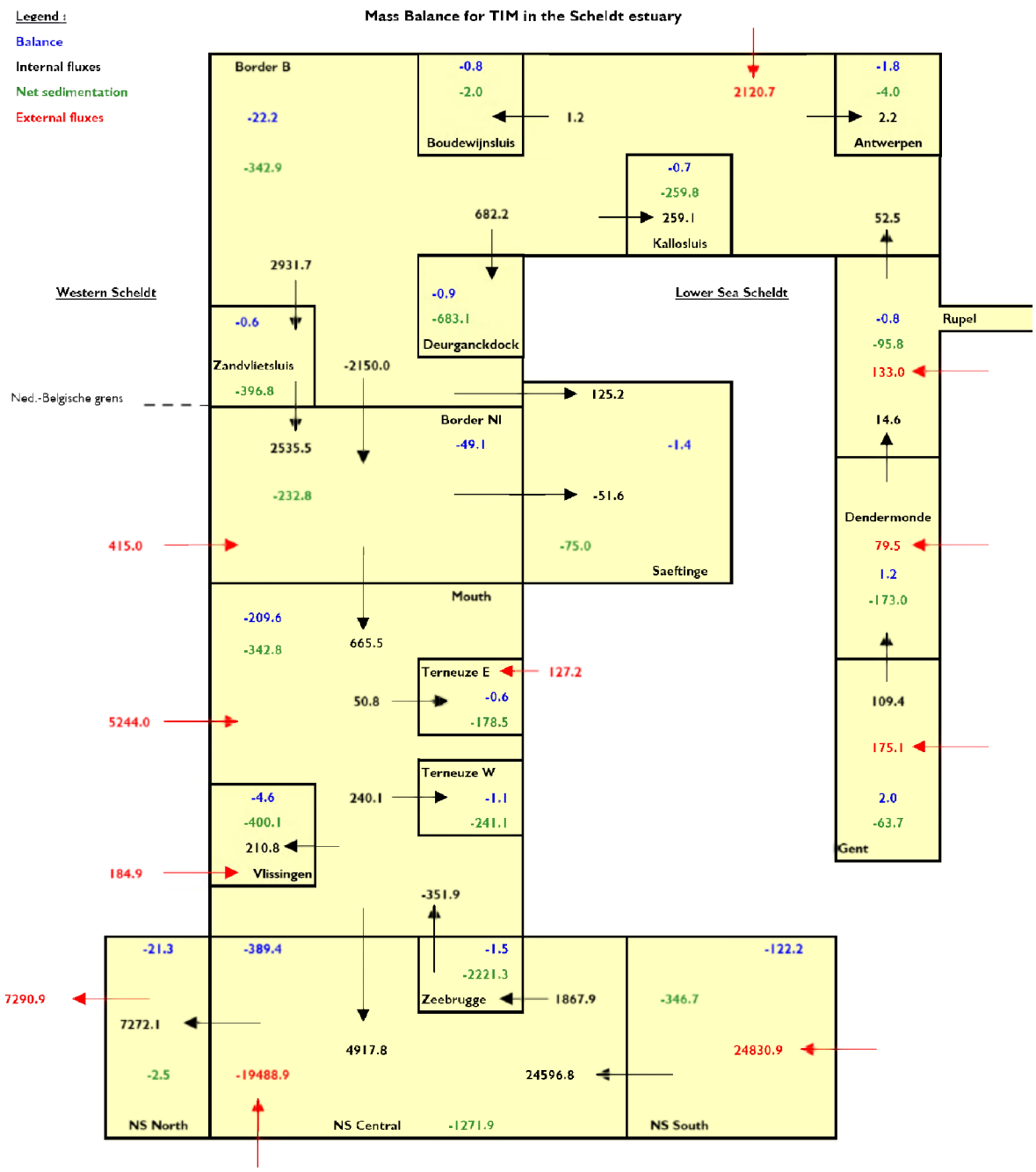

Figure B.8f: Mud balance for simulation Jan – Mar 2003 (q03), expressed in kton/year.

B.9 Validation with improved 3-month hydrodynamics

B.9.1 Large-scale variation

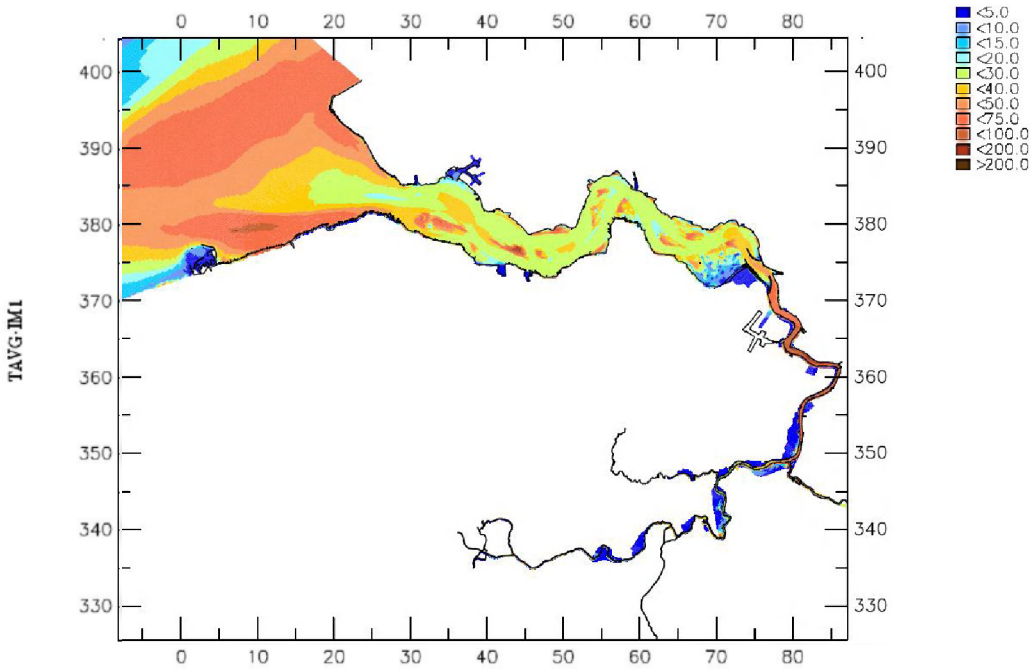

Figure B.9.1a: 14-day averaged SPM surface concentration (mg/l) at end of 3-month simulation (q05a).

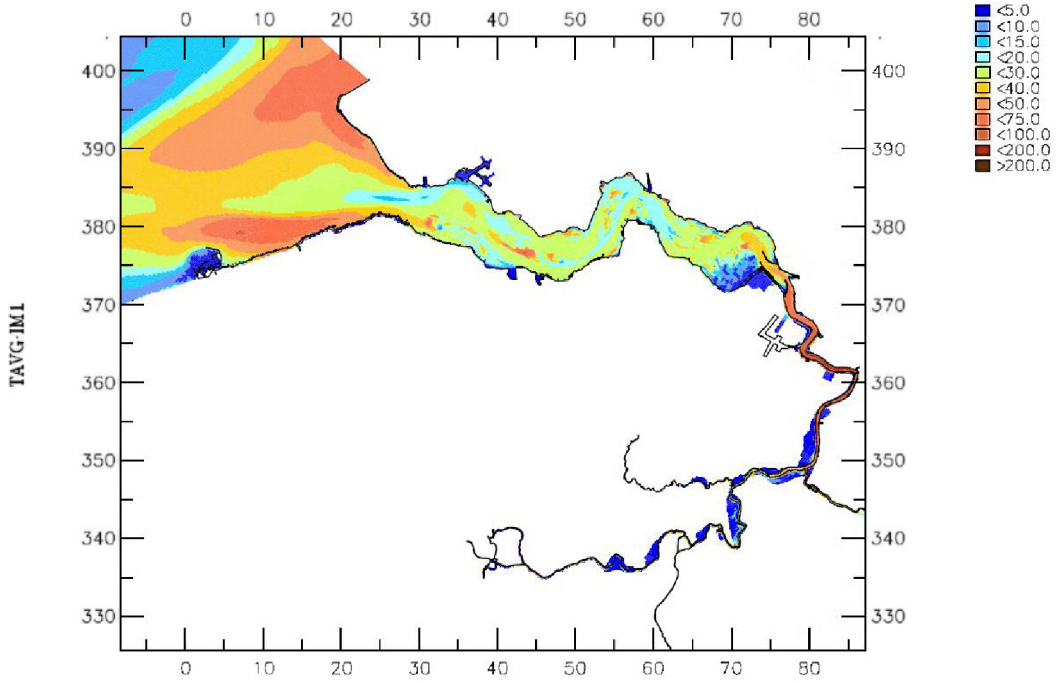

Figure B.9.1b: 14-day averaged SPM surface concentration (mg/l) at end of 3-month simulation (q06).

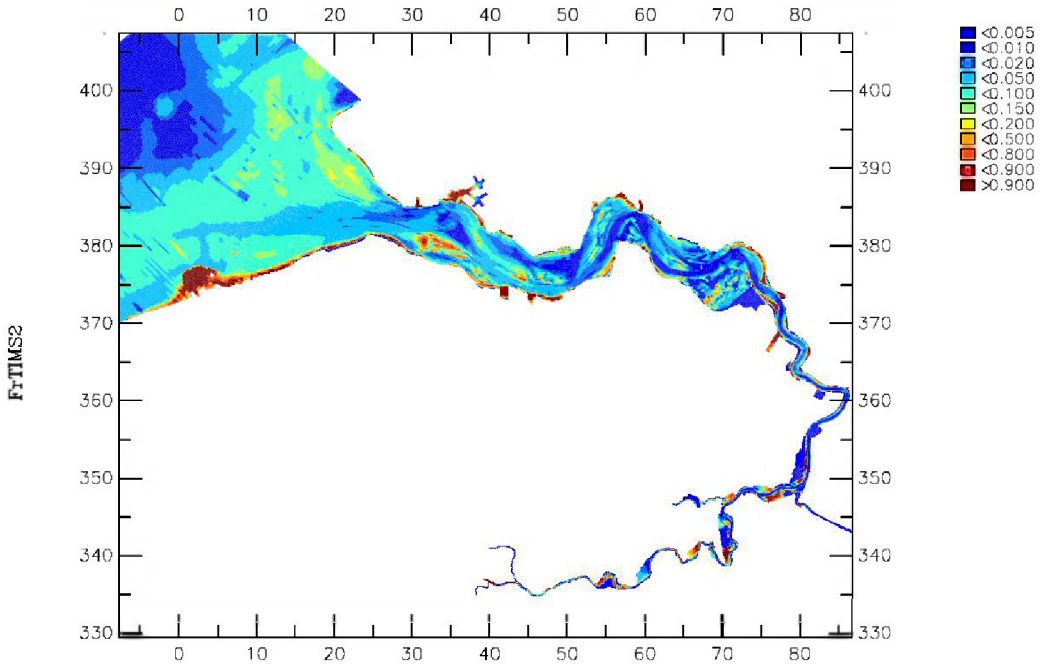

Figure B.9.1c: Mud fraction in sediment bed for 3-month simulation (q05a).

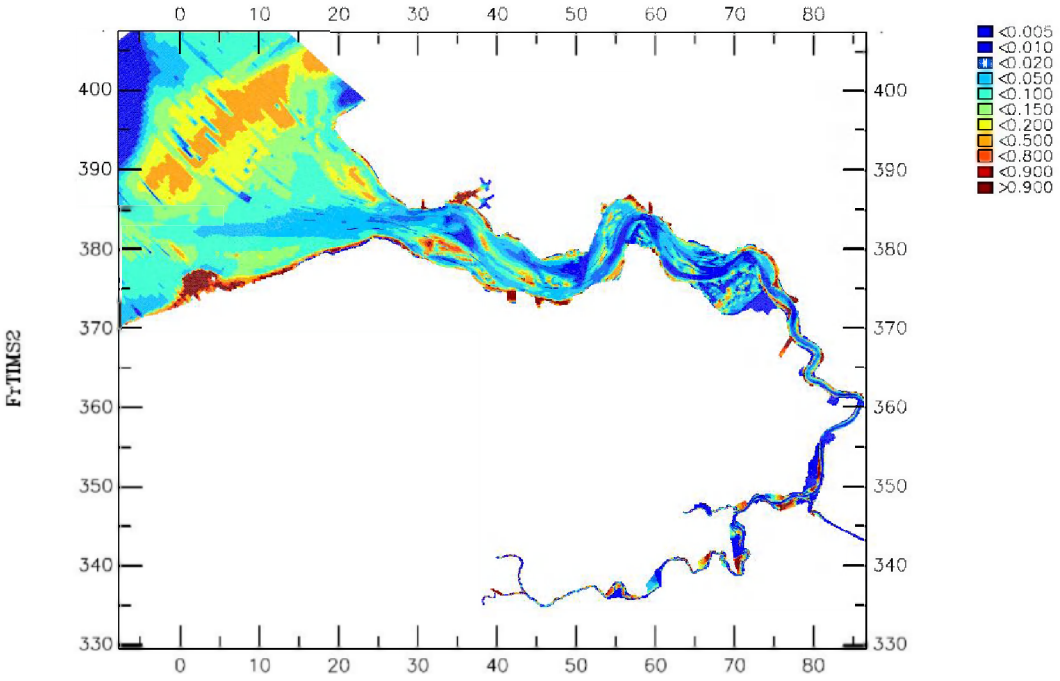

Figure B.9.1d: Mud fraction in sediment bed for 3-month simulation (q06).

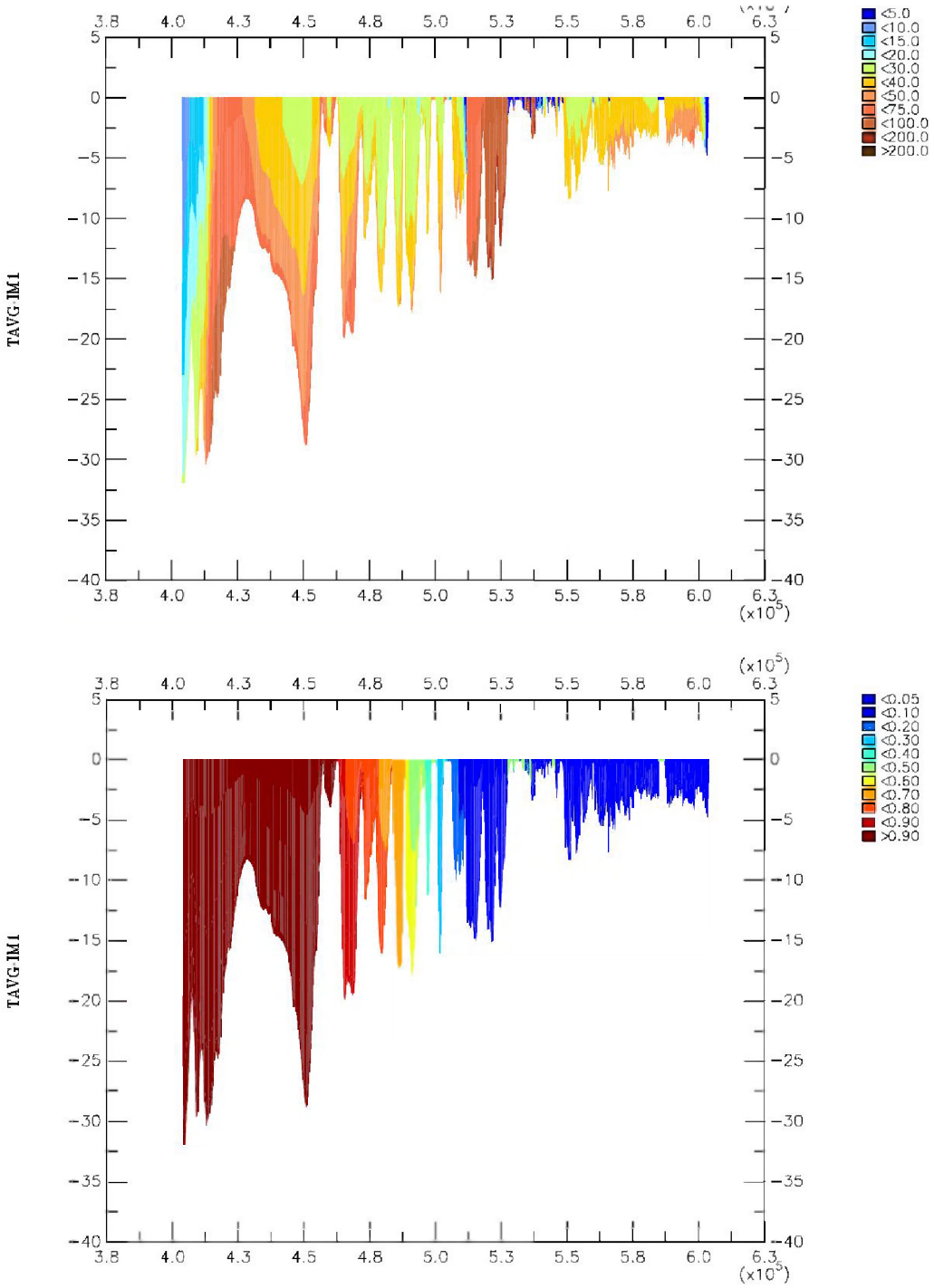

B.9.1e: surface: 14-day winter averaged vertical SPM concentration transect (mg/l) along the estuary (left = sea) for 3-month simulation (q05a); bottom: fraction marine mud.

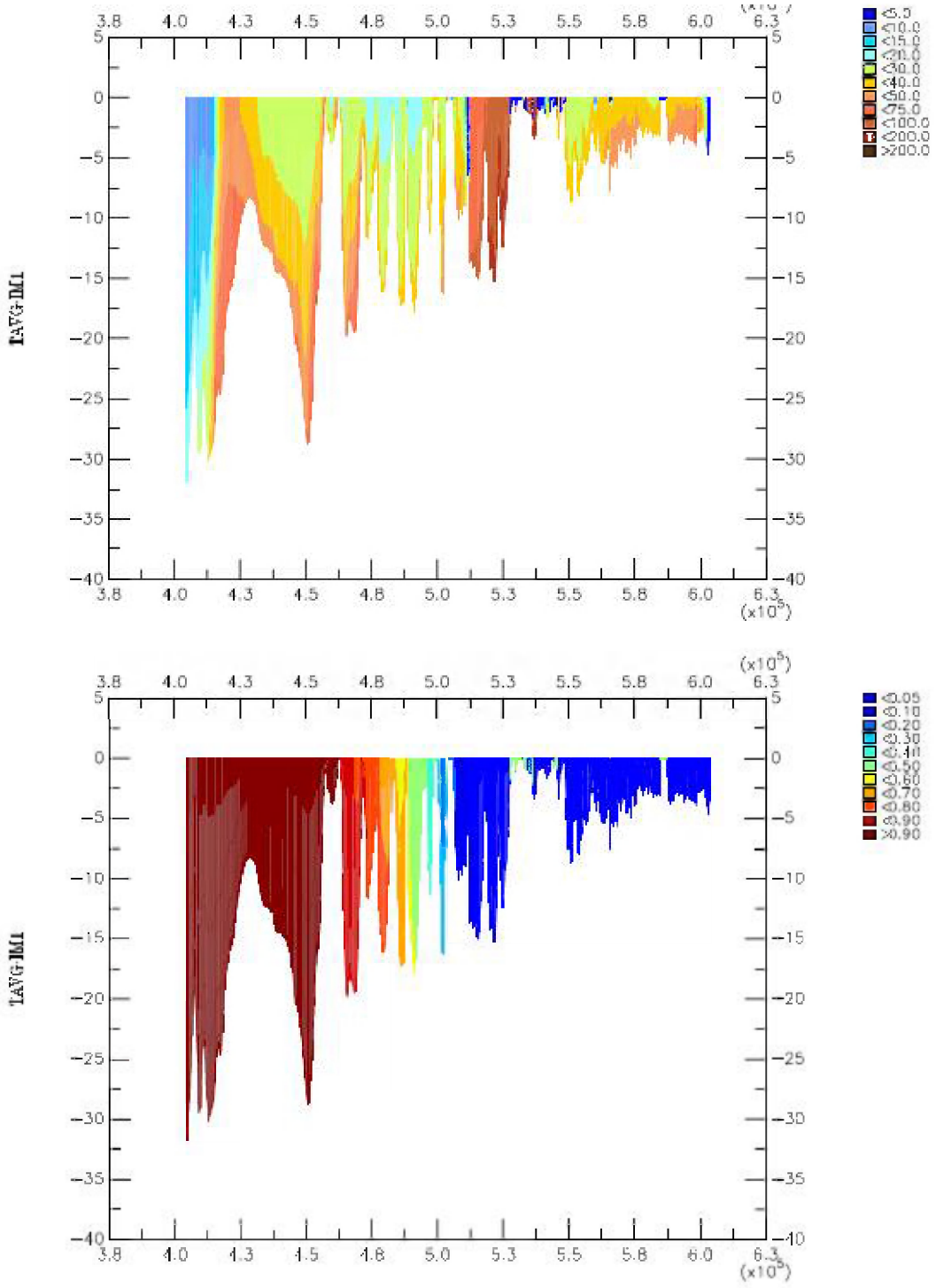

B.9.1f: surface: 14-day winter averaged vertical SPM concentration transect (mg/l) along the estuary (left = sea) for 3-month simulation (q06); bottom: fraction marine mud.

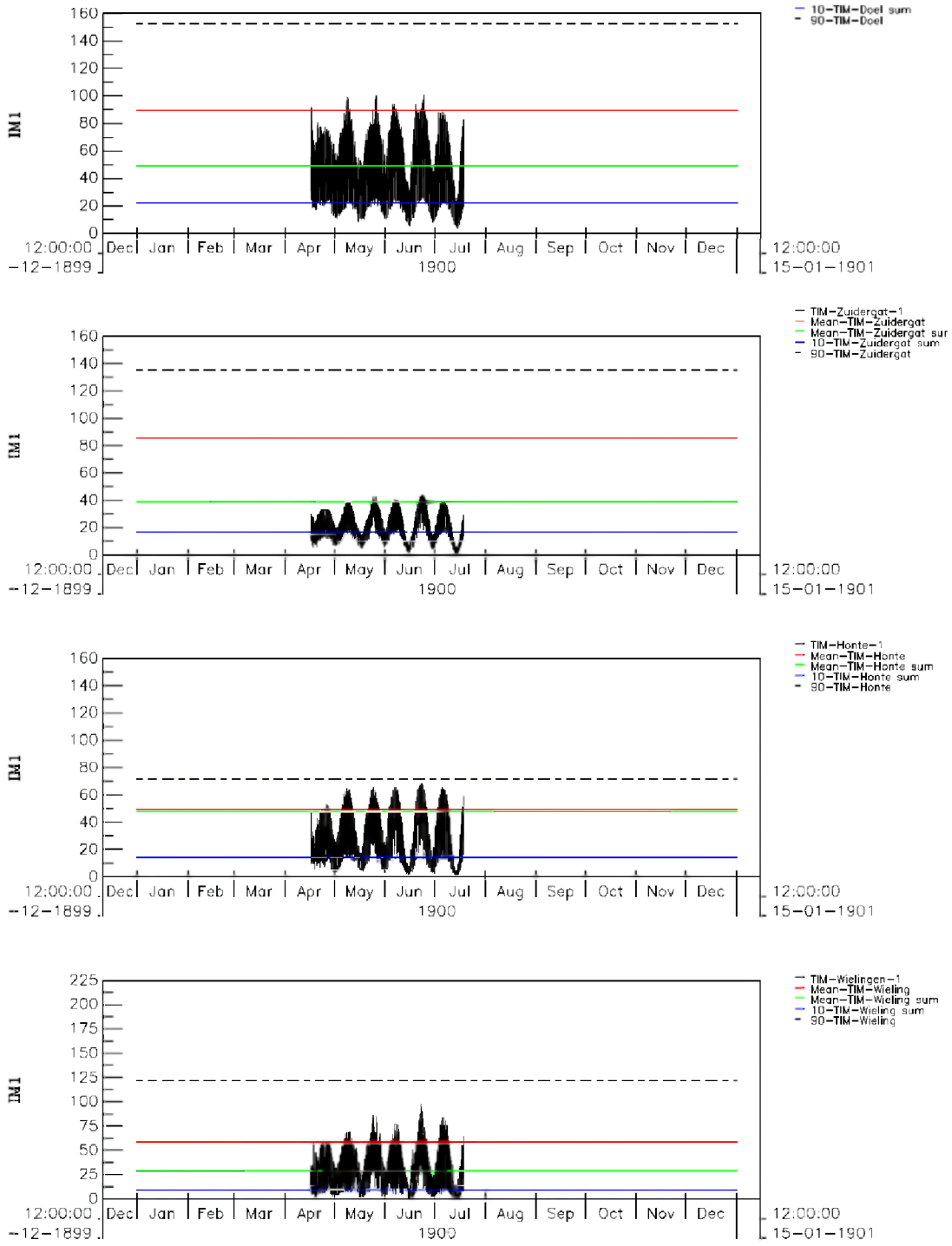

Figure B.9.1g: Computed SPM surface concentration at 4 stations along the Scheldt estuary for a 3-month simulation (q05a). Observed mean levels are indicated with horizontal lines. In blue: 10-percentile level; in green: mean summer level; in red: mean winter level; dashed black: 90-percentile level..

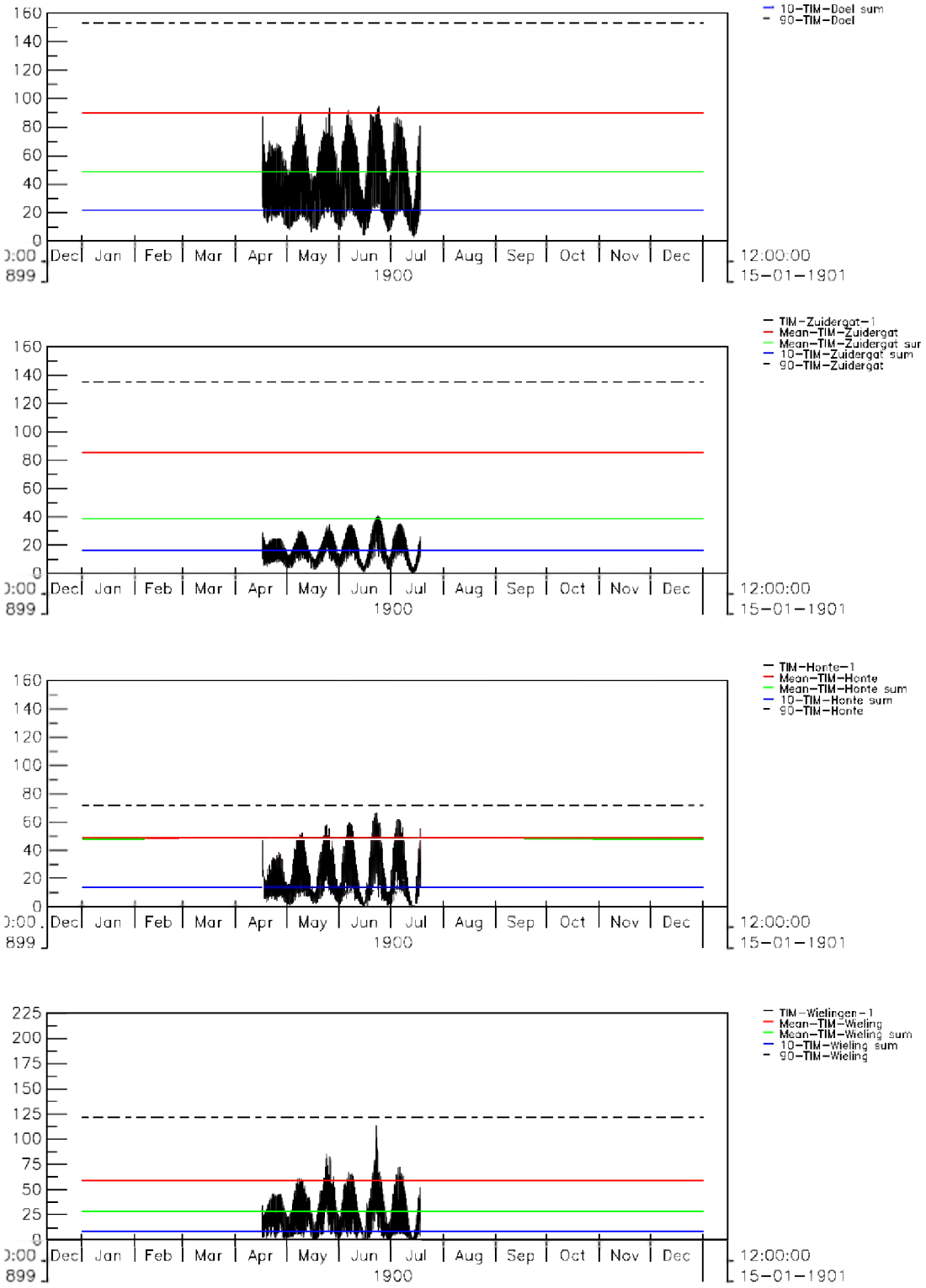

Figure B.9.1h: Computed SPM surface concentration at 4 stations along the Scheldt estuary for a 3-month simulation (q06). Observed mean levels are indicated with horizontal lines. In blue: 10-percentile level; in green: mean summer level; in red: mean winter level; dashed black: 90-percentile level..

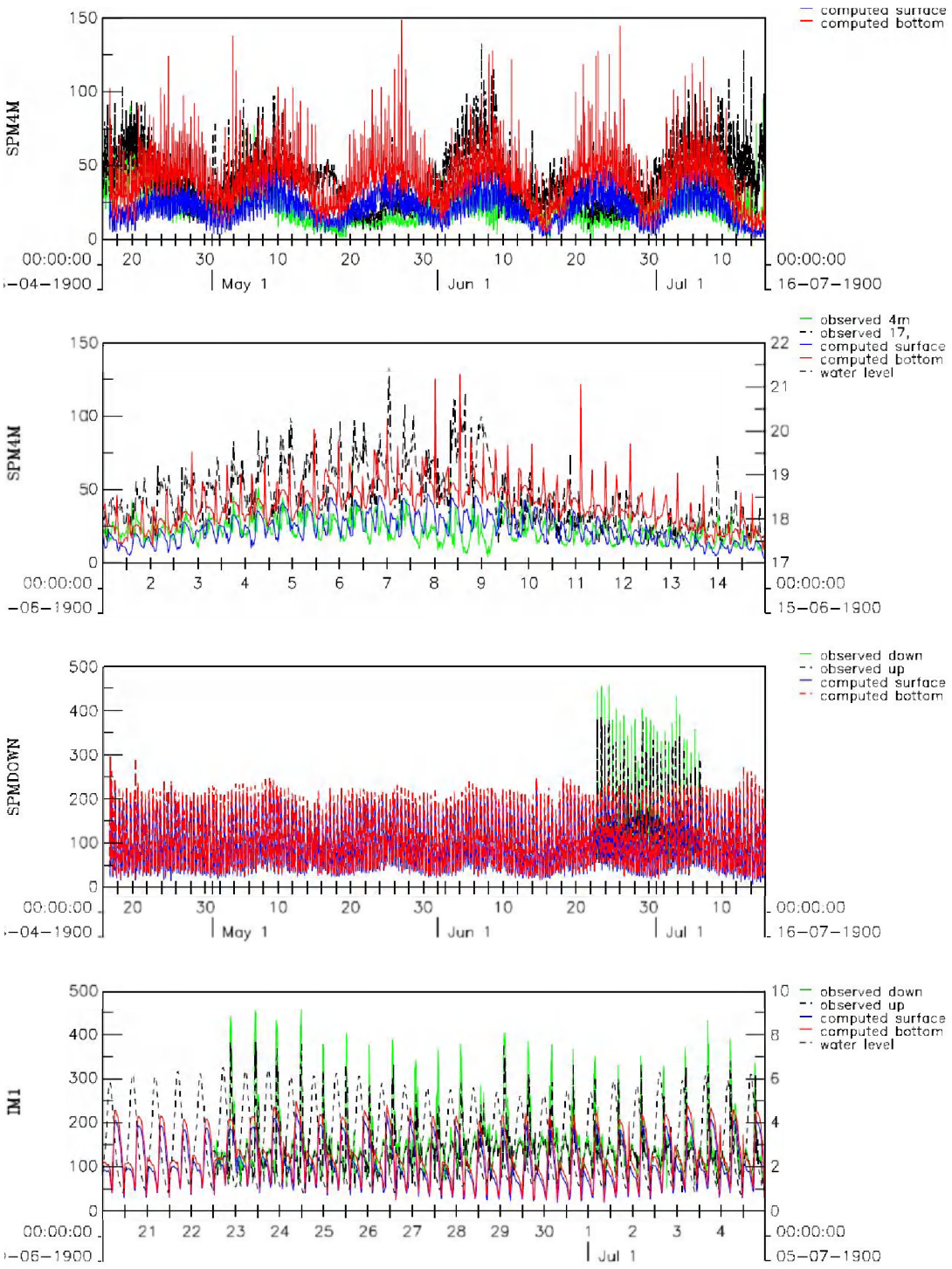

Figure B.9.1i: Mud : Computed SPM surface concentration at 2 stations along the Scheldt estuary for a 3-month simulation (q05a). Upper two panels: at DOW-jetty; lower two panels: at Oosterweel. Observations are included in green (surface) and black (bottom).

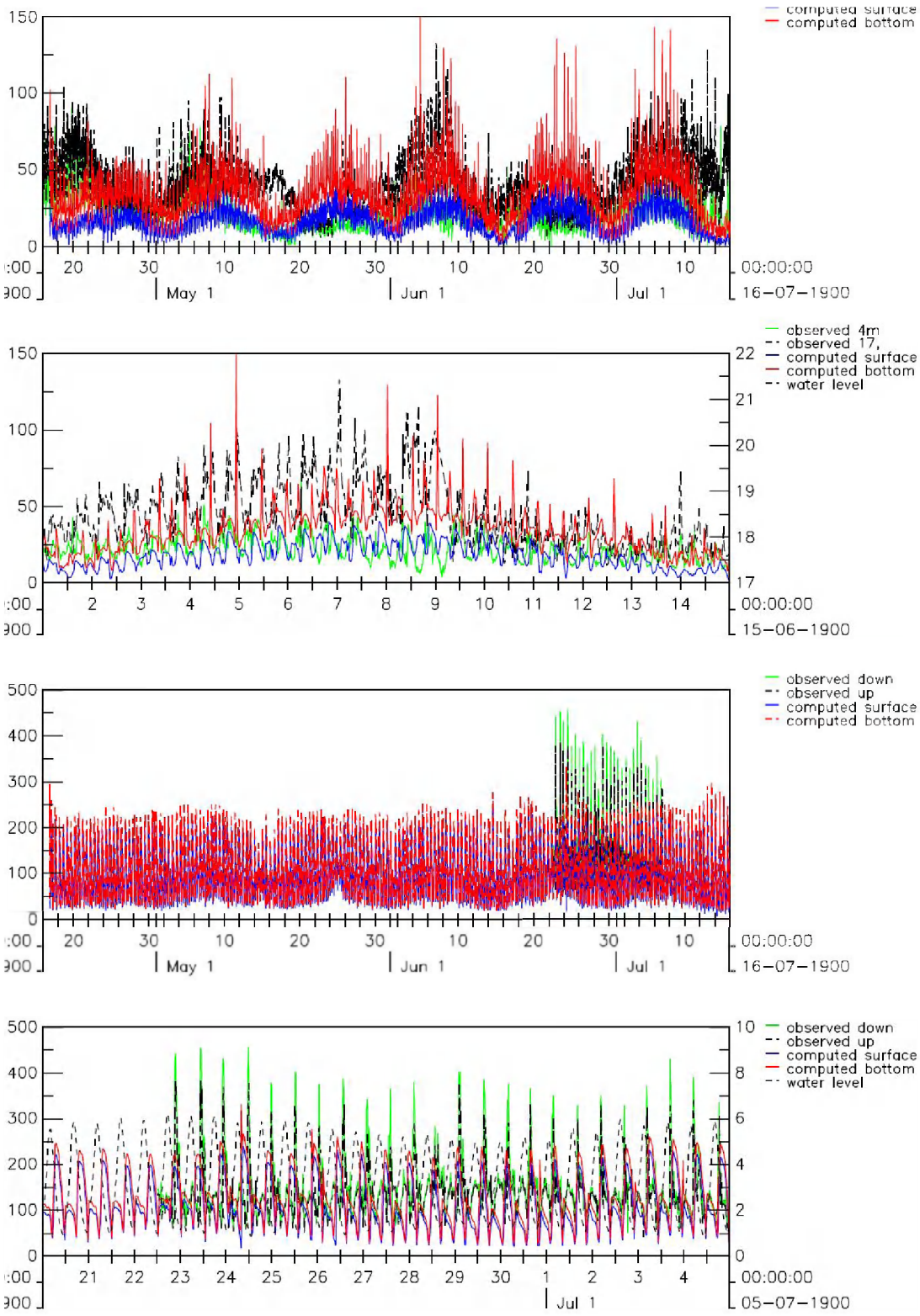

Figure B.9.1j: Mud : Computed SPM surface concentration at 2 stations along the Scheldt estuary for a 3-month simulation (q06). Upper two panels: at DOW-jetty; lower two panels: at Oosterweel. Observations are included in green (surface) and black (bottom).

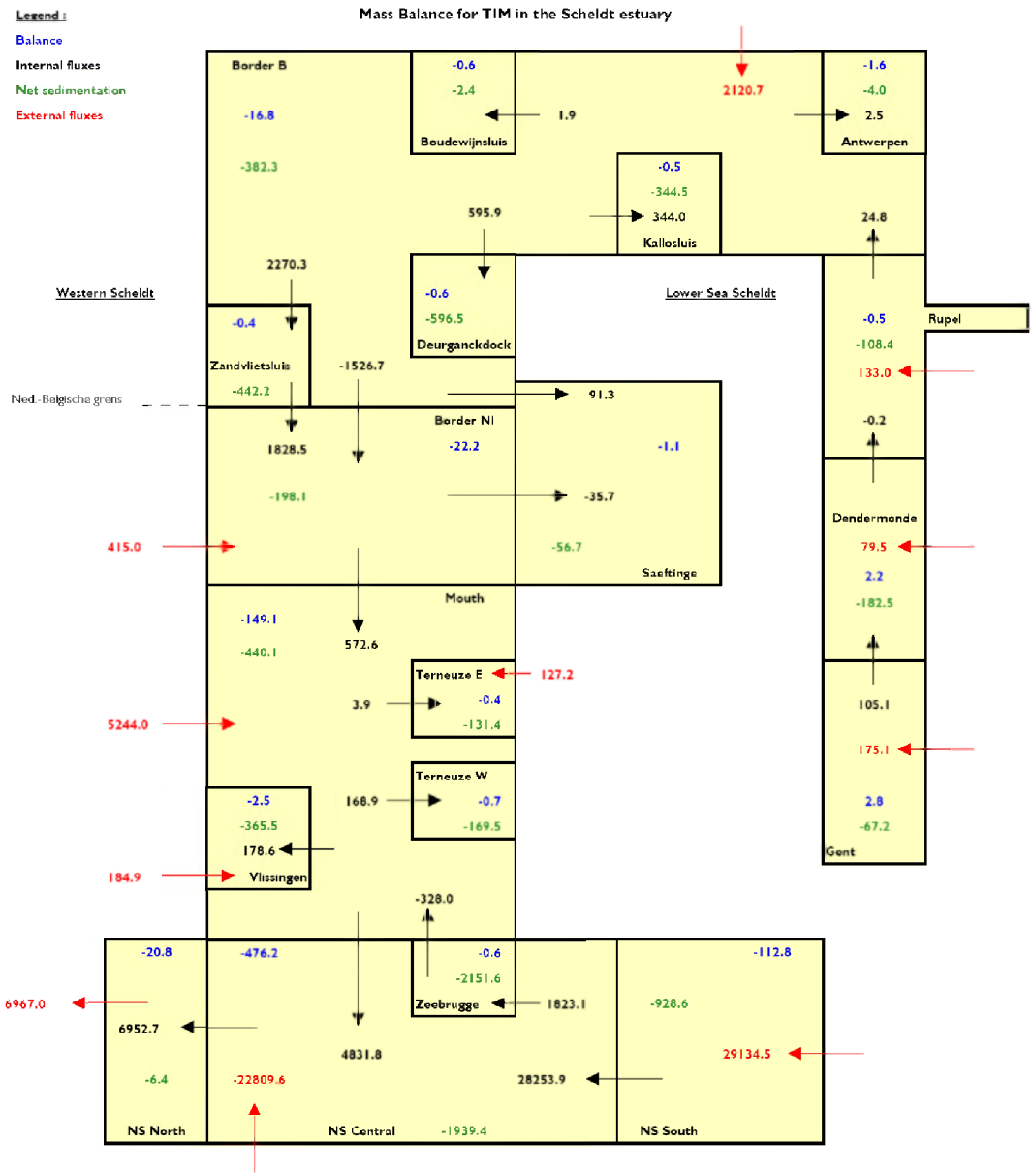

Figure B.9.1k: Mud balance for simulation Jan – Mar 2003 (q05a), expressed in kton/year.

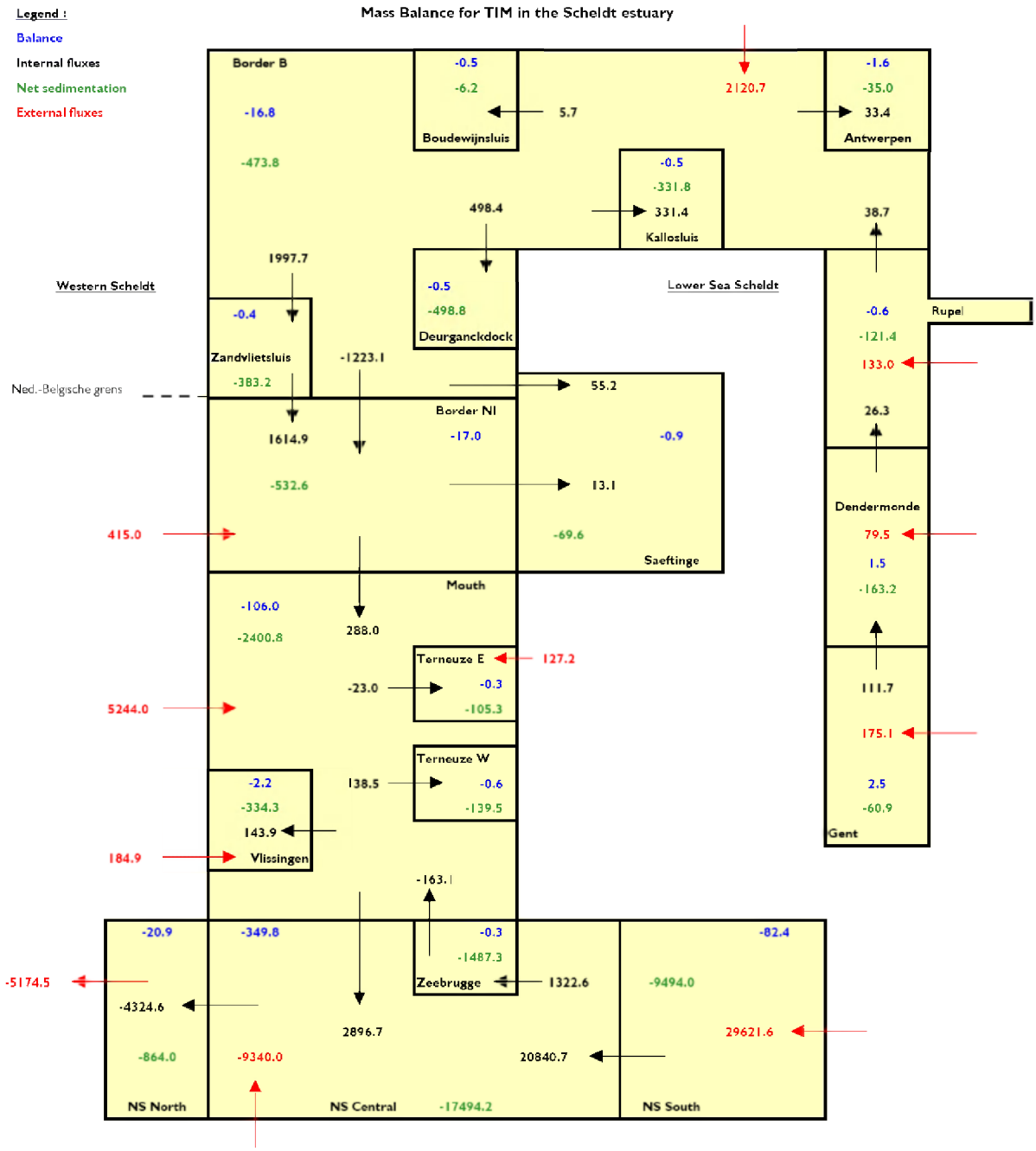

Figure B.9.11: Mud balance for simulation Jan – Mar 2003 (q06), expressed in kton/year.

B.9.2 Validation with observations at DOW-jetty Terneuzen

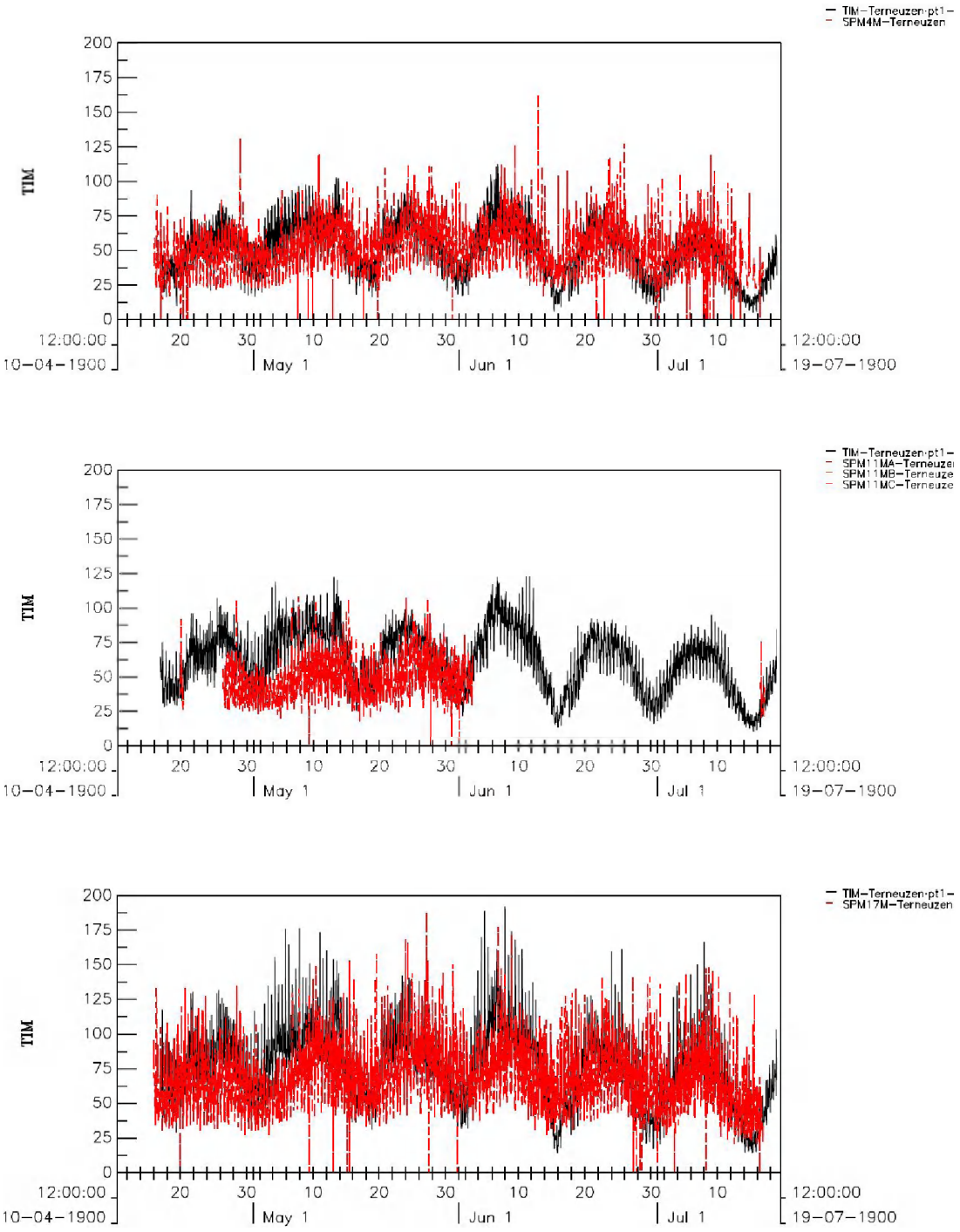

Figure B.9.2a: Computed SPM concentrations at DOW-jetty near Terneuzen for a 3-month period (q10). Observations are included in red and model results in black. Upper panel: obs. NAP-4m, model layer 1. Middle panel: obs. NAP-11m, model layer 2. Lower panel: obs. NAP-17m, model layer 4.

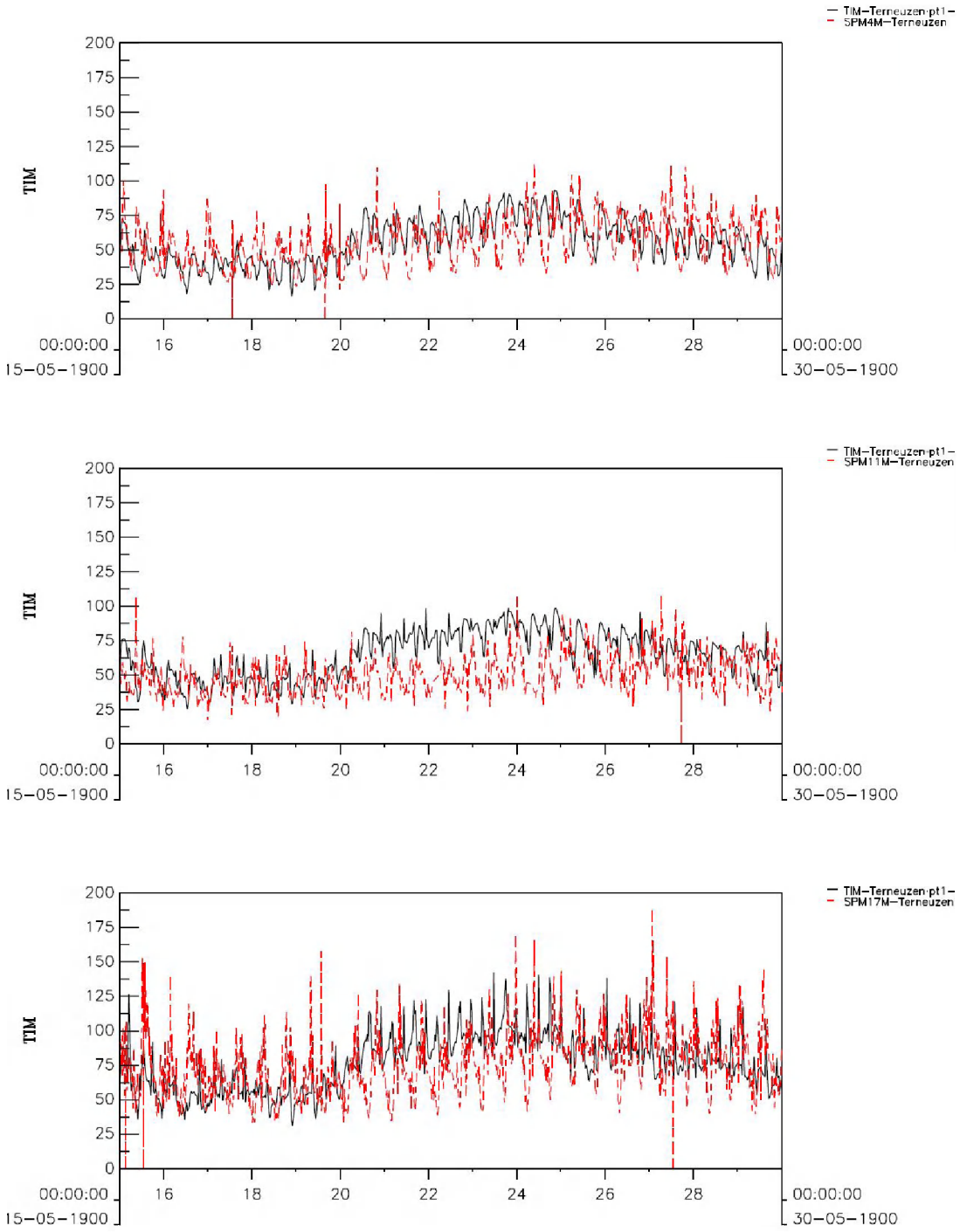

Figure B.9.2b: Computed SPM concentrations at DOW-jetty near Terneuzen for a neap-spring period (q10). Observations are included in red and model results in black. Upper panel: obs. NAP-4m, model layer 1. Middle panel: obs. NAP-11m, model layer 2. Lower panel: obs. NAP-17m, model layer 4.

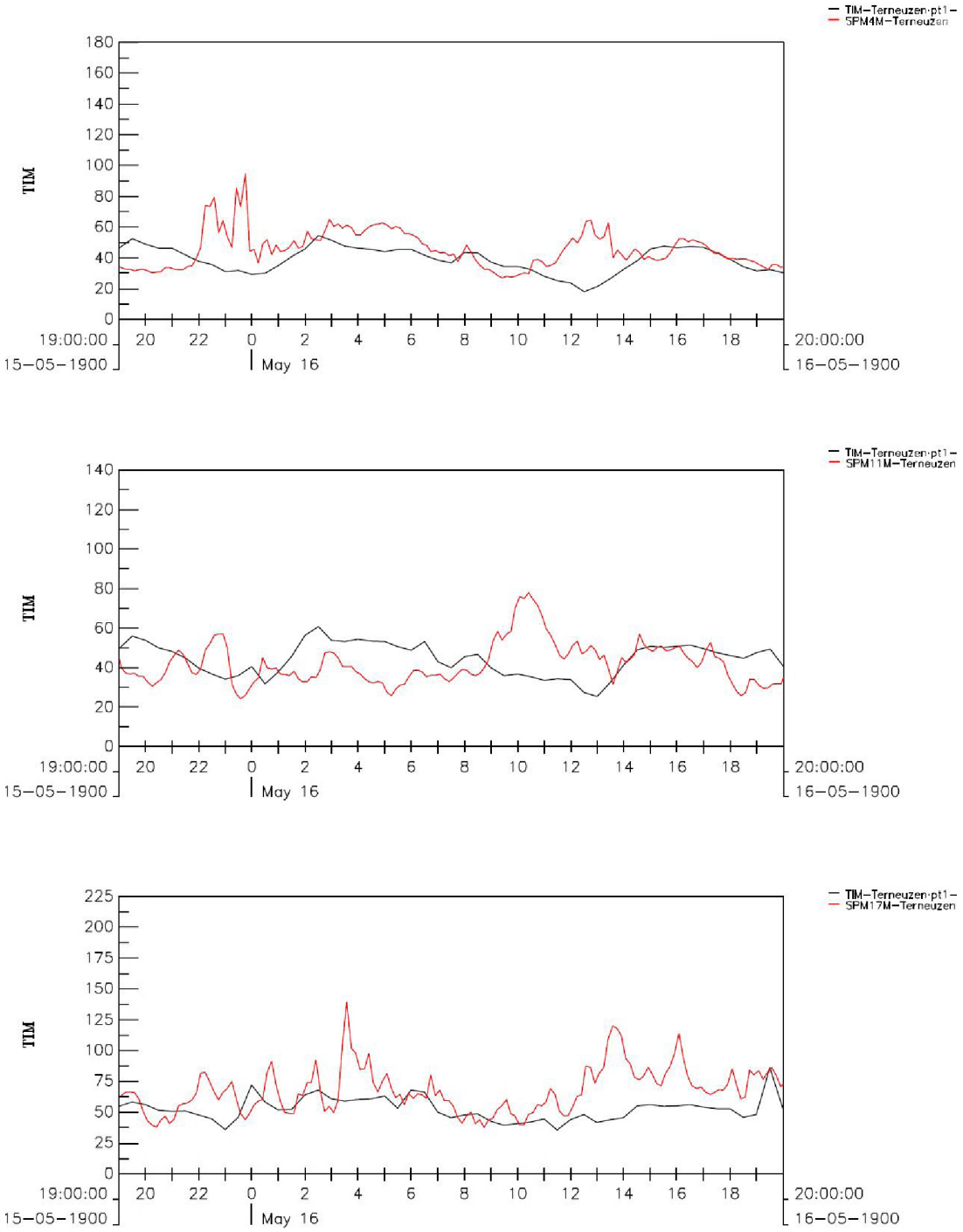

Figure B.9.2c: Computed SPM concentrations at DOW-jetty near Terneuzen for a neap tide (q10). Observations are included in red and model results in black. Upper panel: obs. NAP-4m, model layer 1. Middle panel: obs. NAP-11m, model layer 2. Lower panel: obs. NAP-17m, model layer 4.

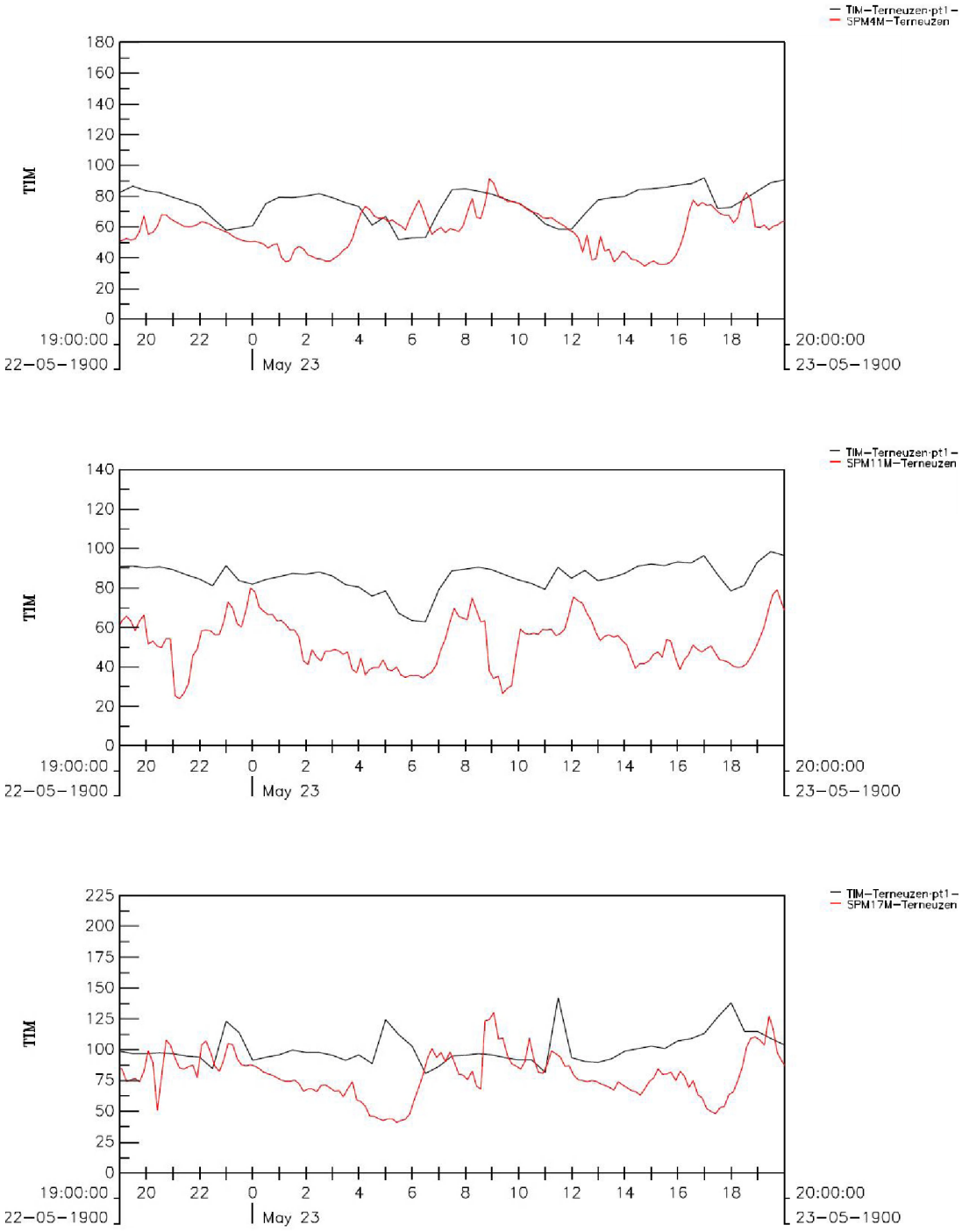

Figure B.9.2d: Computed SPM concentrations at DOW-jetty near Terneuzen for a spring tide (q10). Observations are included in red and model results in black. Upper panel: obs. NAP-4m, model layer 1. Middle panel: obs. NAP-11m, model layer 2. Lower panel: obs. NAP-17m, model layer 4.

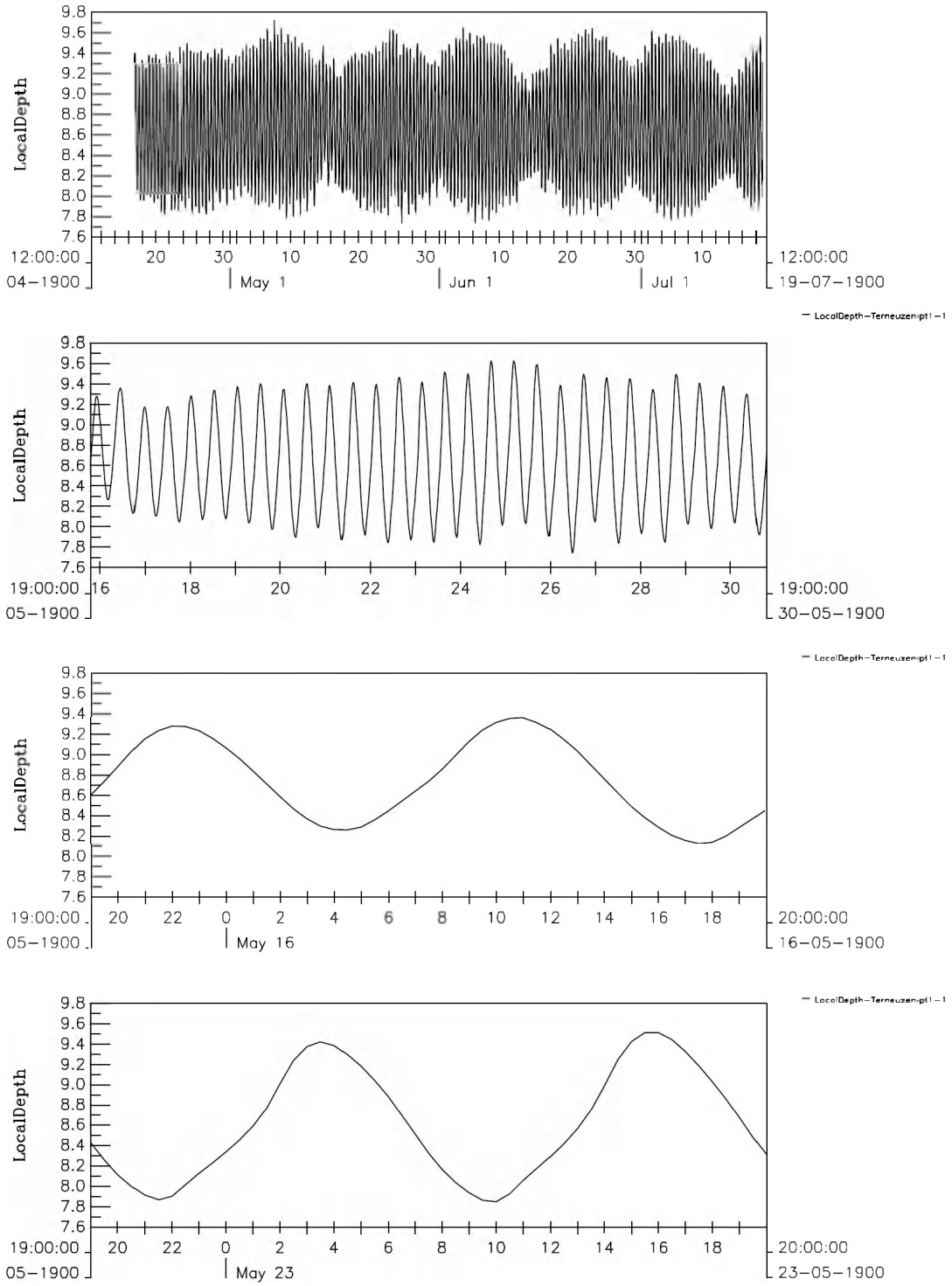

Figure B.9.2e: Computed water depth near Terneuzen (q10). First panel: 3 month period. Second panel: neap-spring period. Third panel: 25 hours during neap tide. Fourth panel: 25 hours during spring tide.

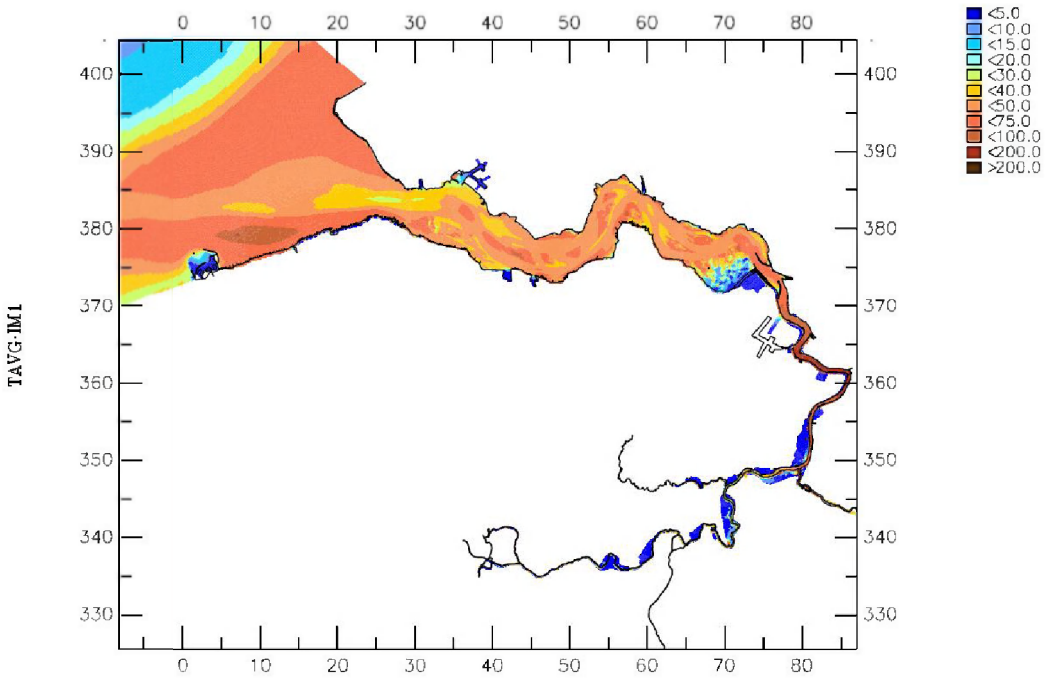

Figure B.9.2f: 14-day averaged SPM surface concentration (mg/l) at end of 3-month simulation (q10).

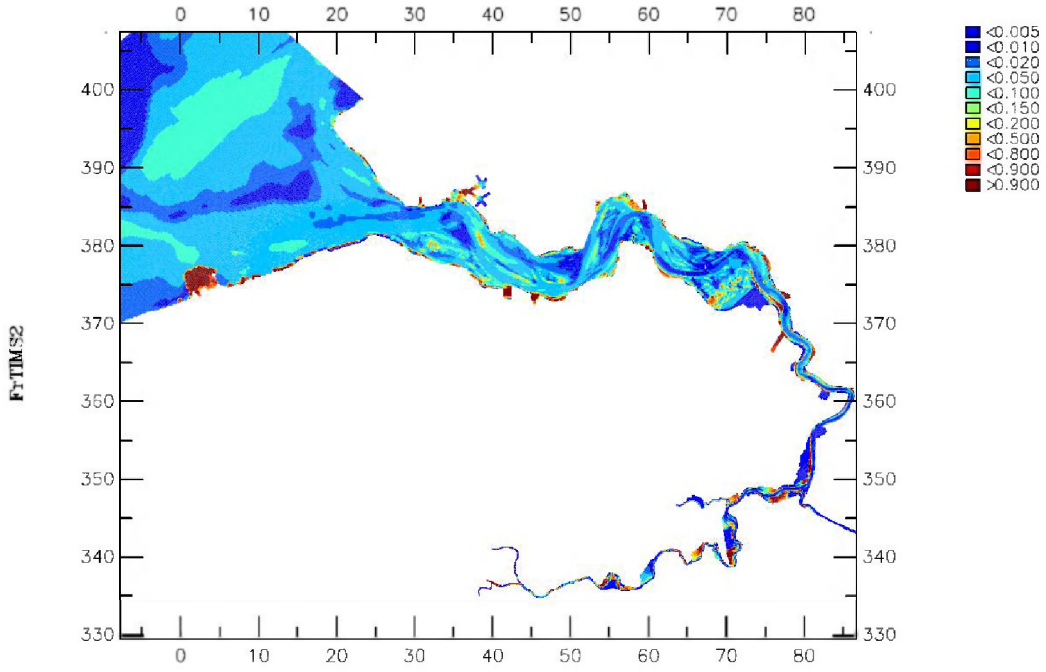

Figure B.9.2g: Mud fraction in sediment bed for 3-month simulation (q10).

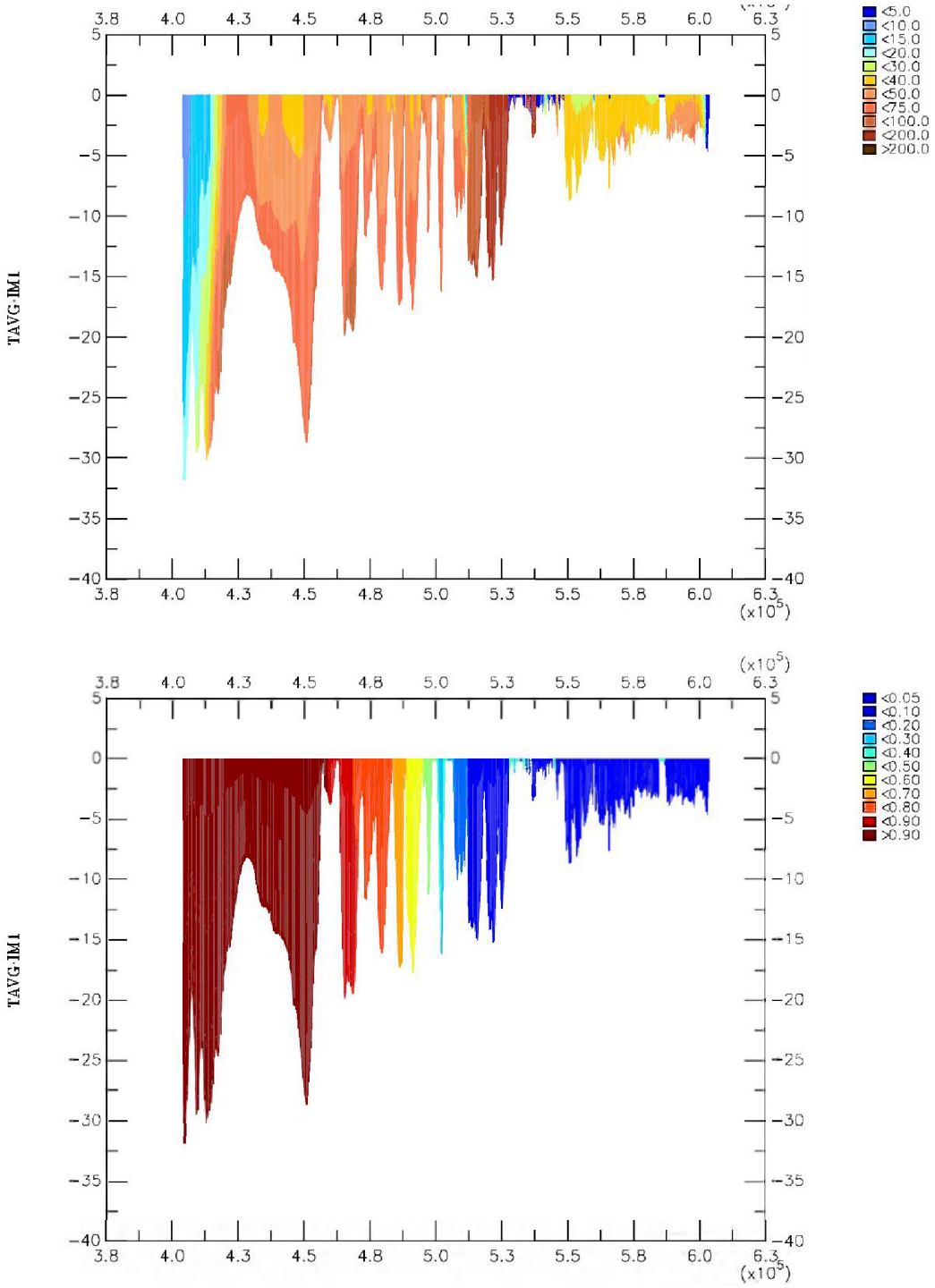

B.9.2h: surface: 14-day winter averaged vertical SPM concentration transect (mg/l) along the estuary (left = sea) for 3-month simulation (q10); bottom: fraction marine mud.

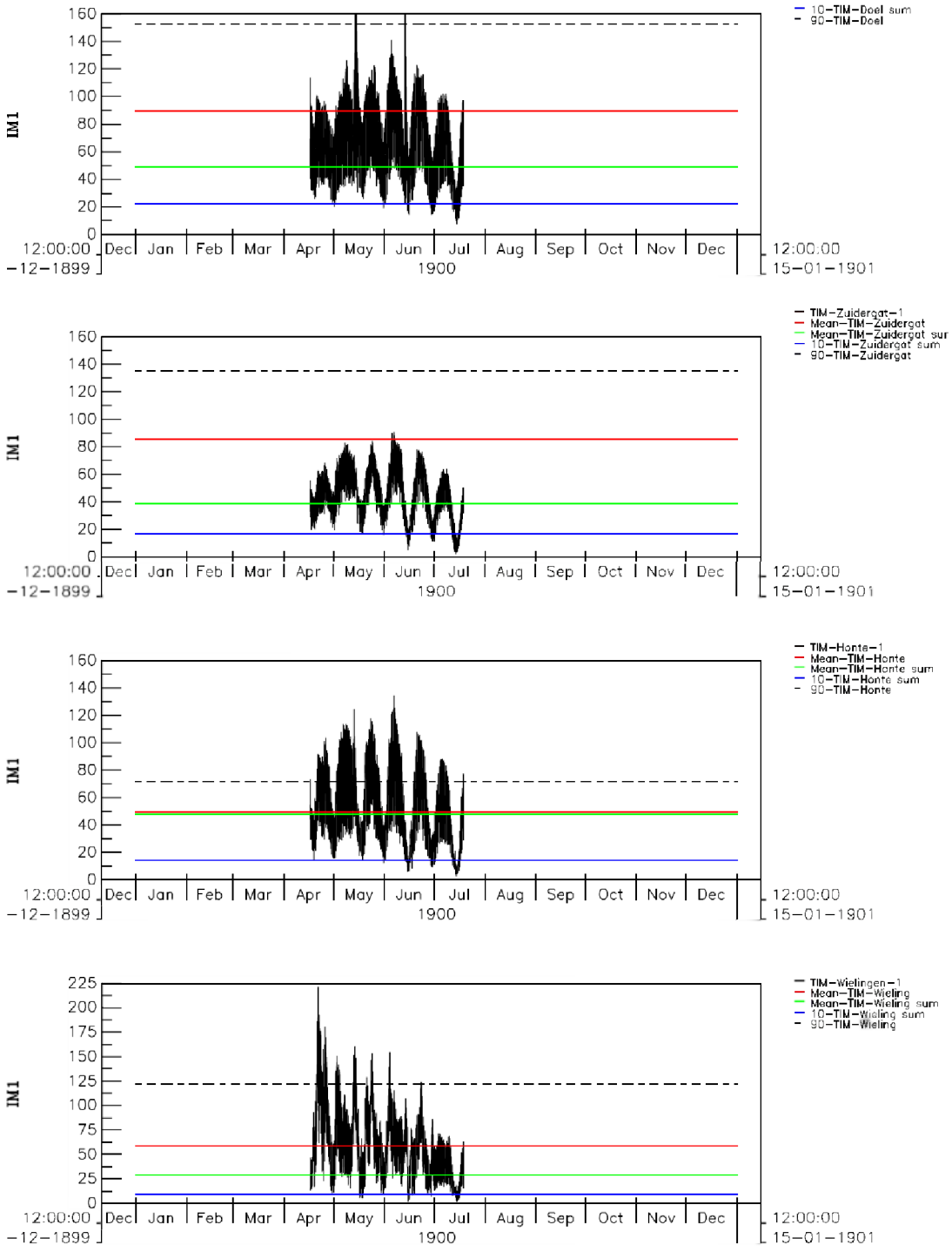

Figure B.9.2i: Computed SPM surface concentration at 4 stations along the Scheldt estuary for a 3-month simulation (q10). Observed mean levels are indicated with horizontal lines. In blue: 10-percentile level; in green: mean summer level; in red: mean winter level; dashed black: 90-percentile level..

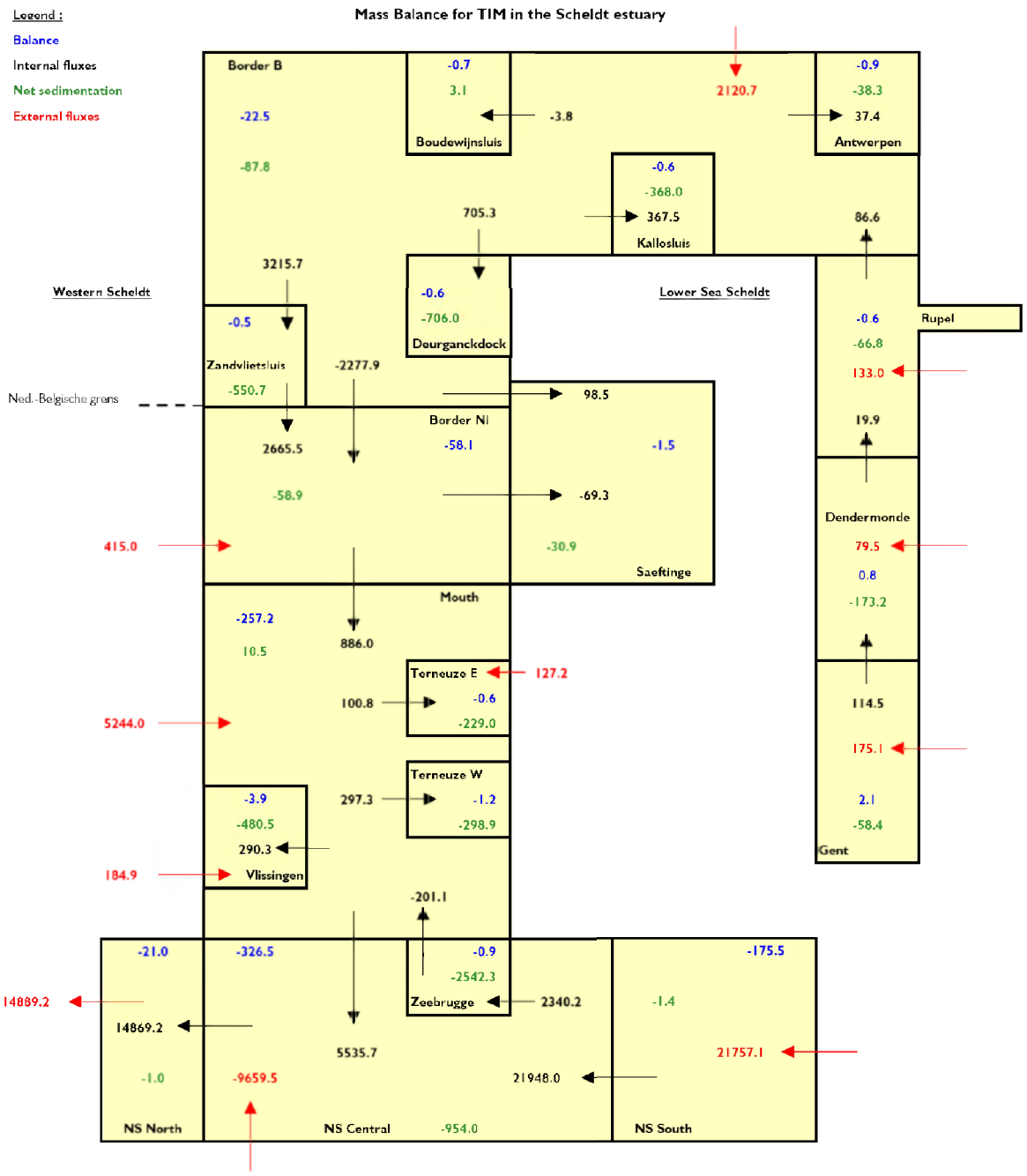

Figure B.9.2j: Mud balance for simulation Jan – Mar 2003 (q10), expressed in kton/year.

B.9.3 Modified dredging and dumping methodology in the model

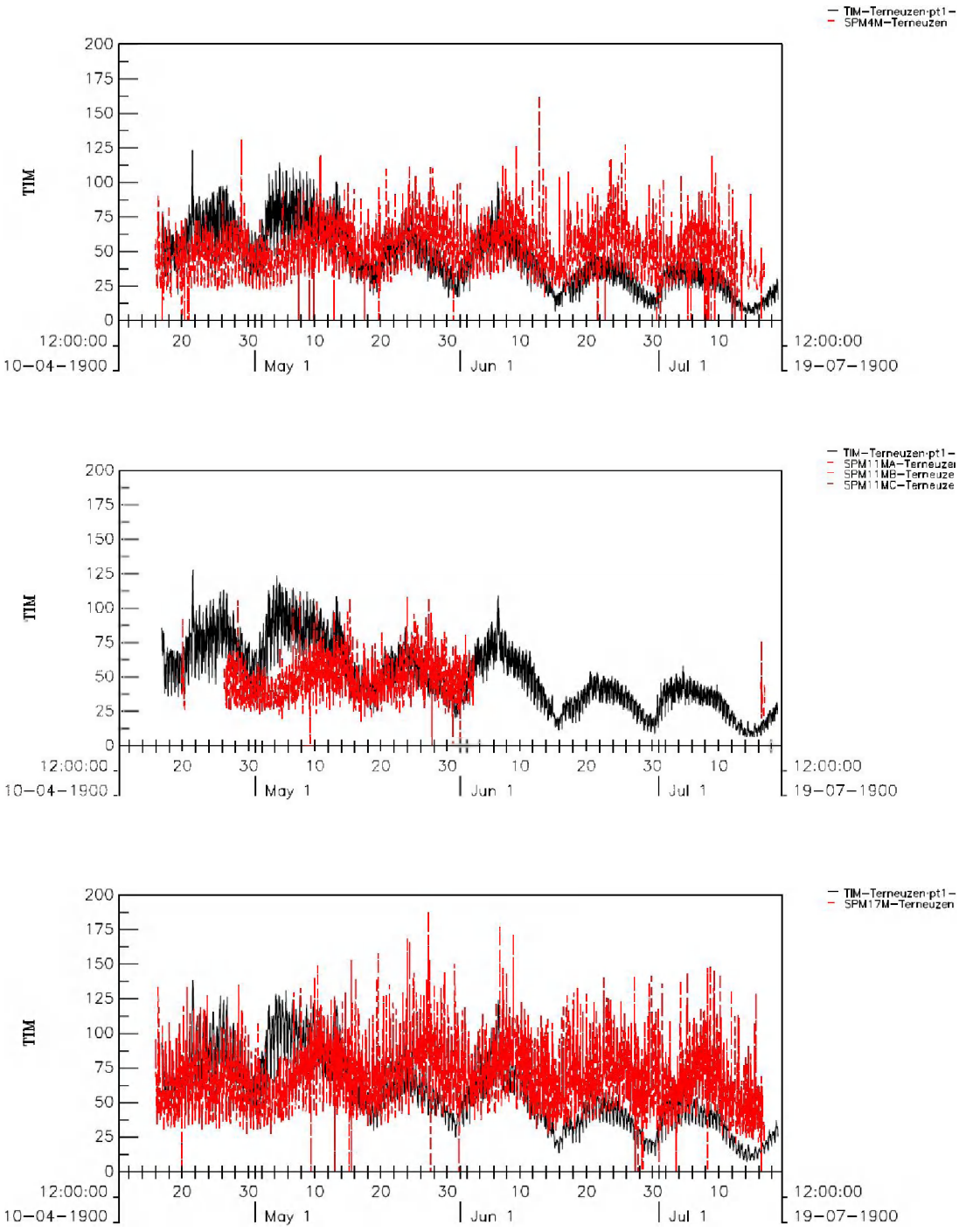

Figure B.9.3a: Computed SPM concentrations at DOW-jetty near Terneuzen for a 3-month period (q09). Observations are included in red and model results in black. Upper panel: obs. NAP-4m, model layer 1. Middle panel: obs. NAP-11m, model layer 2. Lower panel: obs. NAP-17m, model layer 4.

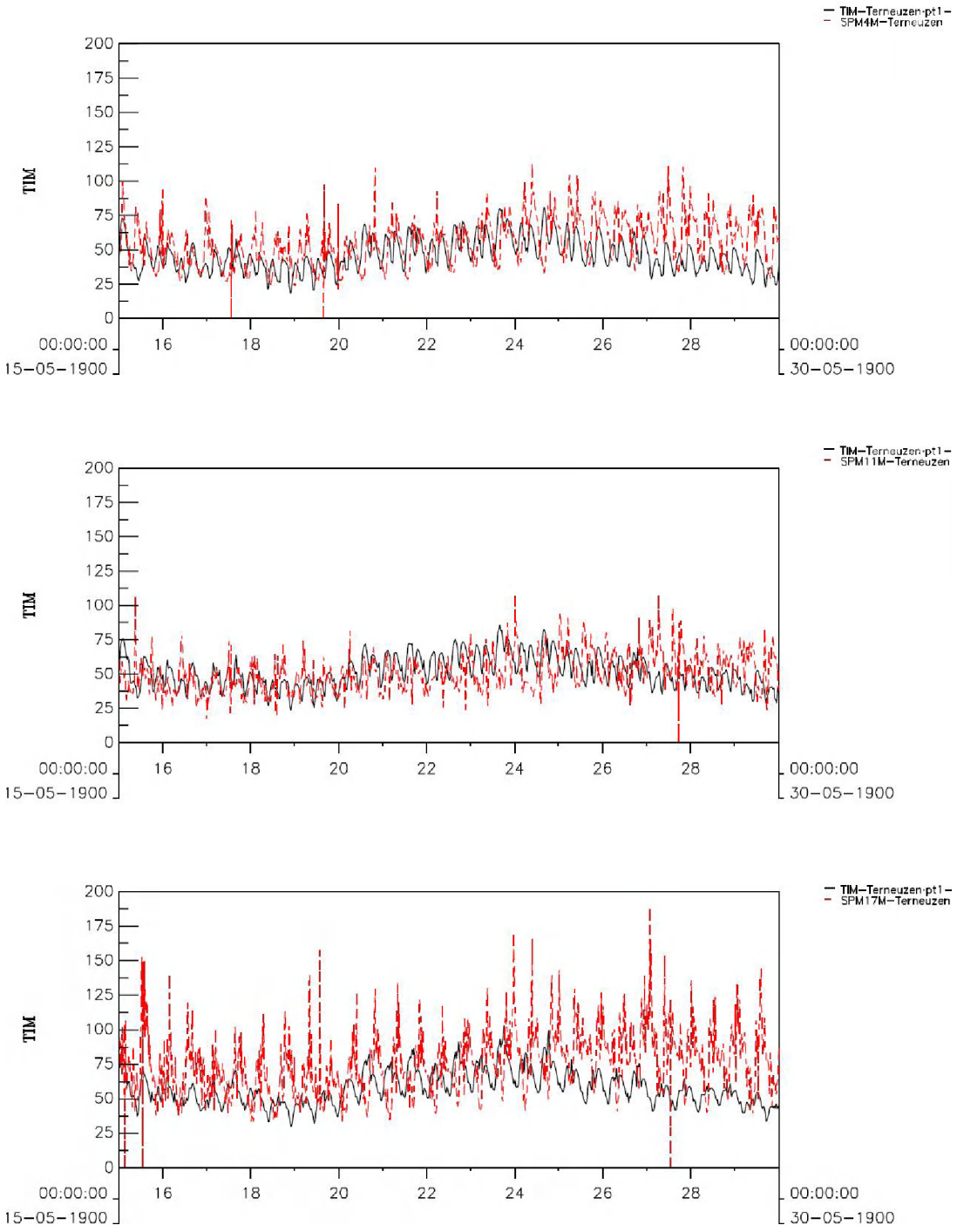

Figure B.9.3b: Computed SPM concentrations at DOW-jetty near Terneuzen for a neap-spring period (q09). Observations are included in red and model results in black. Upper panel: obs. NAP-4m, model layer 1. Middle panel: obs. NAP-11m, model layer 2. Lower panel: obs. NAP-17m, model layer 4.

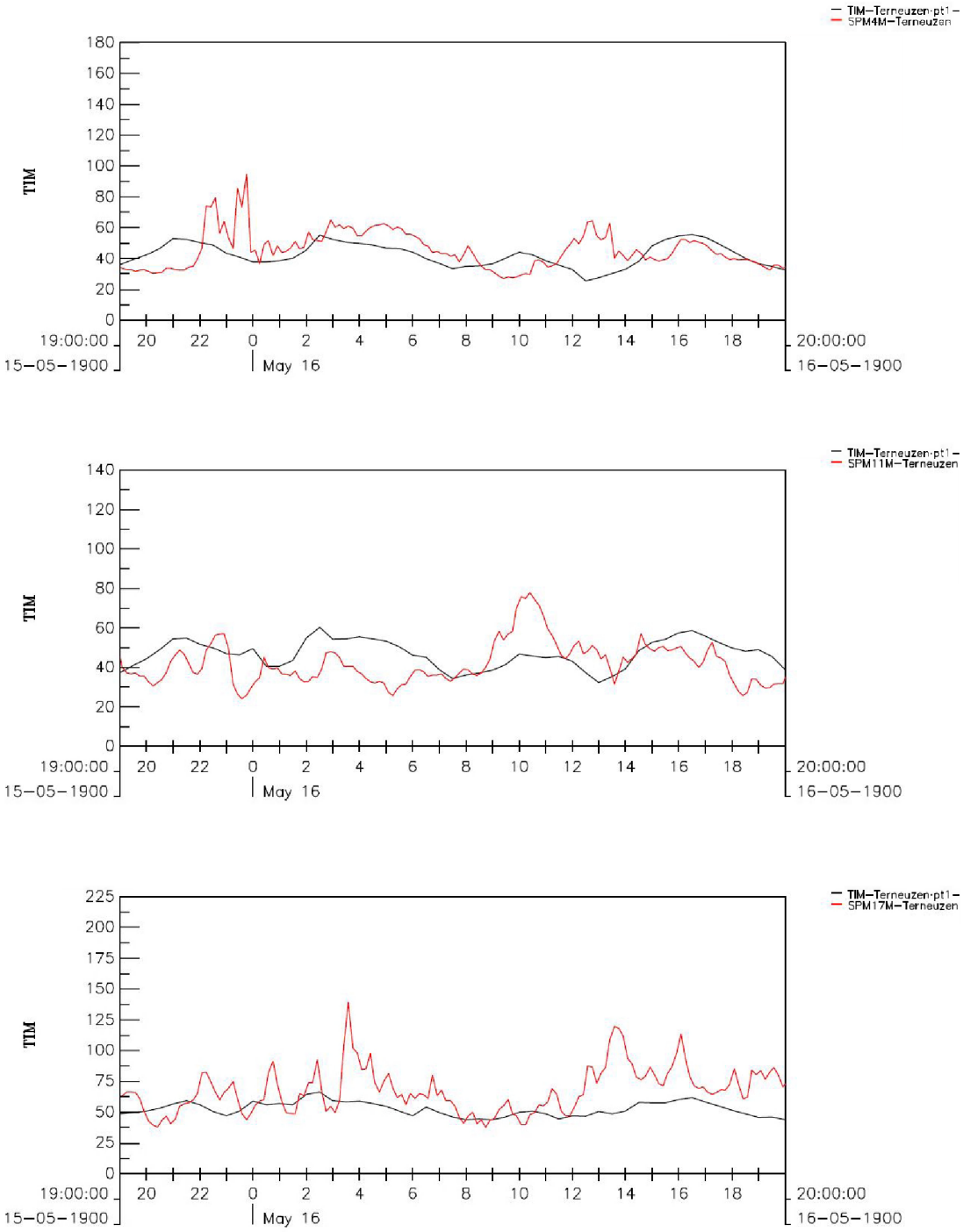

Figure B.9.3c: Computed SPM concentrations at DOW-jetty near Terneuzen for a neap tide (q09). Observations are included in red and model results in black. Upper panel: obs. NAP-4m, model layer 1. Middle panel: obs. NAP-11m, model layer 2. Lower panel: obs. NAP-17m, model layer 4.

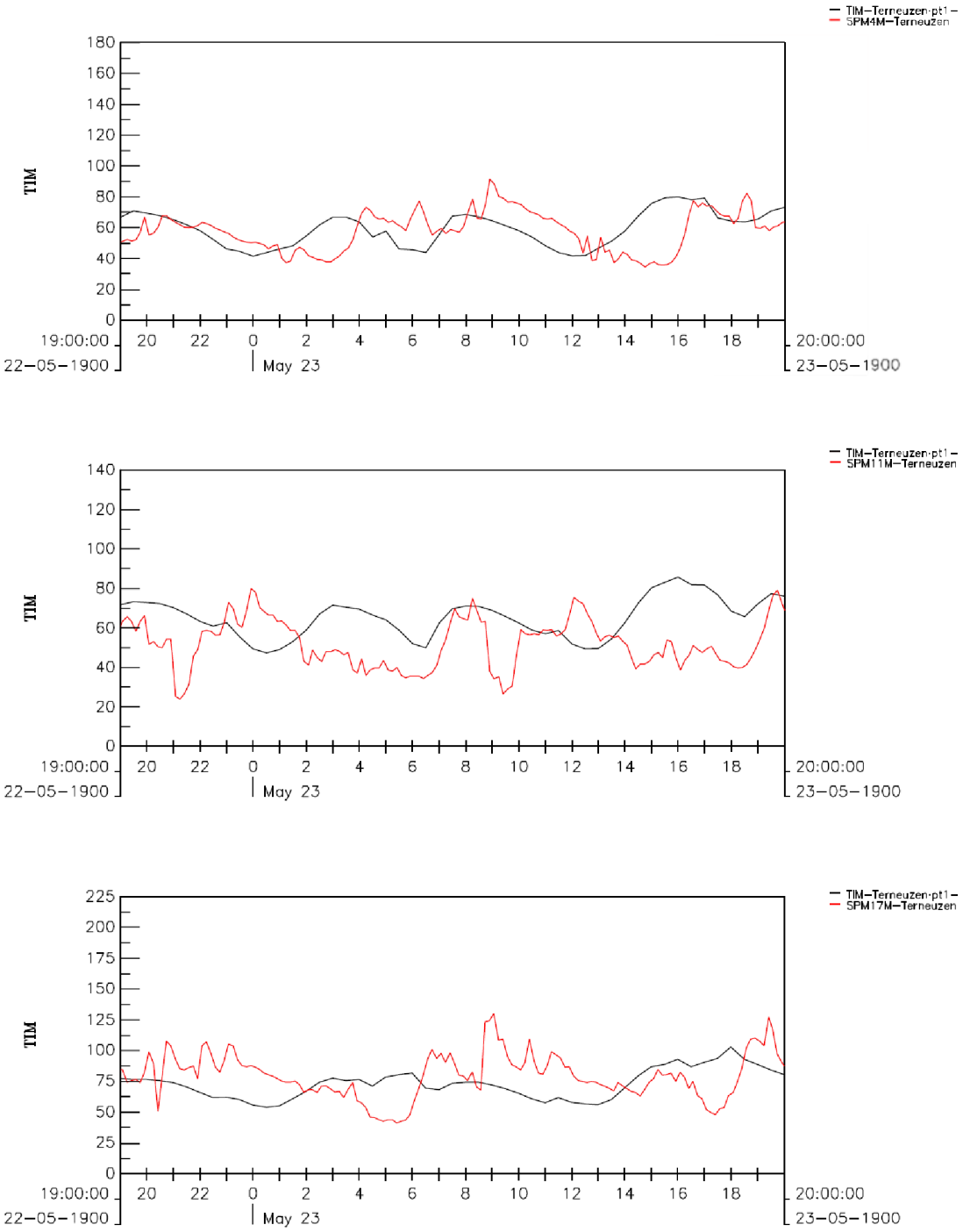

Figure B.9.3d: Computed SPM concentrations at DOW-jetty near Terneuzen for a spring tide (q09). Observations are included in red and model results in black. Upper panel: obs. NAP-4m, model layer 1. Middle panel: obs. NAP-11m, model layer 2. Lower panel: obs. NAP-17m, model layer 4.

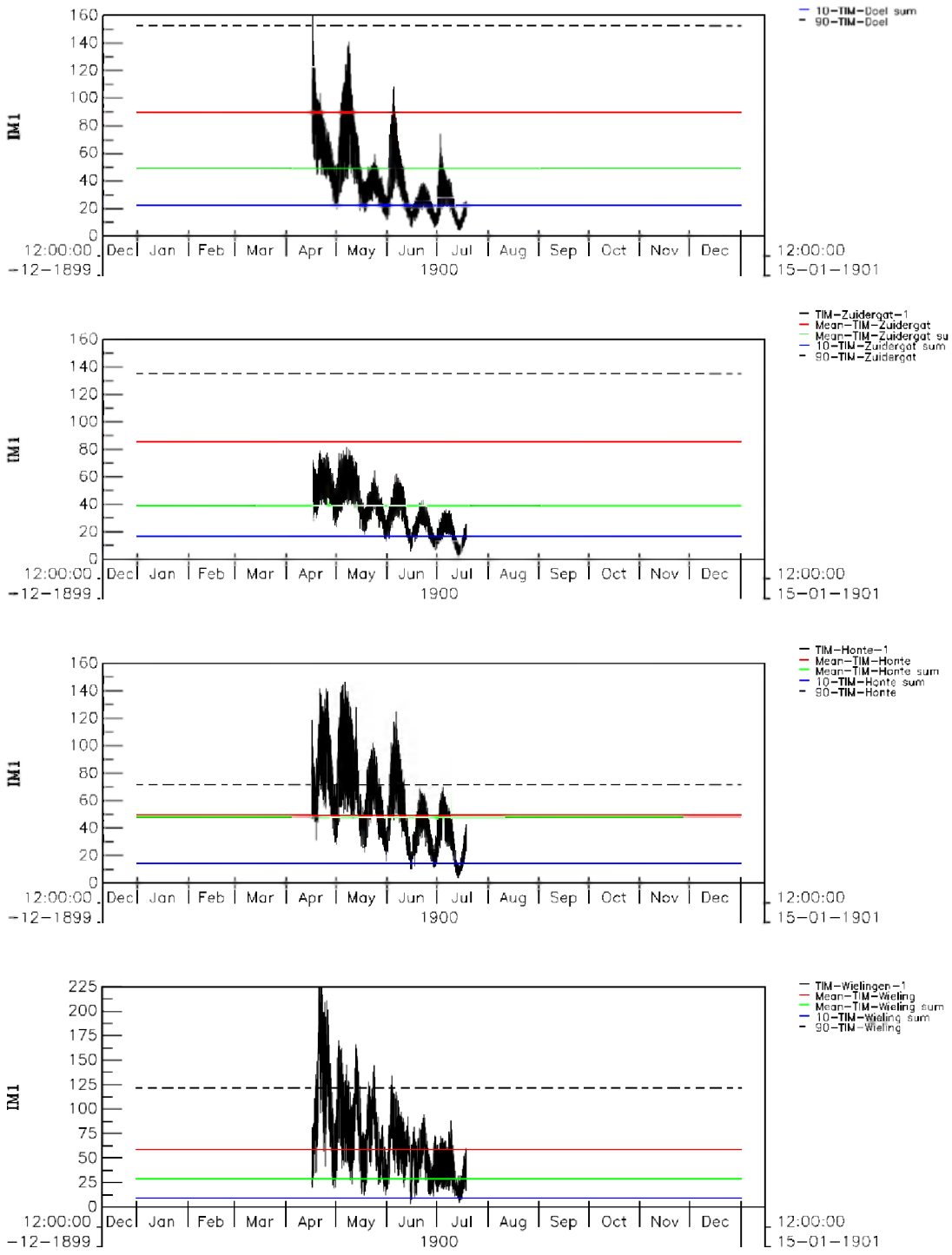

Figure B.9.3e: Computed SPM surface concentration at 4 stations along the Scheldt estuary for a 3-month simulation (q09). Observed mean levels are indicated with horizontal lines. In blue: 10-percentile level; in green: mean summer level; in red: mean winter level; dashed black: 90-percentile level..

B.10 Application to Dutch management issues

B.10.1 Reference (unchanged dumping)

Figure B.10.1a: Mud balance for simulation Jan – Mar 2003 (q10), expressed in kton/year.

B.10.2 Dumping at Sloe

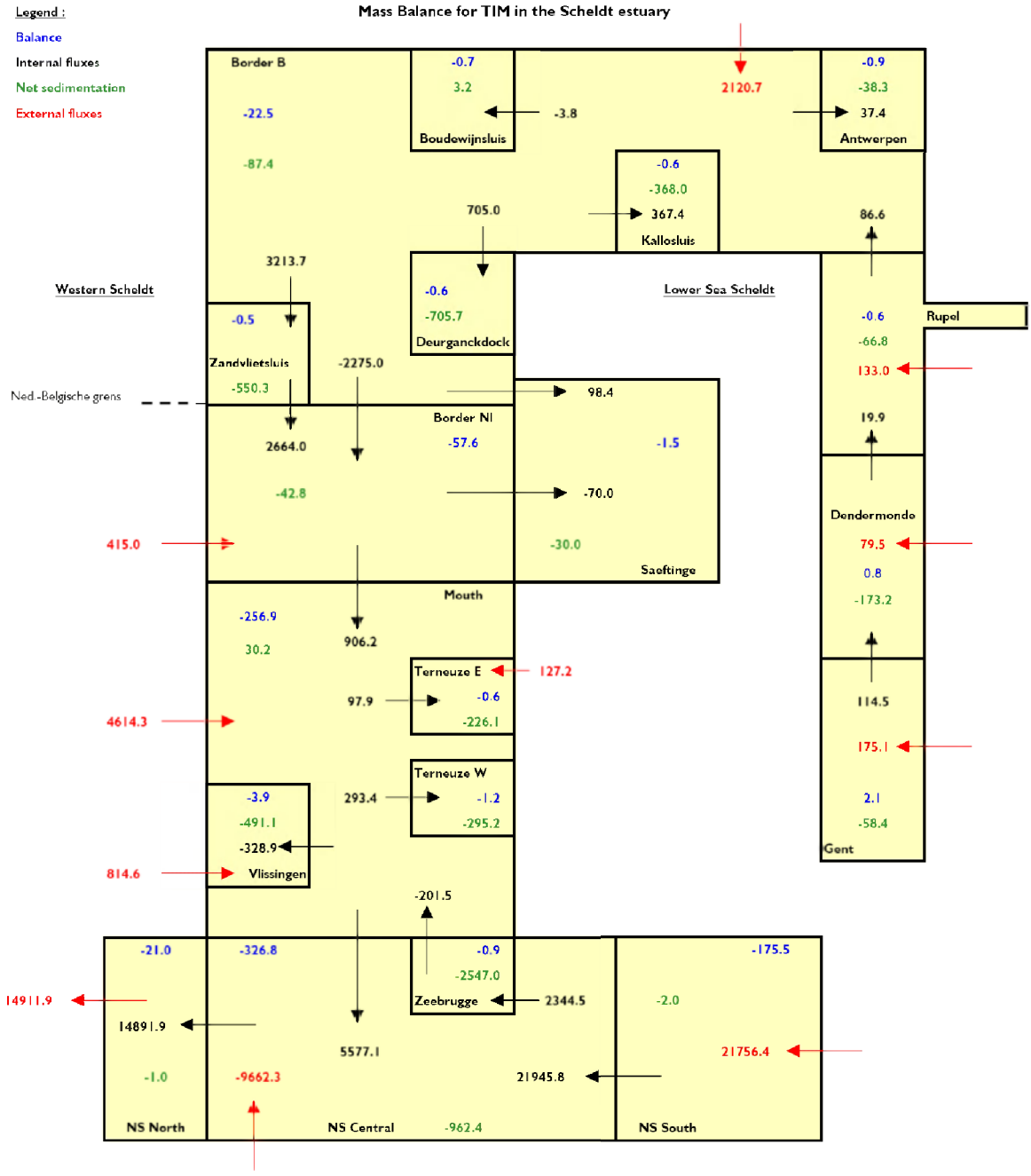

Figure B.10.2a: Mud balance for simulation Jan – Mar 2003 (q10sloe), expressed in kton/year.

B.10.3 Dumping at 12 km East

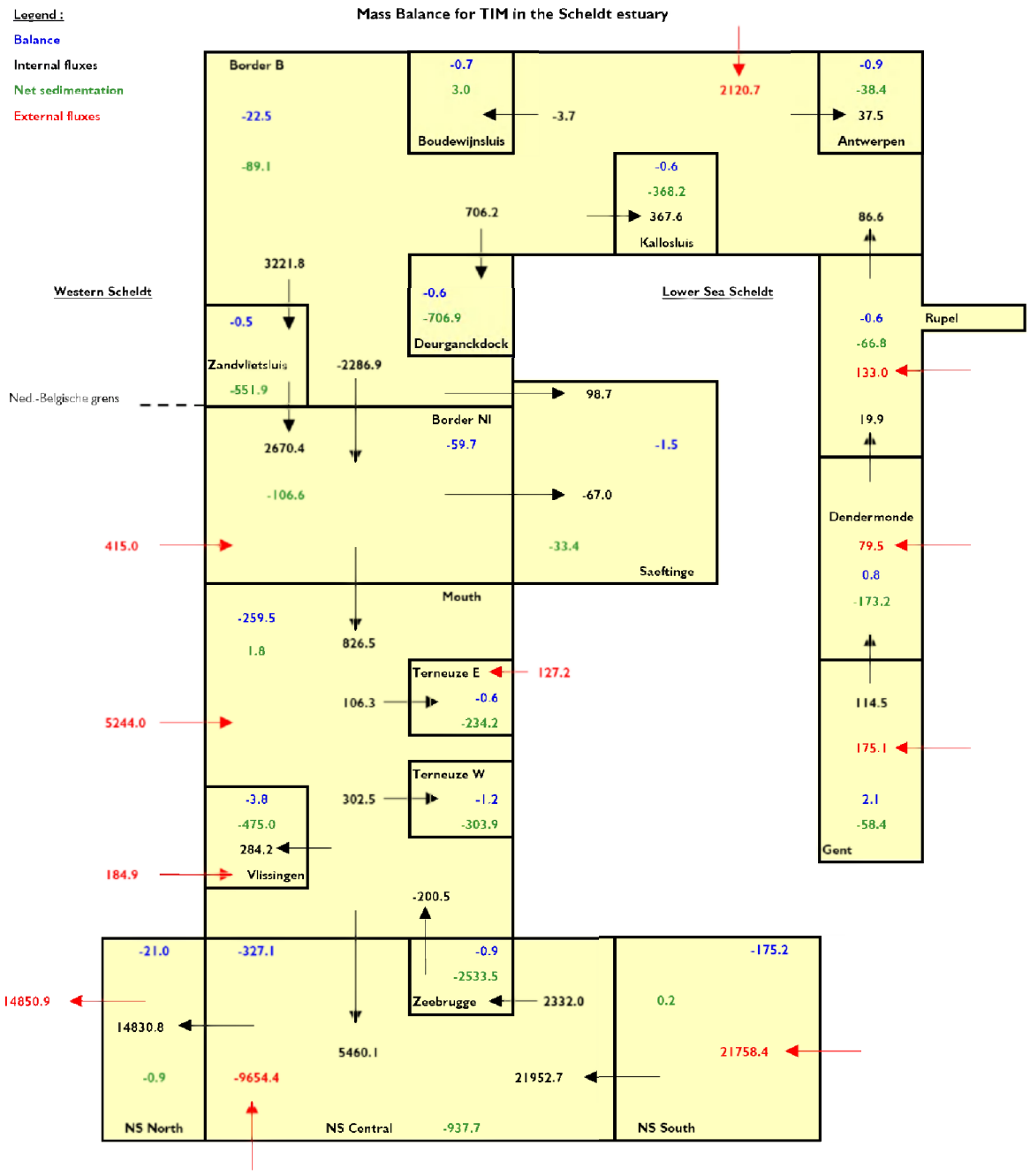

Figure B.10.3a: Mud balance for simulation Jan – Mar 2003 (q10O12km), expressed in kton/year.

B.10.4 Dumping at 6 km East

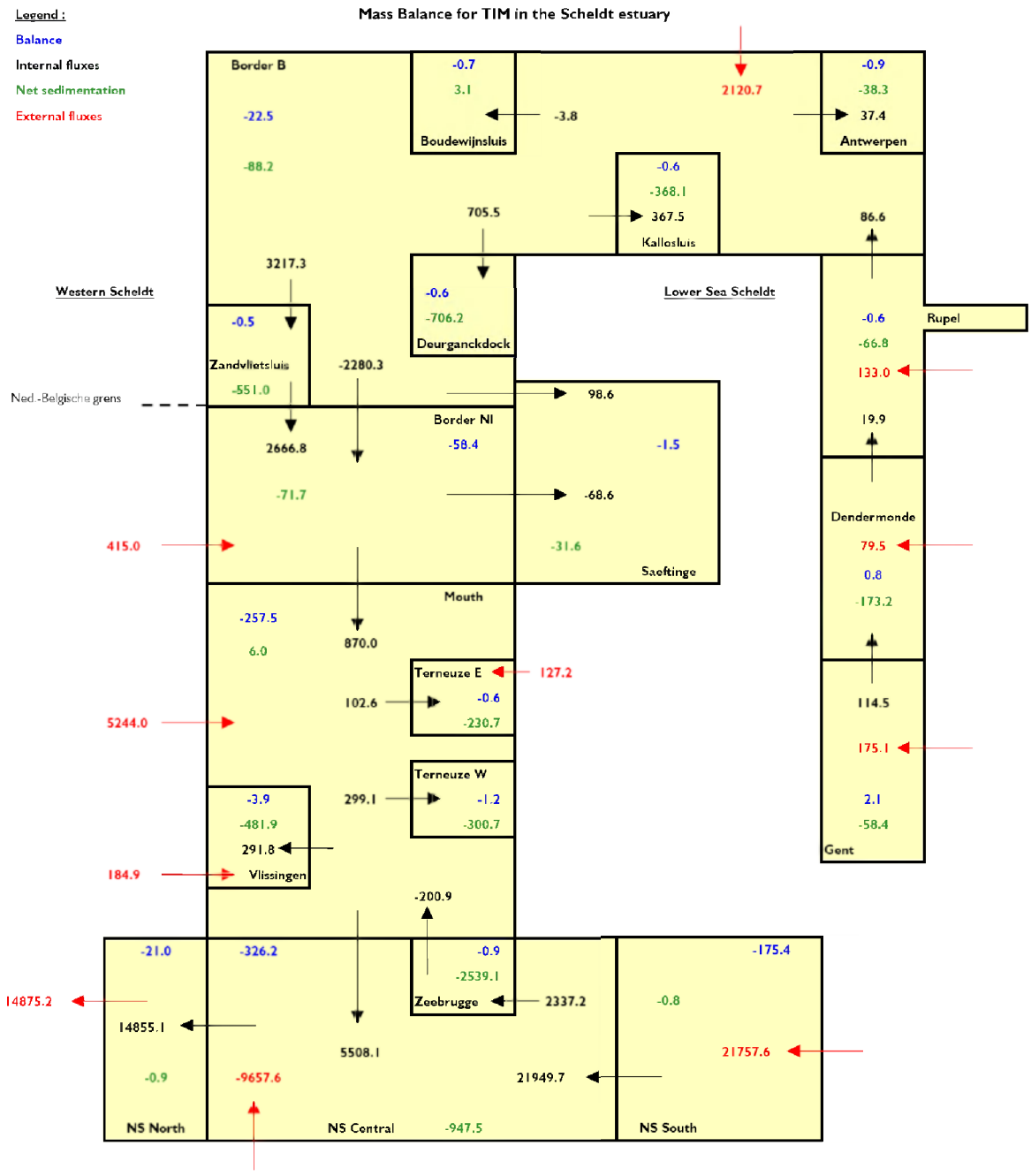

Figure B.10.4a: Mud balance for simulation Jan – Mar 2003 (q10O6km), expressed in kton/year.

B.10.5 Dumping at 12 km West

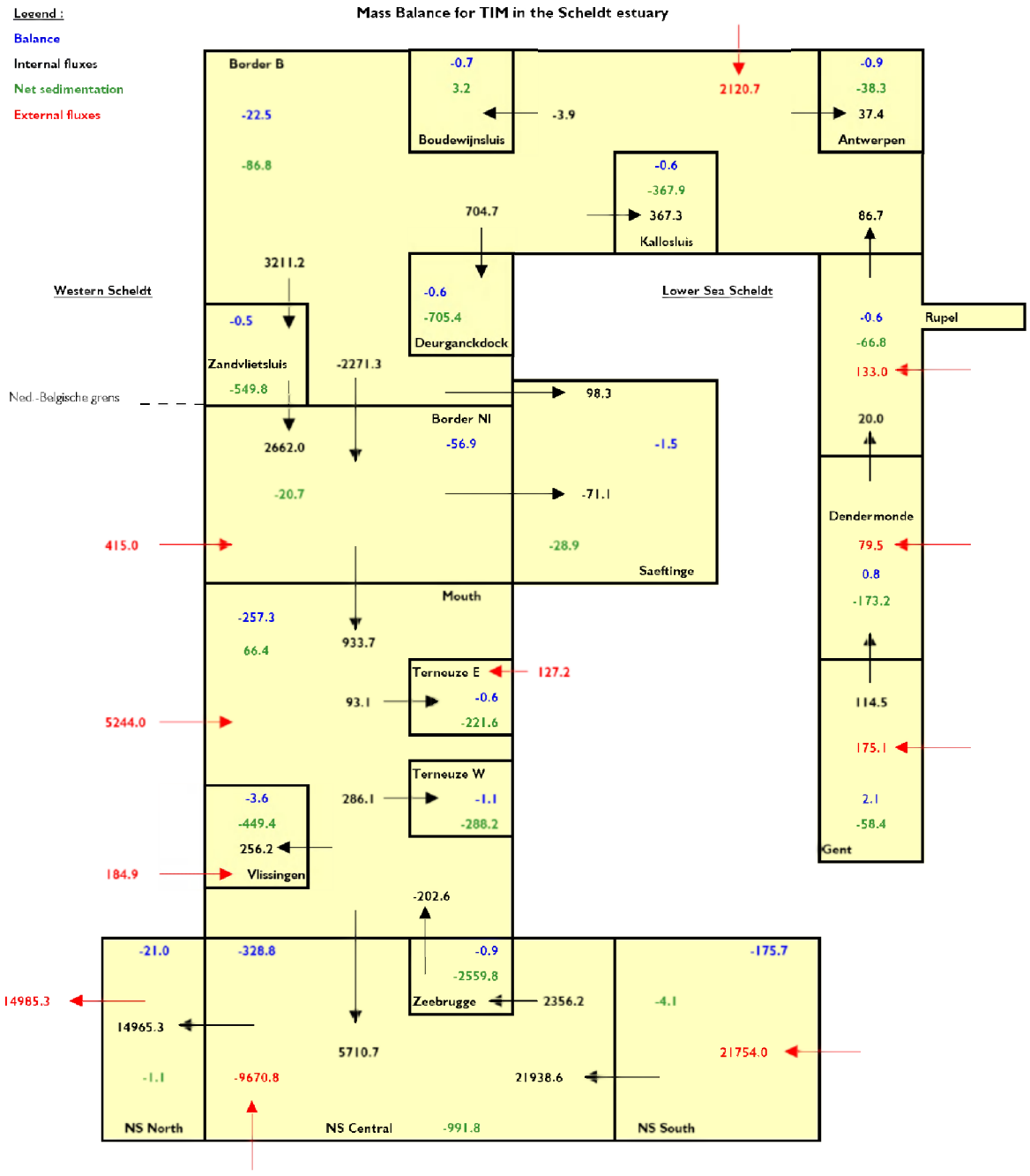

Figure B.10.5a: Mud balance for simulation Jan – Mar 2003 (q10W12km), expressed in kton/year.

B.10.6 Dumping at 6 km West

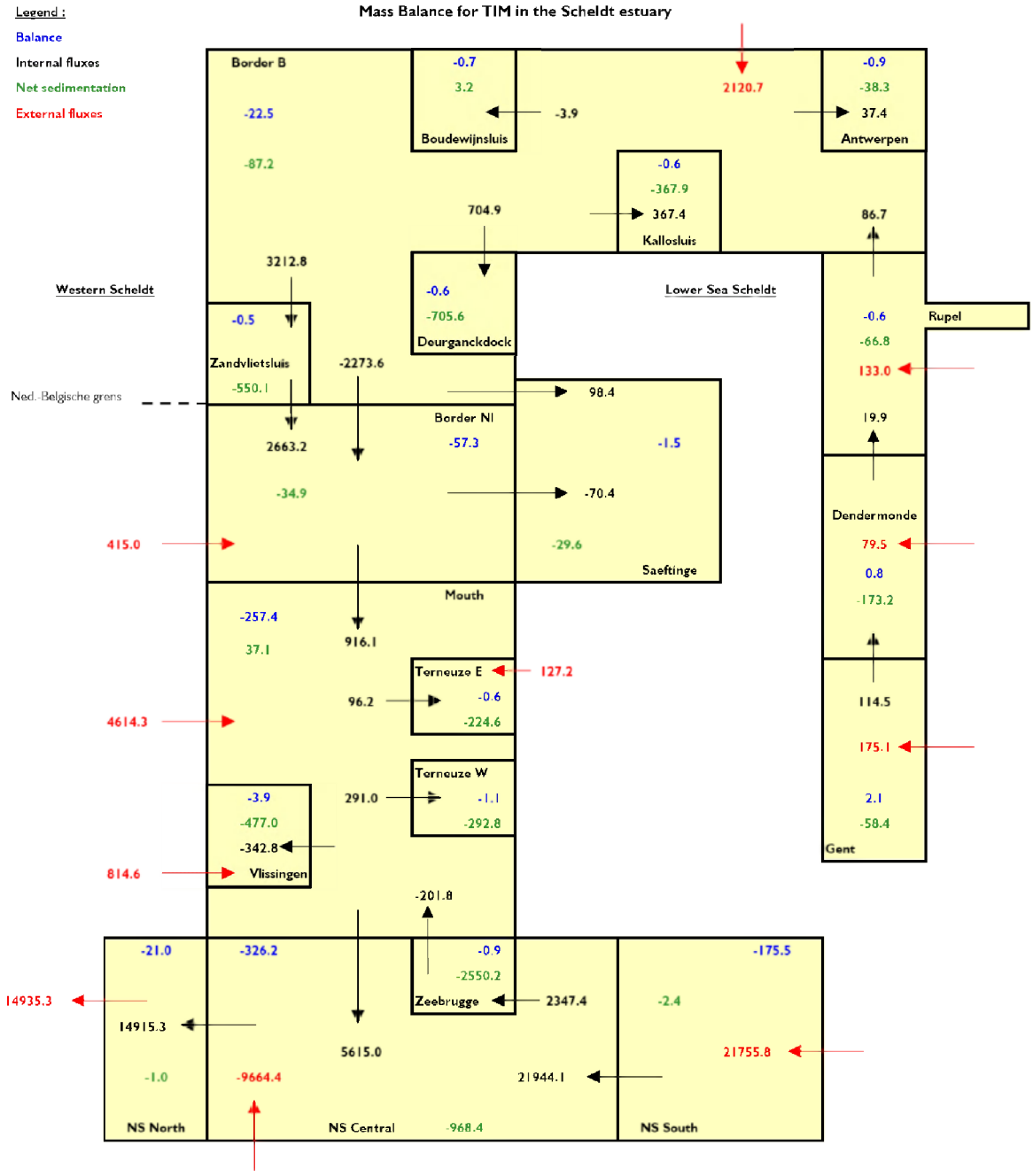

Figure B.10.6a: Mud balance for simulation Jan – Mar 2003 (q10W6km), expressed in kton/year.

B.11 Application to Dutch management issues

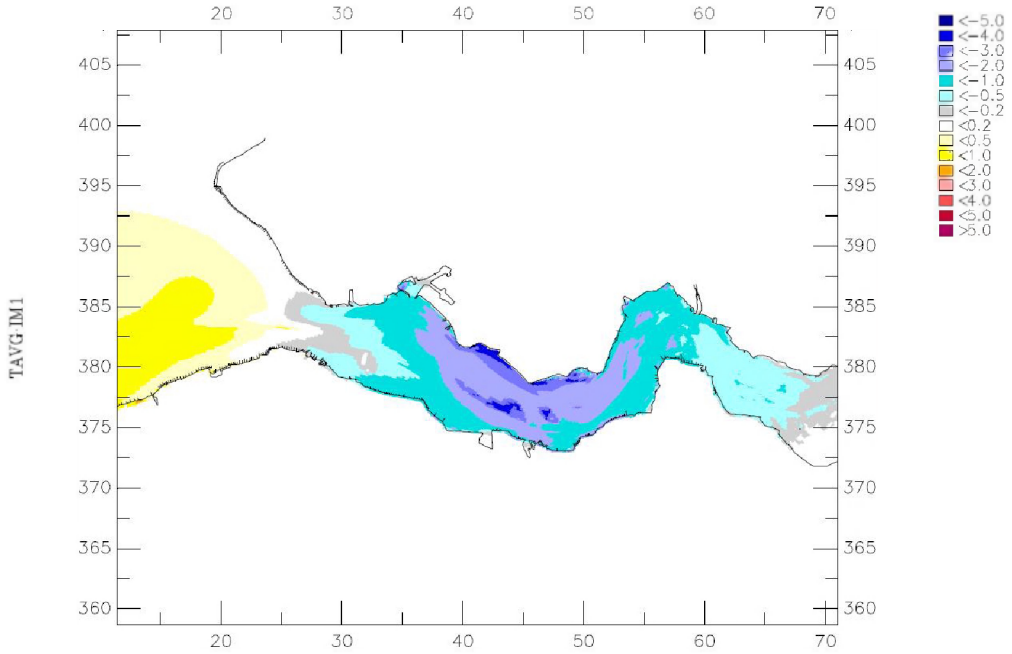

Fig. B.11a: Difference between suspended sediment concentrations (mg/l) of marine mud for run q10 12 km West and reference run (q10) averaged over a period of 14 days.

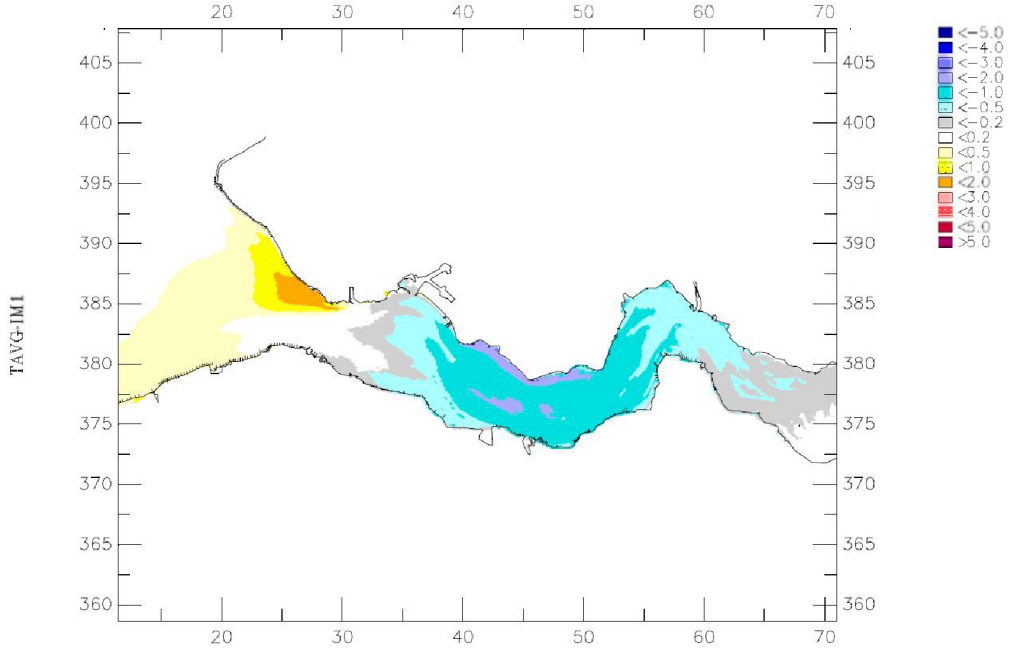

Fig. B.11b: Difference between suspended sediment concentrations (mg/l) of marine mud for run q10 6 km West and reference run (q10) averaged over a period of 14 days.

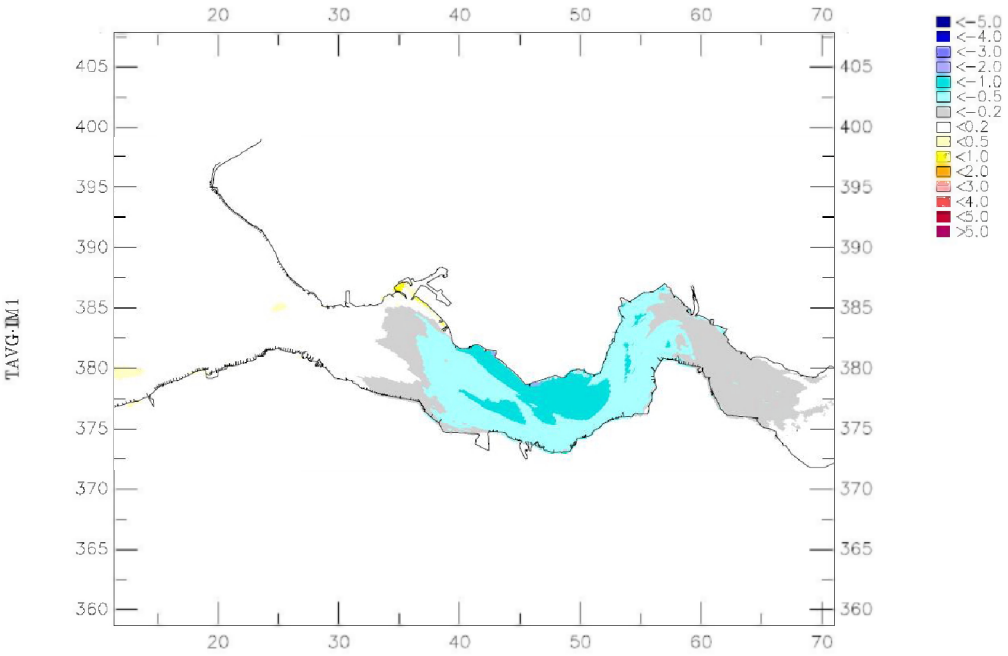

Fig. B.11c: Difference between suspended sediment concentrations (mg/l) of marine mud for run Sloe and reference run (q10) averaged over a period of 14 days.

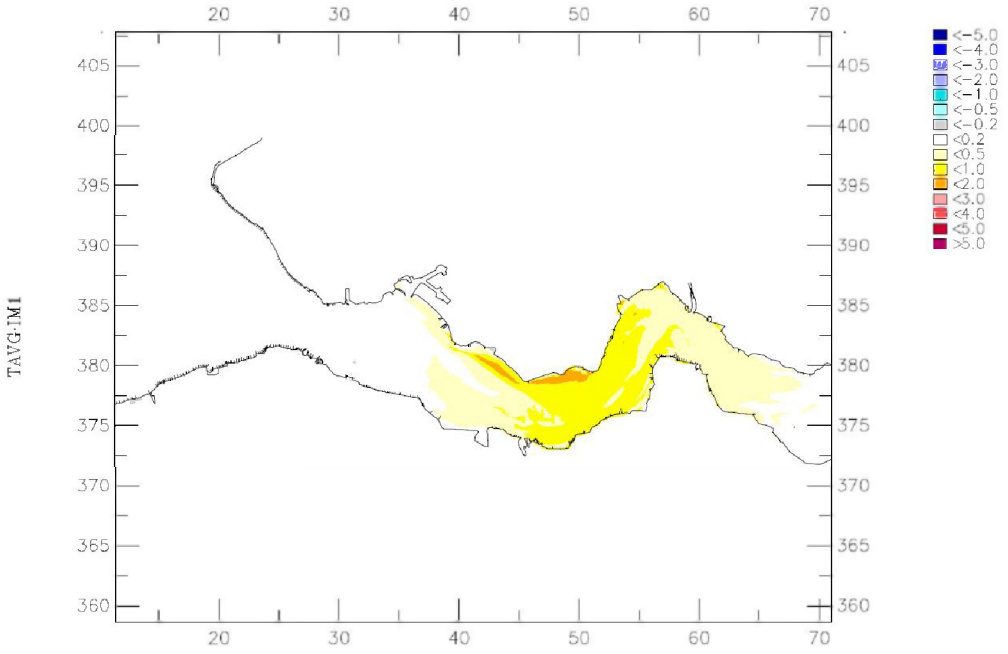

Fig. B.11d: Difference between suspended sediment concentrations (mg/l) of marine mud for run q10 6 km East and reference run (q10) averaged over a period of 14 days.

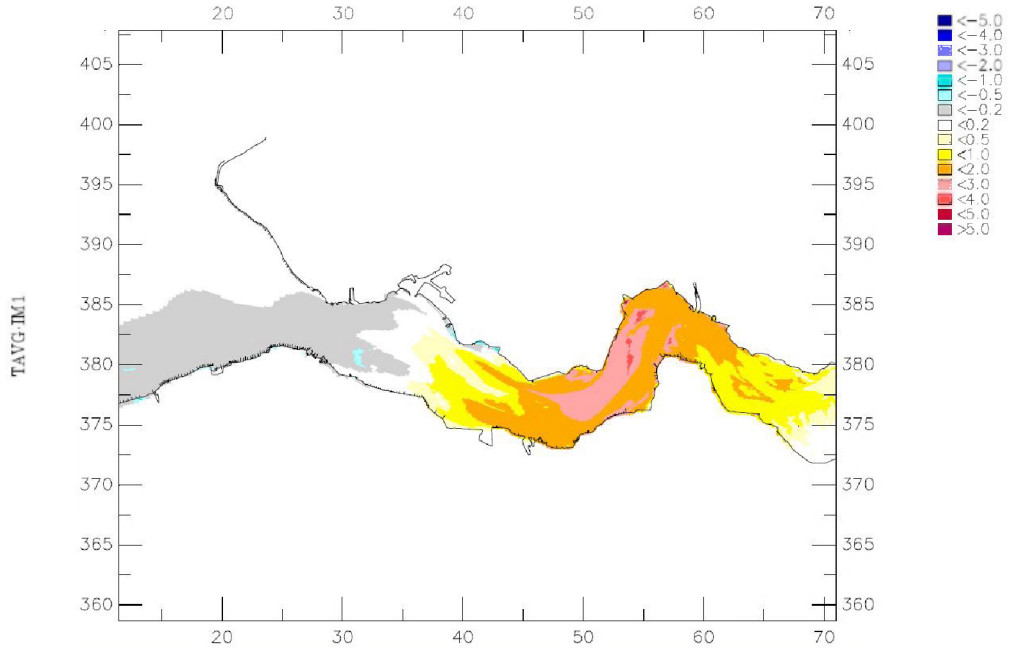

Fig. B.11e: Difference between suspended sediment concentrations (mg/l) of marine mud for run q10 12 km East and reference run (q10) averaged over a period of 14 days.